
Effects of Gradation and Cohesion on Bridge Scour, Vol. 4. Experimental Study of Scour Around Circular Piers in Cohesive Soils

PUBLICATION NO. FHWA-RD-99-186

DECEMBER 1999

PB2000-103273



U.S. Department of Transportation
Federal Highway Administration

Research, Development, and Technology
Turner-Fairbank Highway Research Center
6300 Georgetown Pike
McLean, VA 22101-2296

REPRODUCED BY: **NTIS**
U.S. Department of Commerce
National Technical Information Service
Springfield, Virginia 22161



FOREWORD

This report is volume 4 of a six volume series describing detailed laboratory experiments conducted at Colorado State University for the Federal Highway Administration as part of a study entitled "Effects of Sediment Gradation and Cohesion on Bridge Scour". Volume 4 describes the effects of cohesive soils on local pier scour. This six volume series will be distributed to NTIS only and will not be printed by FHWA. A separate summary report which describes the key results from the six volume series will be published by FHWA and distributed to the FHWA Division Offices.



T. Paul Teng, P.E.
Director, Office of Infrastructure
Research and Development

NOTICE

This document is disseminated under the sponsorship of the Department of Transportation in the interest of information exchange. The United States Government assumes no liability for the contents or use thereof. This report does not constitute a standard, specification, or regulation.

The United States Government does not endorse products or manufacturers. Trade and manufacturers names appear in this report only because they are considered essential to the object of the document.

PROTECTED UNDER INTERNATIONAL COPYRIGHT
ALL RIGHTS RESERVED
NATIONAL TECHNICAL INFORMATION SERVICE
U.S. DEPARTMENT OF COMMERCE

Reproduced from
best available copy.



1. Report No. FHWA-RD-99-186	2. PB2000-103273 	3. Recipient's Catalog No.	
4. Title and Subtitle EFFECTS OF GRADATION AND COHESION ON BRIDGE SCOUR Vol. 4. Experimental Study of Scour Around Circular Piers in Cohesive Soils		5. Report Date December 1999	
		6. Performing Organization Code	
7. Author(s) Albert Molinas and Magdy M. Hosni		8. Performing Organization Report No.	
9. Performance Organization Name and Address Colorado State University Engineering Research Center Fort Collins, Colorado		10. Work Unit No. (TRAIS) NCP# 3D3C1-582	
		11. Contract or Grant No. DTFH61-91-C-00004	
12. Sponsoring Agency and Address Office of Engineering Research and Development Federal Highway Administration 6300 Georgetown Pike MxcLean, Va 22101		13. Type of Report and Period Covered Laboratory Final Report Jan 1991 - Jan 1996	
		14. Sponsoring Agency Code	
15. Supplementary Notes Contracting Officer's Technical Representative: J. Sterling Jones HNR-10			
16. Abstract <p>The effects of cohesion on pier scour was investigated experimentally using four-foot-, eight-foot-, and twenty-foot-wide test flumes at the Engineering Research Center, Colorado State University. In the first part of experiments, clay-sand mixtures with varying amounts of clay were subjected to different approach flow conditions. Experiments were normalized with scour experienced in pure sands. For Montmorillonitic clay mixtures, results showed that in sandy clays increasing the clay content to up to 30 percent may reduce scour by up to 40 percent.</p> <p>Beyond a certain clay content (30-40 percent for the present mixture) parameters such as compaction, initial water content, degree of saturation, shear strength, etc. dominate the pier scour. In the second part of experiments, these effects were investigated for flow conditions with Froude numbers ranging from 0.2 (subcritical) to 1.4 (supercritical). Regression equations reflecting flow and selected cohesive soil parameters to pier scour were derived for the particular pier and flow conditions that were used in the experiments. These experiments showed that pier scour in cohesive material can be expressed in terms of cohesive soil parameters which can be determined in the field.</p> <p>The equations derived from this study do not attempt to relate effects due to pier geometry, flow depth, gradation of sand in the mixtures, etc. and therefore are not intended for general application. These relationships are derived to explain the variability of pier scour with cohesion properties.</p> <p>This publication is the fourth volume of a six volume series. The other volumes are as follows:</p> <ul style="list-style-type: none"> Vol. 1. Effect of Sediment Gradation and Coarse Material Fraction on Clear Water Scour Around Bridge Piers Vol. 2. Experimental Study of Sediment Gradation and Flow Hydrograph Effects on Clear Water Scour Around Circular Piers Vol. 3. Abutment Scour for Nonuniform Mixtures Vol. 5. Effect of Cohesion on Bridge Abutment Scour Vol. 6. Abutment Scour in Uniform and Stratified Sand Mixtures 			
17. Key Words Bridge Scour, Pier Scour, Abutment Scour, Gradation, Coarse Sediment, Cohesion, Clay Scour		18. Distribution Statement No restrictions. This document is available to the public through the National Technical Information Service, Springfield, Va. 22161	
19. Security Classif. (of this report) Unclassified	20. Security Classif. (of this page) Unclassified	21. No. of Pages 191	22. Price

SI* (MODERN METRIC) CONVERSION FACTORS

APPROXIMATE CONVERSIONS TO SI UNITS

APPROXIMATE CONVERSIONS FROM SI UNITS

Symbol	When You Know	Multiply By	To Find	Symbol	When You Know	Multiply By	To Find	Symbol
LENGTH								
in	inches	25.4	millimeters	mm	millimeters	0.039	inches	in
ft	feet	0.305	meters	m	meters	3.28	feet	ft
yd	yards	0.914	kilometers	km	meters	1.09	yards	yd
mi	miles	1.61			kilometers	0.621	miles	mi
AREA								
in ²	square inches	645.2	square millimeters	mm ²	square millimeters	0.0016	square inches	in ²
ft ²	square feet	0.093	square meters	m ²	square meters	10.764	square feet	ft ²
yd ²	square yards	0.836	square meters	m ²	square meters	1.195	square yards	yd ²
ac	acres	0.405	hectares	ha	hectares	2.47	acres	ac
mi ²	square miles	2.59	square kilometers	km ²	square kilometers	0.386	square miles	mi ²
VOLUME								
fl oz	fluid ounces	29.57	milliliters	mL	milliliters	0.034	fluid ounces	fl oz
gal	gallons	3.785	liters	L	liters	0.264	gallons	gal
ft ³	cubic feet	0.028	cubic meters	m ³	cubic meters	35.71	cubic feet	ft ³
yd ³	cubic yards	0.765	cubic meters	m ³	cubic meters	1.307	cubic yards	yd ³
MASS								
oz	ounces	28.35	grams	g	grams	0.035	ounces	oz
lb	pounds	0.454	kilograms	kg	kilograms	2.202	pounds	lb
T	short tons (2000 lb)	0.907	megagrams (or "metric ton")	Mg (or "t")	megagrams (or "metric ton")	1.103	short tons (2000 lb)	T
TEMPERATURE (exact)								
°F	Fahrenheit temperature	5(F-32)/9 or (F-32)/1.8	Celcius temperature	°C	Celcius temperature	1.8C + 32	Fahrenheit temperature	°F
ILLUMINATION								
fc	foot-candles	10.76	lux	lx	lux	0.0929	foot-candles	fc
ft	foot-Lamberts	3.426	candela/m ²	cd/m ²	candela/m ²	0.2919	foot-Lamberts	ft
FORCE and PRESSURE or STRESS								
lbf	poundforce	4.45	newtons	N	newtons	0.225	poundforce	lbf
lbf/in ²	poundforce per square inch	6.89	kilopascals	kPa	kilopascals	0.145	poundforce per square inch	lbf/in ²

NOTE: Volumes greater than 1000 l shall be shown in m³.

(Revised September 1993)

* SI is the symbol for the International System of Units. Appropriate rounding should be made to comply with Section 4 of ASTM E380.

EFFECTS OF GRADATION AND COHESION ON BRIDGE SCOUR

VOLUME IV

TABLE OF CONTENTS

	Page
I. INTRODUCTION AND OBJECTIVES	
1-1 Introduction	1
1-2 Objectives	3
1-3 Methodology	4
II. SCOUR AROUND BRIDGE PIERS	
2-1 Introduction	7
2-2 Definition and Classification of Scour.....	7
2-3 Mechanism of Local Scour at Bridge Piers	10
2-4 Parameters affecting Local Pier Scour	13
III. REVIEW OF LITERATURE	
3-1 Introduction	18
3-2 Previous Studies of Pier Scour in Non-Cohesive Soils	19
3-3 Review of the Properties of Mineral Clays	27
3-3-1 Clay Mineralogy	27
3-3-2 Soil Structure and Fabric	28
3-3-3 Structure and Composition of Clay Minerals	28
3-3-4 Ions (Cations, anions) Exchange	30
3-3-5 Flocculation and Dispersion of Mineral Clays	32
3-3-6 Effect of Dielectric Dispersion	32
3-3-7 Effect of Compaction on Cohesive Soils	33
3-3-8 Plasticity of Mineral Clays	34
3-4 Previous Studies of Scour or Erosion in Cohesive Soils	36

TABLE OF CONTENTS (Cont.)

	Page
IV. EXPERIMENTAL FACILITIES AND TEST PROCEDURES	
4-1 Introduction	48
4-2 Experimental Facilities	48
4-2-1 Flumes	48
4-2-2 Piers	54
4-2-3 Current Meter	54
4-2-4 Point Gage	55
4-3 Soils Selection and Bed Material Preparation ..	55
4-4 Experimental Procedures	60
4-5 Experimental Measurements	65
V. ANALYSIS OF THE EXPERIMENTAL RESULTS	
5-1 Introduction	70
5-2 Dimensional Analysis	71
5-3 Analysis of Pier Scour in Cohesive- Non Cohesive Soil Mixtures	74
5-3-1 Geometry of Scour Hole in the Mixtures	74
5-3-2 Effect of Flow Intensity on Pier Scour in Mixtures	91
5-3-3 Effect of the Test Duration on Pier Scour in Mixtures	96
5-3-4 Regression Analysis for Pier Scour in Mixtures	99
5-4 Analysis of Pier Scour in Compacted Unsaturated Cohesive Soil	100
5-4-1 Geometry of Scour Hole in Unsaturated Cohesive Soils	103
5-4-2 Effect of Flow Intensity on Pier Scour in Unsaturated Cohesive Soils	108
5-4-3 Effect of the Test Duration on Pier Scour in Unsaturated Cohesive Soils	115
5-4-4 Regression Analysis for Pier Scour in Unsaturated Cohesive Soils	120

TABLE OF CONTENTS (Cont.)

	Page
5-5 Analysis of Pier Scour in Saturated Cohesive Soils	124
5-5-1 Geometry of Pier Scour in Saturated Cohesive Soils	124
5-5-2 Effect of the Approach Flow and IWC on Pier Scour in Saturated Cohesive Soils ..	128
5-5-3 Effect of Test Duration on Pier Scour in Saturated Cohesive Soils	136
5-5-4 Regression Analysis for Pier Scour in Saturated Cohesive Soils	141
5-5-5 Effect of Dry-Wet Cycle on Pier Scour in Saturated Cohesive Soils	146
5-5-6 General Equation for Pier Scour in Cohesive Soils	150
5-6 Sensitivity Analysis	151
VI. SUMMARY, CONCLUSIONS, AND RECOMMENDATIONS	
6-1 Summary	164
6-2 Conclusions	167
6-3 Recommendations for Further Research	169
Bibliography	172

EFFECTS OF GRADATION AND COHESION ON BRIDGE SCOUR

VOLUME IV

LIST OF FIGURES

Figure	Page
2-1 a) Scour Depth as a Function of Time	9
b) Scour Depth as a Function of Shear Velocity	9
2-2 Diagrammatic Flow Pattern at Cylindrical Pier (After Raudkivi 1986)	12
2-3 Common Pier Shapes	15
2-4 Scour Shapes Around Piers Aligned and Angled to the Flow Direction (After Laursen and Toch 1956)	17
2-5 Alignment Factor $K\alpha$ for Piers not Aligned with Flow (After Laursen and Toch 1956)	17
3-1 Effect of Compaction on Soil Structure (After Lambe 1958)	35
4-1 Plan View of the Seventeen-Foot Wide Experimental Flume	50
4-2 Plan View of the Eight-Foot Wide Experimental Flume	53
4-3 Plan View of the Four-Foot Wide Experimental Flume	53
4-4 Grain Size Distribution of the Masonry Sand	57
4-5 Grain Size Distribution of the Cohesive Soil	58
4-6 Velocity Measurements Grid	67
5-1 View of the Scour Hole for Pier A (0% Clay) at the End of Run R32, $Q=9$ cfs	77
5-2 View of the Scour Hole for Pier B (20% Clay) at the End of Run R32, $Q=9$ cfs	77
5-3 View of the Scour Hole for Pier B (30% Clay) at the End of Run R20, $Q=13.5$ cfs	78
5-4 View of the Scour Hole for Pier C (40% Clay) at the End of Run R20, $Q=13.5$ cfs	78

LIST OF FIGURES (Cont.)

Figure	Page
5-5 Effect of Clay Content on the Cross Section Geometry Along the Center Line of Pier PA for Runs R30 and R32 (0% Clay)	79
5-6 Effect of Clay Content on the Cross Section Geometry Along the Center Line of Pier PB for Runs R13, R16, and R21 (5% Clay)	80
5-7 Effect of Clay Content on the Cross Section Geometry Along the Center Line of Pier PB for Runs R30 and R32 (20% Clay)	81
5-8 Effect of Clay Content on the Cross Section Geometry Along the Center Line of Pier PC for Runs R30 and R32 (40% Clay)	82
5-9 Effect of Clay Content on the Cross Section Geometry Along the Center Line of Piers PA, PB, and PC for Run R30	83
5-10 Effect of Clay Content on the Cross Section Geometry Along the Center Line of Piers PA, PB, and PC for Run R31	84
5-11 Effect of Clay Content on the Slope of the Scour Hole.....	86
5-12 Effect of Clay Content in Sandy Soils on (d_s/b) versus (V_s/b^3)	87
5-13 Effect of Clay Content in Sandy Soils on Pier Scour Ratio.....	88
5-14 Effect of Clay Content in Sandy Soils on Reduction Factor (K)	90
5-15 Vertical Velocity Distribution Across the Test Flume at the Approach of Piers PB and PC at Sec. 53 for Run R16	92
5-16 Vertical Velocity Distribution Across the Test Flume at the Approach of Pier PA at Sec. 53 for Run R16	92
5-17 Vertical Velocity Distribution Across the Test Flume at the Approach of Pier PA at Sec. 37.6 for Run 30	93

LIST OF FIGURES (Cont.)

Figure	Page
5-18 Vertical Velocity Distribution Across the Test Flume at the Approach of Pier PB at Sec. 73 for Run R30	93
5-19 Effect of Clay Content on the Scour Ratio for Various Approach Velocities	94
5-20 Effect of Clay Content on the Scour Ratio for Various Froude Numbers	95
5-21 Effect of Clay Content on Scour Development for Run R32	97
5-22 Effect of Clay Content on Scour Development for Run R21	98
5-23 Comparison Between the Observed and Predicted Scour Ratios in Sandy-Clayey Soil	102
5-24 View of the Scour Hole for Pier A (58% Comp.) at the End of R27, Q=11 cfs	106
5-25 View of the Scour Hole for Pier C (80% Comp.) at the End of R27, Q=11 cfs	106
5-26 View of Scour Hole for Pier C (80% Comp.) at the End of R17, Q=9.96 cfs	107
5-27 View of the Scour Hole for Pier E (73% Comp.) at the End of R26, Q=10 cfs	107
5-28 Effect of Compaction on the Cross Section Geometry Along the Center Line of Pier PA for Runs R33 and R35 (58% Comp.)	109
5-29 Effect of Compaction on the Cross Section Geometry Along the Center Line of Pier PB for Runs R33 and R35 (73% Comp.)	110
5-30 Effect of Compaction on the Cross Section Geometry Along the Center Line of Pier PC for Runs R33 and R35 (87% Comp.)	111
5-31 Effect of Compaction on the Cross Section Geometry Along the Center Line of Piers PA, PB, and PC for Run R35	112

LIST OF FIGURES (Cont.)

Figure	Page
5-32 Effect of Compaction on the Scour Ratio	113
5-33 Effect of Compaction on (d_s/b) versus (V_s/b^3)	114
5-34 Effect of Compaction on the Scour Ratio for Various Approach Velocities	116
5-35 Effect of Compaction on the Scour Ratio for Various Froude Numbers	117
5-36 Effect of Compaction on Scour Development for Run R25	118
5-37 Effect of Compaction on Scour Development for Run R35	119
5-38 Comparison Between the Observed and Predicted Scour Ratios in Unsaturated Cohesive Soil	123
5-39 View of the Scour Hole for Pier A (35% IWC) at the End of R36, $Q=17.7$ cfs	126
5-40 View of the Scour Hole for Pier C (45% IWC) at the End of Run R36, $Q=17.7$ cfs	126
5-41 View of the Scour Hole for Pier A (40% IWC) at the End of R36, $Q=17.7$ cfs	127
5-42 View of the Scour Hole for Pier A (32% IWC) at the End of R41, $Q=1.95$ cfs	127
5-43 Effect of IWC of Saturated Clay on the Cross Section Geometry Along the Center Line of Pier PA for Runs R36, R37, and R38 (35% IWC)	129
5-44 Effect of IWC of Saturated Clay on the Cross Section Geometry Along the Center Line of Pier PB for Runs R36, R37, and R38 (40% IWC)	130
5-45 Effect of IWC of Saturated Clay on the Cross Section Geometry Along the Center Line of Pier PC for Runs R36, R37, and R38 (45% IWC)	131
5-46 Effect of IWC of Saturated Clay on the Cross Section Geometry Along the Center Line of Piers PA, PB, and PC for Run R36	132

LIST OF FIGURES (Cont.)

Figure	Page
5-47 Effect of IWC of Saturated Clay on the Cross Section Geometry Along the Center Line of Piers PA, PB, and PC for Run R34	133
5-48 Effect of IWC of Saturated Clay on (d_s/b) versus (V_s/b^3)	134
5-49 Effect of the IWC of Saturated Clay on the Scour Ratio	135
5-50 Effect of the IWC of Saturated Clay on the Scour Ratio for Various Approach Velocities	137
5-51 Effect of Froude Number on the Scour Ratio for Saturated Clay at 32% IWC	138
5-52 Effect of the IWC of Saturated Clay on Scour Development for Run R38	139
5-53 Effect of the IWC of Saturated Clay on Scour Development for Run R34	140
5-54 Comparison Between the Observed and Predicted Scour Ratios in Saturated Cohesive Soil	145
5-55 Soil Surface Conditions after 6 Days of Dry Period	148
5-56 Soil Surface Conditions after 22 Days of Dry Period	148
5-57 Soil Surface Conditions after 30 Days of Dry Period	149
5-58 Soil Surface Conditions after 120 Days of Dry Period	149
5-59 Comparison Between the Observed and Predicted Scour Ratios in Unsaturated and Saturated Cohesive Soil ...	153
5-60 Comparison Between the Developed Equations	154

EFFECTS OF GRADATION AND COHESION ON BRIDGE SCOUR

VOLUME IV

LIST OF TABLES

Table	Page
3-1 Coefficient K_1 for Pier Types	22
3-2 Coefficient K_2 for Flow Angle of Attack	22
4-1 The Flumes Used in the Study	54
4-2 Properties of Cohesive Soil Used in the Study	56
4-3 Conditions of Compactions	61
5-1 Summary of Experimental Conditions and Results for Set 1	75
5-2 Regression Output from SAS Program for Set 1	101
5-3 Summary of Experimental Conditions and Results for Set 2, Subset 2.A	104
5-4 Summary of Experimental Conditions and Results for Set 2, Subset 2.B	105
5-5 Regression Output from SAS Program for Set 2	122
5-6 Summary of Experimental Conditions and Results for Set 3	125
5-7 Regression Output from SAS Program for Set 3	144
5-8 Effect of Dry-Wet Cycle on Saturated Clay	147
5-9 Regression Output from SAS Program for the General Equation	152
5-10 Results of the Sensitivity Analysis for Set 1, Run R13-PB	158
5-11 Results of the Sensitivity Analysis for Set 1, Run R31-PC	158
5-12 Results of the Sensitivity Analysis for Set 2, Run R35-PA	159
5-13 Results of the Sensitivity Analysis for Set 2, Run R33-PC	159

LIST OF TABLES (Cont.)

Table	Page
5-14 Results of the Sensitivity Analysis for Set 3, Run R36-PA	160
5-15 Results of the Sensitivity Analysis for Set 3, Run R38-PC	160
5-16 Results of the Sensitivity Analysis for the General Equation, Run R36-PB	161
5-17 Error in the Predicted Scour Depth Due to 2% Error in the Measured Parameter for Set 1	162
5-18 Error in the Predicted Scour Depth Due to 2% Error in the Measured Parameter for Set 2	162
5-19 Error in the Predicted Scour Depth Due to 2% Error in the Measured Parameter for Set 3	163
5-20 Error in the Predicted Scour Depth Due to 2% Error in the Measured Parameter for the General Equation	163

LIST OF SYMBOLS

Symbol	Description
ρ	Water density, γ/g
μ	Dynamic viscosity
g	Gravitational acceleration
b	Pier width
L	Pier length
V	Approach velocity
Y	Approach flow depth
F_r	Froude number, $V/(gY)^{1/2}$
F_c	Critical Froude number
d_s	Scour depth
V_s	Scour volume
B	Upper diameter of the scour hole
Z	Side slope of the scour hole
α	Flow angle of attack
γ	Kinematic viscosity
τ	Shear stress
D_{50}	Sediment size at which 50% of material is finer
K	Reduction factor depending on the clay content in sandy soils
q	Discharge per unit width
t	Time
ϕ	Coefficient factor for pier type

LIST OF SYMBOLS (Cont.)

Symbol	Description
G	Gradation
ρ_s	Sediment density
W	Sediment fall velocity
S_1	Stream bed slope
H_s	Scour depth from water surface
S	Vane shear strength
CEC	Cation-exchange capacity
ESP	Exchangeable Sodium percentage
SAR	Sodium adsorption ratio
L.L	Liquid limit
P.L	Plastic limit
P.I	Plasticity index (P.I = L.L-P.L)
C	A parameter describing the amount of clay content in sandy soil (dry weight of clay/dry weight of mixture).
Comp.	Degree of compaction of cohesive soil, $\rho_d / (\rho_d)_{opt}$
ρ_d	Dry unit density
$(\rho_d)_{opt}$	Optimum dry density
ρ_w	Wet unit density
W_w	Wet weight of sample
W_s	Dry weight of sample
IWC	Initial water content, $(W_w - W_s) / W_s$
SROHV2	$S / (\rho V^2)$

CHAPTER I
INTRODUCTION AND OBJECTIVES

1-1 Introduction

The formation of local scour holes around bridge piers is almost an unavoidable problem in alluvial channel beds subjected to the erosive action of oncoming river flows. The design and construction of bridges spanning across alluvial channels requires the knowledge, or at least as accurate an estimate as possible of maximum scour depth which might occur during the anticipated life of the bridge near the piers.

A unifying theory for estimating scour depth at piers is still in an embryonic stage, mainly due to the complex nature of the scour problems. Major scouring usually occurs during floods which are unsteady flows, and may even have different flow directions from normal flows.

Scour is caused by three-dimensional boundary-layer separation at the pier, resulting in erosion of bed material by the local flow structure, which is characterized by a high level of turbulence and vorticity. The investigation of scour at bridge piers has been on-going for several decades.

Numerous experimental and analytical investigations of local pier scour were conducted in alluvial channels and series of prediction equations were developed by researchers

to estimate the maximum scour depth at bridge piers under different approach flow, sediment size and gradation, pier type and size conditions.

Unfortunately, these studies have been confined to non-cohesive soils. This is undoubtedly due to not only the abundance of streams with these types of beds but also because sand and gravel are easier to both characterize and model physically. The local scour in cohesive materials has been considered only by Abt and Ruff (1980) who measured scour downstream of a culvert outlet and Nicollet (1975) who observed scour around a pier in the laboratory.

The scour of cohesive materials is fundamentally different from that of non-cohesive materials. Firstly, it involves not only complex mechanical phenomena including shear stress and shear strength, but also the chemical and physical bonding of the individual particles. The scour process in this environmental is for instance, significantly affected by the amount and type of minerals clay, microscopic and macroscopic clay properties, water content, pH and temperature of the eroding water, and the thixotropy and consolidation of clay. Secondly, cohesive materials once eroded, remain in suspension such that clear water scour conditions always prevail. That is, very little incoming sediment is deposited in the scour hole and the scour depth increases as the flow intensity increases.

Thirdly, The slope of the scour hole in cohesive soils can be very steep and in some cases, approaching 90° (vertical).

The local scour at bridge pier continues for a sufficiently long time until the hydrodynamic forces in the scour hole are no longer able to remove particles from the hole. At this condition, the scour hole reaches an equilibrium condition, and the scour depth does not change appreciably unless the flow conditions change.

The main interest of this research is to experimentally study the magnitude and geometry of the equilibrium local scour at bridge pier placed in cohesive soil. It is believed that the systematic investigation of local pier scour in cohesive materials is an important step in the evaluation of bridge safety especially for bridges with limited service life. The research presented in this dissertation investigates the scour depth using literature review, theory, and through laboratory experiments.

1-2 Objectives

The objectives of this research is to formulate an empirical criteria for the prediction of pier scour in a mixture of cohesive and non-cohesive soils, and in cohesive soils. In order to develop an effective laboratory experimentation program, the study identified several

objectives. These objectives are as follows:

Primary Objectives

- 1) Develop a method for predicting the equilibrium bridge pier scour depth placed in a mixture of cohesive and non-cohesive soil and in cohesive soil.
- 2) Provide design criteria for the prediction of natural scour hole dimensions at bridge piers.
- 3) Provide the time rate of scour at bridge pier in cohesive soils, and in mixtures of sandy and clayey soils.

Secondary Objectives

- 4) Perform a survey of previous experimental, theoretical, and field studies related to cohesive soils through an extensive literature review.
- 5) Identify flow conditions and soil characteristics which have a great effect on the equilibrium pier scour.
- 6) Establish a data base of the equilibrium depth and volume of the scour holes.

1-3 Methodology

To accomplish the goals of this investigation, three physical models were conducted and fifty five scour test runs were carried out in the Hydraulics Laboratory of Colorado State University sponsored by the Department of Transportation, Federal Highway Administration.

The scope of work entailed three different sets of experiments. In the first set, thirty nine experimental data points were obtained to examine the effect of clay content in non-cohesive soils. The second set (thirty nine experimental data points) which contains two Subsets, 2.A and 2.B, investigates the compaction effect of unsaturated cohesive soils. The third set (thirty three experimental data points) concentrated on the effect of initial water content (IWC) of saturated cohesive soils on pier scour depth.

Chapter II is devoted to the classifications and mechanism of local scour at a bridge pier. In this chapter, analysis and influence of pier scour parameters are also presented.

Chapter III presents the previous investigations of pier scour in non-cohesive soils. A review of the background information on the nature and behavior of minerals clay related to soil erosion is also discussed followed by the previous experimental and theoretical studies on scour or erosion of cohesive soils.

Chapter IV describes the experimental facilities, the bed materials, and the experimental techniques used in this investigation.

Chapter V is devoted to the data reduction and analysis. Complete analysis and discussion of the results are included. The analysis entailed dimensional analysis, regression analysis of the experimental data, and sensitivity analysis for the developed equations. Charts and functional relationships between the equilibrium scour depth and key variables affecting pier scour are given in this chapter.

The last Chapter (VI) contains summary, conclusions, and makes recommendations for further research.

CHAPTER II

SCOUR AROUND BRIDGE PIERS

2-1 Introduction

Local scour can be defined as the removal of the bed materials through the action of flowing water in a specific location. The main cause of concern about the stability of bridges is the occurrence of scour at their supports. The scouring may occur at piers, at abutments or at river banks. This chapter presents the classification of scour as well as the mechanism of local scour at bridge piers. The many parameters which influence scour depth around piers are also illustrated at the end of this Chapter.

2-2 Definition and Classification of Scour

In a general sense, scour can be defined as the erosive action of running water in streams that excavates and carries away material from stream bed and banks. The total scour at a bridge site can be classified into the following three components:

- 1- General scour, which would occur whether a bridge is present or not.
- 2- Constriction scour, which is caused by constriction of the waterway by the bridge and its approaches.

- 3- Local scour due to the interference with flow by piers and abutments which accelerate the flow creating vortices that remove the material around them (Richardson et al.1975).

Laursen (1952) stated the general basic characteristics of local scour as:

- 1- The rate of scour will equal the difference between the capacity for transport out of the scoured area and the rate of supply of the material.
- 2- The rate of scour will decrease as the flow section is enlarged.
- 3- There will be a limiting extend to scour.
- 4- This limit will be approached asymptotically."

Furthermore, local scour in non-cohesive soils may be classified as live bed scour and clear water scour. For the case of clear water scour, the scour depth increases almost linearly with time and shear velocity until the limiting scour depth is approached (see Figure 2-1). Live bed scour (also known as scour with sediment transport) occurs when the bed material upstream of piers or abutments is moving, which is to say the shear stress in the undisturbed flow is higher than the threshold value. According to the response of passage of bed forms, live bed scour fluctuates about an equilibrium scour depth, at which, the rate of sediment removed from the

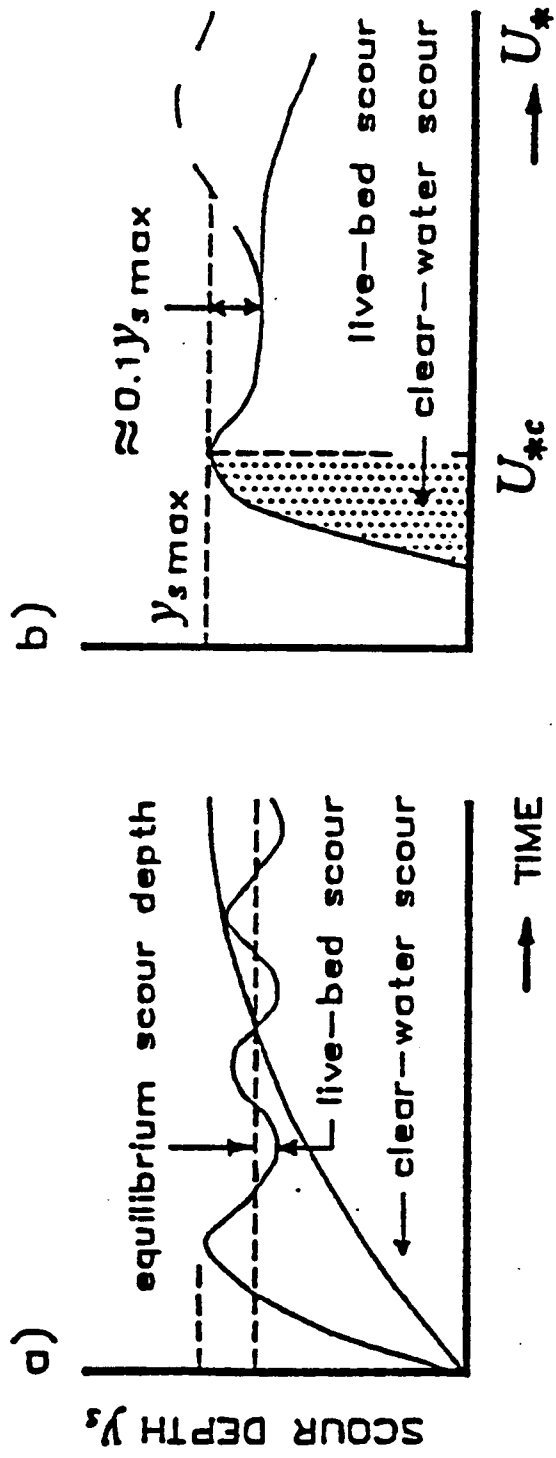


Figure 2-1. a) Scour Depth as a Function of Time
 b) Scour Depth as a Function of Shear Velocity

scour hole equals the rate of sediment supplied to the scour hole from upstream. In case of cohesive soils, clear water scour is always occurring since the cohesive materials remain in suspension once they are eroded (Andres 1983).

2-3 Mechanism of Local Scour at Bridge Piers

In summary, when an obstruction such as a blunt-nosed pier is placed in a flow field, locally the systems of vortices are developed around the pier. These systems of vortices are the basic mechanism of local scour, and this fact were reported by many investigators including Posey (1949), Laursen and Toch (1956), Shen (1967), and Melville (1975). The vortex systems can be summarized in the following features:

1) The Downflow

As the pier blocks a uniform flow, the approach flow goes to zero at the upstream face of the pier. Since the approach flow velocity decreases from the free surface downward to zero at the bed, the stagnation pressure, $\rho u^2/2$, will also decrease in the vertical plane of symmetry. This downward pressure gradient drives the downflow.

According to Melville (1975), the downflow acts as a vertical jet in eroding the bed. The equilibrium condition is attained when the scour depth is just sufficient so that the magnitude of the vertically downward flow can no longer dislodge the surface grains.

2) The Horseshoe Vortex System

The horseshoe vortex develops as a result of separation of flow at the upstream rim of the pier. Melville (1975) reported that the horseshoe is a consequence of scour, not the cause of it, and it is initially small and weak. With the formation of the scour hole, the vortex rapidly extends downstream past the sides of the pier for a few pier diameters, before losing its identity and becoming part of general turbulence. Also, the horseshoe vortex pushes the downflow velocity within the scour hole closer to the pier.

3) Wake Vortices

The stagnation pressure causes not only downflow but also sideways acceleration of the flow past the cylinder. The separation of the flow at the sides of the pier creates the wake vortices at the interfaces to the main stream. These vortices are translated downstream with the flow and interact with the horseshoe vortex at the bed causing it to oscillate laterally and vertically. The strength of the wake vortex system depends on pier shape and fluid velocity, and acts as little tornadoes lifting sediment from the bed.

4) The Bow Wave

The bow wave develops at the surface with rotation in the opposite sense to that in the horseshoe vortex. In case of shallow flows, the bow wave interferes with the approach flow and causes a reduction in the strength of the downflow.

Figure 2-2 shows the flow patterns at a cylindrical pier.

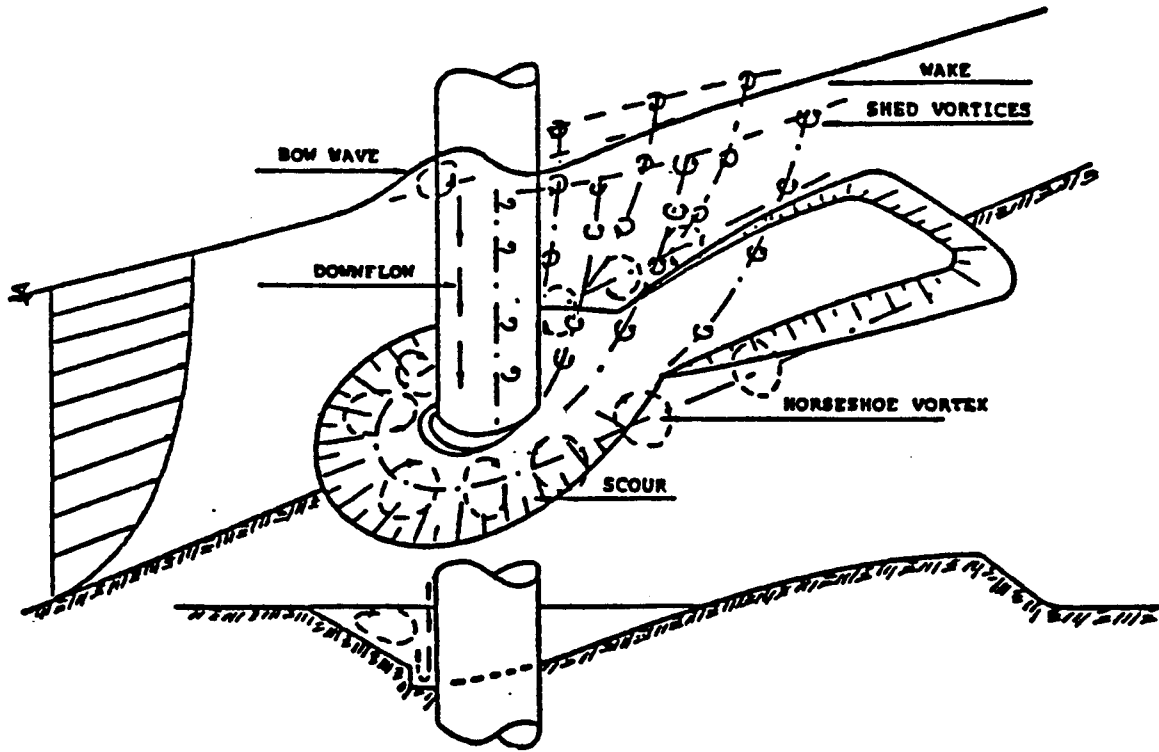


Figure 2-2. Diagrammatic Flow Pattern at Cylindrical Pier
(After Raudkivi 1986)

2-4 Parameters affecting Local Pier Scour

The treatments of the pier scour problem usually start with the statement that the scour depth depends on fluid parameters, flow conditions, stream bed material, pier parameters, and time. These parameters can be stated as:

1- Fluid variables

ρ = fluid density.

μ = dynamic viscosity.

g = gravity acceleration.

2- Flow variables

V_1 = approach flow velocity.

Y_1 = approach flow depth.

S_1 = stream bed slope.

3- Channel bed materials

a) Non cohesive materials

D = sediment diameter.

W = sediment fall velocity.

ρ_s =sediment density.

G = gradation.

b) Cohesive materials

the chemical and physical properties of mineral cohesive soils.

4) Pier parameters

b = pier width.

ϕ = pier shape.

L = pier length.

α = the flow angle of attack.

The dimension and shape of bridge pier has a strong influence on the equilibrium scour depth. As shown in Figure 2-3, the bridge piers can be classified as blunt-nosed and sharp-nosed piers. The blunt-nosed pier, such as square or round noses, has a strong horseshoe-vortex system and thus the maximum scour depth occurs at the pier nose. With the sharp-nosed pier, the horseshoe-vortex system is very weak and maximum scour depth occurs near the downstream end.

For the square-nosed pier, the maximum scour depth is about 20 percent larger than a sharp-nosed pier, and, 10 percent larger than a round-nosed pier. Piers shape and their coefficients are presented with the equation of CSU (1975).

Additionally, if the pier is not perfectly aligned with the flow, the effect of pier shape other than circular, may be entirely lost. Furthermore, the turbulence is significantly increased when the pier is not aligned with the flow. The scour depth is a function of the projected width of the pier, which directly proportional to the flow angle of attack.

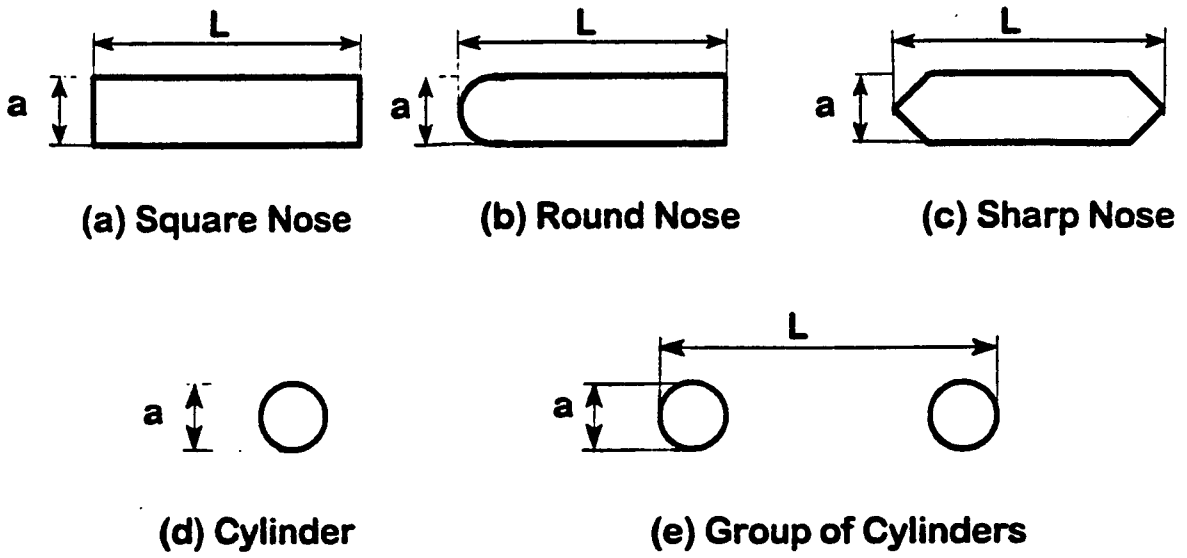


Figure 2-3. Common Pier Shapes

Figure 2-4 shows that as the angle of attack increases, the point of maximum scour depth moves along the exposed side of the pier towards the rear end of the pier. The effect of the angle of attack on pier scour depth has been tested by Laursen and Toch (1956). They developed an empirical relation for the ratio K_a of scour depth to an angle of attack to that at zero angle of attack. As shown in Figure 2-5, the angle of attack depends on the ratio of the length of the pier to its width (Laursen and Toch 1956).

With regards to the effect of the flow depth relative to the pier diameter, several references states that this parameter has a great effect on scour depth. But for flow depth greater than three pier diameters, this parameter can be neglected.

Because of the complexities and costs of measuring, analyzing, and evaluating all of the above mentioned variables, many researchers simplify and reduce the above variables to the following:

1. density ρ and dynamic viscosity μ of the fluid;
2. mean sediment diameter D_{50} , gradation, and density ρ_s ;
3. approach flow depth Y_1 and mean velocity V_1 ;
4. pier diameter b , shape ϕ , and orientation (angle α).

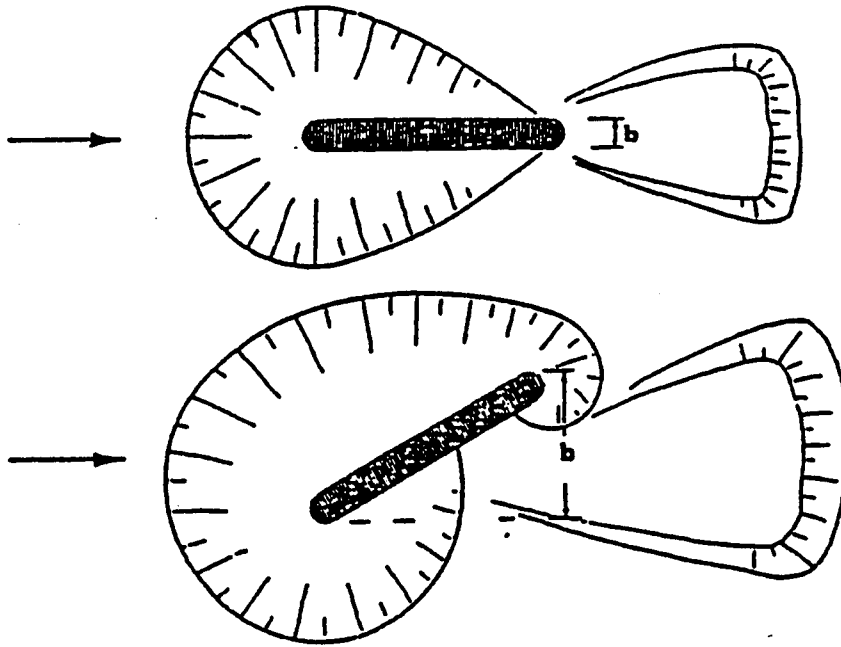


Figure 2-4. Scour Shapes Around Piers Aligned and Angled to the Flow Direction (After Laursen and Toch 1956)

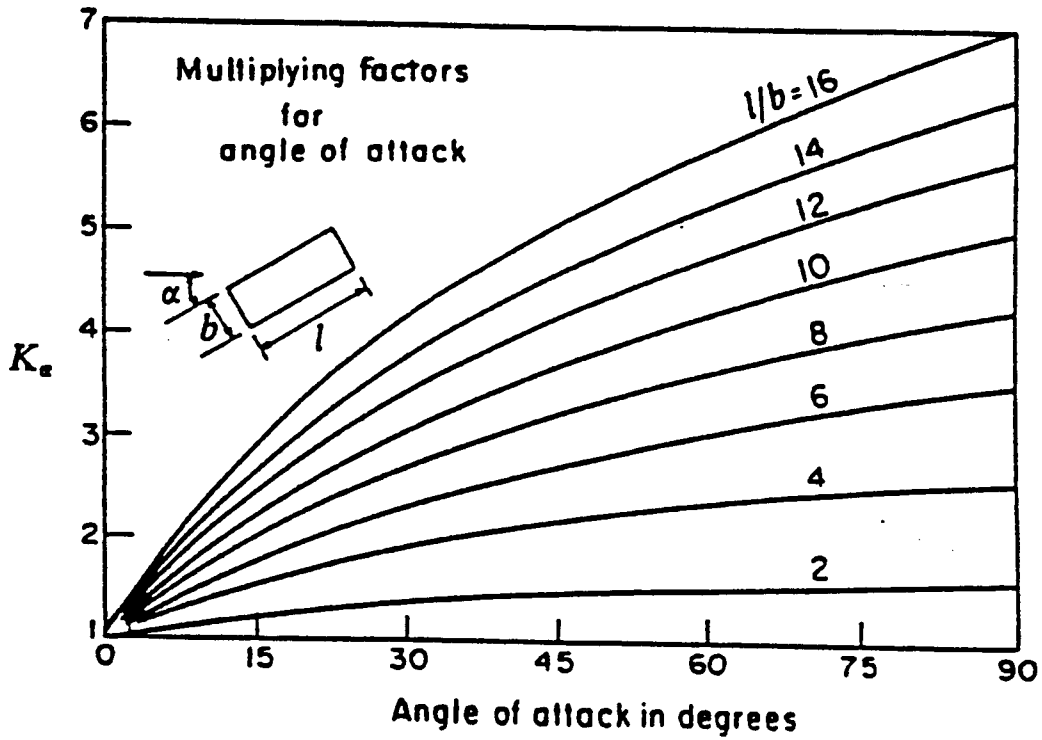


Figure 2-5. Alignment Factor K_a for Piers not Aligned with Flow (After Laursen and Toch 1956)

CHAPTER III

REVIEW OF LITERATURE

3-1 Introduction

Presently, information pertaining to pier scour in cohesive soils is not available. From the review of past and present literature, it is found that pier scour studies have been concentrated in the area of non-cohesive materials, although a considerable number of the bridges are located in sites of silty or clayey soils. Therefore, future efforts have to be devoted to investigate pier scour in cohesive soils.

In this chapter, Section 3-2 summarizes the important concepts and results of some investigations dealing with pier scour in non-cohesive soils. The next section, Section 3-3, presents the important concepts and properties of mineral clays which may have a great influence on the scour or erosion of cohesive soils. Finally, Section 3-4 at the end of this chapter presents some references, cites research on cohesive soils, and identifies specific trends, indicators or conclusions that may relate to local scour in cohesive soils.

3-2 Previous Studies of Pier Scour in Non-Cohesive Soils

The investigations of local scour at bridge piers have been on-going for several decades. For non-cohesive materials, several equations for predicting scour depth at bridge pier were proposed by different researchers. Starting from 1938, the following are examples of these formulas:

Inglis-Poona (1938)

$$\frac{Y_s}{b} = 1.70 \left(\frac{q^{2/3}}{b} \right)^{0.78} \quad (\text{ft-unit}) \quad (3-1)$$

in which

Y_s = depth of scour.

q = discharge per unit width.

b = width of pier.

The equation was derived for clear water scour and zero angle of attack, based on a series of experimental data of a rectangular round-nosed pier.

Blench (1965)

$$\frac{H_s}{y_r} = 1.8 \left(\frac{b}{y_r} \right)^{1/4} \quad (3-2)$$

in which

H_s = scour depth from water surface.

y_r = regime depth = $1.48 (q^2 / F_b)^{3/2}$.

$F_b = 1.9 (D)^{1/2}$.

D = mean diameter of bed sand, in mm.

q =average discharge intensity, in m^2/s ; and
 b =width of pier.

This equation is based on the Inglis-Poona experiments. A contradiction applies because the conditions of the Poona tests were those of clear water scour and regime theory. The regime theory implies a low to moderate rate of sediment movement.

Ahmed (1962)

$$H_s = K q^{2/3} \quad (3-3)$$

in which

H_s =scour depth from water surface.

q =discharge per unit width; and

K =a multiplying factor that varies from 1.3 to 2.3

according to the general situation of the bridge and other conditions.

The equation was derived based on field experience and model studies, and applicable only for live bed scour. It is developed for bridges in the case of deep sand fills.

CSU's equation (1975).

$$\frac{Y_s}{Y_1} = 2.0 K_1 K_2 \left(\frac{a}{Y_1} \right)^{0.65} (Fr_a)^{0.43} \quad (3-4)$$

in which

Y_s = scour depth.

Y_1 = flow depth just upstream of the pier.

K_1 = coefficient for pier shape from Table 3-1.

K_2 = coefficient for angle of attack of flow from Table 3-2.

a = pier width.

Fr_a = Froude number = $V_1 / (gY_1)^{1/2}$; and

V_1 = approach average velocity.

This equation was derived from laboratory data, and it is recommended for both live bed and clear water scour. For live bed scour, the predicted equilibrium scour depth will be 30 % greater if dunes are present. In case of clear water scour, plane bed or with antidunes, the equation predicts the maximum scour depth.

Table 3-1, Coefficient K_1 for pier types

Type of piers	K_1
Square nose	1.1
Round nose	1.0
Circular Cylinder	1.0
Sharp nose	0.9
Group of Cylinders	1.0

Table 3-2, Coefficient K_2 for flow angle of attack.

Angle	$L/a = 4$	$L/a = 8$	$L/a = 12$
0	1.0	1.0	1.0
15	1.5	2.0	2.5
30	2.0	2.5	3.5
45	2.3	3.3	4.3
90	2.5	3.9	5.0

Angle = skew angle of flow.

L = length of the pier.

Ettema equation (1980)

$$\left(\frac{Y_s}{Y_1}\right)_{\max} = \left[\frac{2.3 b}{Y_1}\right] \quad (3-5)$$

in which

Y_s = maximum equilibrium local clear water scour depth in uniform material.

Y_1 = flow depth.

b = pier diameter.

Davoren equation (1985)

$$Y_s = 0.395 Y_1 \quad (3-6)$$

where

Y_s = scour depth from mean bed elevation(m).

Y_1 = approach flow depth(m).

Froehlich (1987)

$$\frac{Y_s}{b} = 0.32 \phi \left(\frac{b}{b}\right)^{0.62} \left(\frac{Y_1}{b}\right)^{0.46} F_r^{0.2} \left(\frac{b}{D_{50}}\right)^{0.08} \quad (3-7)$$

in which

ϕ = coefficient factor for pier type.

= 1.3 for square-nosed pier.

= 1.0 for a round-nosed pier.

= 0.7 for a sharp-nosed pier.

b' = pier width projected normal to the approach flow.

$$= b \cos \alpha + l \sin \alpha .$$

α = flow angle of attack.

l = pier length.

F_r = Froude number = $V_1 / (gY_1)^{1/2}$.

D_{50} = sediment mean diameter.

The equation was derived based on field measurements and multiple-linear-regression analysis of previous data. Froehlich's equation leads to a good agreement with some field data when a factor of safety, 1, was added in such a way that:

$$\frac{Y_s}{b}(\text{design}) = \frac{Y_s}{b}(\text{calculated}) + 1 \quad (3-8)$$

Melville and Sutherland Equation (1988)

$$\frac{Y_s}{Y_1} = K_1 K_y K_d K_o K_s K_a \frac{b}{Y_1} \quad (3-9)$$

where

Y_s = scour depth;

Y_1 = flow depth;

b = pier diameter normal to the flow;

K_1 = flow intensity factor;

K_y = flow depth factor;

K_d = sediment size factor;

K_o = sediment gradation factor;

K_s = pier shape factor; and

$K\alpha$ = pier alignment factor.

The K values can be obtained using the graphs proposed by the authors (1988).

Abdou (1993) performed large-scale experiments to investigate the effect of sediment gradation coefficient and the effect of increasing the size of coarse material fraction that exists in a sediment mixture on local pier scour. The study included six different sediment mixtures with a constant mean diameter. Abdou derived the following equations based on the dimensional and regression analysis:

For $\sigma_g = 1.38$

$$\frac{Y_s}{Y_1} = 144.5 (F_r)^{3.47} \quad (3-10)$$

For $\sigma_g = 2.43$

$$\frac{Y_s}{Y_1} = 38.0 (F_r)^{3.03} \quad (3-11)$$

For $\sigma_g = 3.4$

$$\frac{Y_s}{Y_1} = 23.0 (F_r)^{3.2} \quad (3-12)$$

$$\left[\frac{Y_s}{Y_1} \right] = 148.0 (F_r)^{2.93} \left(\frac{d_{90}}{d_{50}} \right)^{-1.48} \quad (3-13)$$

in which

Y_s = local scour depth.

Y_1 = mean flow depth.

F_r = Froude number.

d_{90} = sediment size (diameter) for which 90% of the sediment material by weight is finer.

d_{50} = sediment size (diameter) for which 50% of the sediment material by weight is finer.

σ_g = Geometric standard deviation of sediment mixture,

$$\sigma_g = (d_{84}/d_{16})^{0.5}.$$

Noshi (1993) studied the relation between the maximum scour depth of a hydrograph and the steady long-duration flow. He used three different time steps which were 2.5, 5, and 7.5 minutes. The resulting developed equations were:

$$\left(\frac{Y_s}{Y_1}\right)_{5min.Hyd.} = 0.4 \left[\frac{Y_s}{Y_1}\right]^{2.44} \sigma_g^{1.58} \quad (3-14)$$

$$\left(\frac{Y_s}{Y_1}\right)_{2.5min.Hyd.} = 0.0459 + 0.79 \left[\frac{Y_s}{Y_1}\right]_{5min.Hyd.} \quad (3-15)$$

$$\left(\frac{Y_s}{Y_1}\right)_{7.5min.Hyd.} = 1.67 \left[\frac{Y_s}{Y_1}\right]_{5min.Hyd.}^{1.41} \quad (3-16)$$

$$\left[\frac{Y_s}{Y_1}\right] = K_g [6.18 F_r - 5.22 F_r^2 - 0.716] \quad (3-17)$$

in which

Y_s = maximum clear water scour depth in uniform or/ and graded bed material.

Y_1 = mean flow depth.

F_r = Froude number.

$$K_g = 2.82 \sigma_g^{(-1.33)} F_r^{0.849}$$

σ_g = geometric standard deviation of the particle size distribution.

The equations were developed based on laboratory data and regression analysis.

3-3 Review of the Properties of Mineral Clays

3-3-1 Clay Mineralogy

Knowledge of the nature and behavior of mineral clays is very essential to understand the fundamental factors affecting the erosion resistance or erosion rate of cohesive soil under a given flow condition. Clay exhibits greater specific surface area than sand and silt, therefore it is the most active in physicochemical processes.

Mineral clay particles are flat shaped, and carry negative electric charges on their surface. These charges are unbalanced because of the incomplete charge neutralization of terminal atoms on lattice edges. Hence, they are balanced externally by exchangeable ions (mostly cations). This cations-exchange phenomenon is very important in soil physics and soil chemistry.

On the basis of the force existing between water and soil, the water in a clay fall into three categories: adsorbed water, double layer water, and free water. The adsorbed water

is strongly held by the soil; the double layer water is all the water attracted to the soil; and free water is the water which is not attracted to the soil at all. Hence, the interaction between water and the clay particles is the primary mechanism governing the erosion of cohesive soils.

3-3-2 Soil Structure and Fabric

The term "fabric" refers only to the geometric arrangement of the particles, particle groups, and pore spaces in a soil. While the term "structure" refers to the combined effect of fabric, composition, and interparticle forces. The soil structure strongly affects the engineering properties and behavior of the soil particles.

3-3-3 Structure and Composition of Clay Minerals

Basically, clay minerals are formed by the stacking of silica, brucite sheets, and gibbsite (aluminum octahedral sheet). The most prevalent clay minerals are the layered aluminosilicates which are formed of crystals. These crystals are composed of a tetrahedron of four oxygen atoms surrounding a central cation, usually Si^{4+} , and an octahedron of six oxygen atoms or hydroxyl surrounding a larger cation of lesser valency, usually Al^{3+} or Mg^{2+} .

The tetrahedra are joined together at their basal corners by means of shared oxygen atoms. Similarly, the octahedral are joined along their edges to form a triangular array. The

layered aluminosilicate mineral clays are classified according to the ratio of tetrahedral layers to octahedral layers, into two principal types; 1:1, and 2:1 minerals.

In 1:1 minerals, such as Kaolinite, one tetrahedral sheet is attached to one octahedral sheet.

In 2:1 minerals, like Montmorillonite, two tetrahedral sheets, one on each side are attached to one octahedral sheet. The bonding between these sheets is electrical, very strong and may be sufficiently weak to response to changes in environmental conditions. According to Marshall (1964), the main types of electrical bonds are:

1) Primary valence bonds

These bonds are the strongest bonds to hold atoms together in the basic mineral units. They can be classified into three categories; Ionic bonds, Covalent bonds, and Heter polar bonds. The Ionic bonds are the result of the exchange of electrons by the linked atoms as in mica. The larger the layer charge, the stronger the bond. The Covalent bonds are the cause of sharing of electrons by the linked atoms, and the Heter polar bonds result from an unequal sharing of electrons.

2) Hydrogen bonds

These bonds exist in the layer of OH groups, as in Kaolinite. The hydrogen bonds occur when an atom of hydrogen is rather strongly attracted by two other atoms as in water molecules. These bonds are strong and prevent the layer to separate in the presence of water.

3) Secondary forces (Van der Waals bonds)

These bonds arise from electrical moments existing within the units. The secondary forces are an order of magnitude weaker than the primary and the hydrogen bonds. These bonds contribute to clay strength and cause soils to hold water.

In general, the layers bonded by Van der Waals are greatly influenced by applied stress and can be changed in the soil-water system.

3-3-4 Ions (Cations, anions) Exchange

Clay minerals have the property of adsorbing certain anions, cations, and remaining in an exchangeable state. These anions and cations are replaced by other anions or cations of a water solution. The common exchangeable cations are Calcium (Ca^{2+}), Magnesium (Mg^{2+}), Potassium (K^+), and Sodium (Na^+). While the common exchangeable anions are sulfate (SO_4^{2-}), chloride (Cl^-), and phosphate (PO_3^{4-}).

In Montmorillonite minerals, the cation-exchange reaction is slower, while in Kaolinite minerals, the cation exchange reactions are more rapidly. In general, the cation-exchange capacity (CEC) is the result of the broken bond around the edge of the silica-alumina unit. The amount of exchangeable sodium (Na) relative to the other exchangeable cations in the soil has an important influence on the structural status of soils and is described in terms of the exchangeable Sodium

percentage (ESP) as:

$$ESP = \frac{\text{exchangeableNa}^+}{\text{Cation exchange Capacity}} \times 100 \quad (3-18)$$

Soils with ESP greater than about 2%, may behave as dispersive clays in water (Mitchell, 1992). The most common method to estimate ESP is Gapon's equation. The practical form of the Gapon's equation is:

$$\left[\frac{Na^+}{Ca^{2+}+Mg^{2+}} \right]_s = K \left[\frac{Na^+}{\sqrt{(Ca^{2+}+Mg^{2+})/2}} \right]_e \quad (3-19)$$

The subscript "s" refers to the adsorbed layer, the subscript "e" refers to the equilibrium solution, and "K" is a selected constant. The constant K has a value of 0.017 (meq/l)^{-1/2} for a wide range of soils. The right hand side of the last equation is defined as the sodium adsorption ratio (SAR) in milliequivalent per liter, where

$$\left[\frac{Na^+}{\sqrt{(Ca^{2+}+Mg^{2+})/2}} \right]_e = SAR \quad (\text{meq/l})^{1/2} \quad (3-20)$$

The SAR can be determined easily by chemical analysis of the pore water than the ESP.

Many studies (e.g., Sherard et al., 1972; Arulanandan et al., 1973) have indicated that the ESP and SAR are uniquely related for most soils, and are a good indication of the

resistance of clay soil structure to breakdown and particle dispersion.

3-3-5 Flocculation and Dispersion of Mineral Clays

When two mineral clay particles come into contact, forces both of repulsion and attraction can come into play. If the repulsion forces are dominant, the particles separate and the clay is said to be dispersed, which is an important factor in erosion of cohesive soils. On the other hand, when the attractive forces prevail, the clay becomes flocculated and the greater resistance to erosion might be.

The main types of flocculation are salt and nonsalt flocculation. The salt flocculation is the result of high salt concentration in the bulk solution, while nonsalt flocculation is due to positive charged clay attracted to negatively charged clay surface.

For Montmorillonite clay, the flocculation is mostly salt, while in Kaolinite clay, the nonsalt flocculation is predominant. The repulsive force derives from the like charges of the ionic swarms surrounding each particle, while the attractive forces result when two clay platelet, one positive charge and the other negative charge, are brought together.

3-3-6 Effect of Dielectric Dispersion ($\Delta\epsilon$)

In order to examine the effect of type and amount of clay fraction on erosion process, a method proposed by Arulanandan

et al. (1970) was adopted. This method is based on applying an alternating electric field to the soil-water system. A response is produced which can be measured in terms of a resistance (R) and a capacitance (C). The value of " C/C_0 " is defined as the dielectric constant, which reflects the ability of the clay to store electrical energy. The parameter C_0 refers to the capacitance of a condenser with only vacuum between the electrodes.

The dielectric constant of soil-water system varies for each frequency. As a result of increasing the frequency, the accumulation charges on clay particle decreases the ability of the system to store electrical potential energy. This change of dielectric constant with frequency is defined as dielectric dispersion ($\Delta\epsilon$), which mainly depend upon the type and amount of mineral clays.

Alizadeh (1974) showed that, at low values of SAR, the dielectric dispersion increased as the clay content increased, which in turn increased the critical shear stress.

3-3-7 Effect of Compaction on Cohesive Soils

The fundamentals of compaction of cohesive soil was established by Proctor (1930). He concluded that the amount of shear strain obtained after compaction of soils, is mainly based on the water content, compactive effort, strength of the pre-existing fabric, and the method of compaction.

As shown in Figure 3-1, at the same compactive effort, the soil fabric becomes more oriented with increasing water content. Hence, at dry of optimum, the soils are always flocculated, whereas at wet of optimum, the fabric becomes more oriented or dispersed. If the compactive effort is increased, the soil tends to become more oriented, even in case of dry of optimum water content.

In general, the effects of compaction include breakdown of flocculated aggregates, the destruction of shear planes, the elimination of larger pores, and the production of a more homogeneous arrangement or more dispersed fabric soil.

For the compacted clays, the strength and swelling are greater for those compacted dry of optimum, while shrinkage of the compacted clays is greater for those compacted wet of optimum. The main methods of compactions are impact (hammer), kneading (temper), and static loading (piston).

3-3-8 Plasticity of Mineral Clays

Plasticity may be defined as the property of mineral clay which permits the material to be shaped by the application of a force without rupturing and to retain the shape produced after the stress is removed. In general, clay materials develop plasticity when they are mixed with relatively small amount of water.

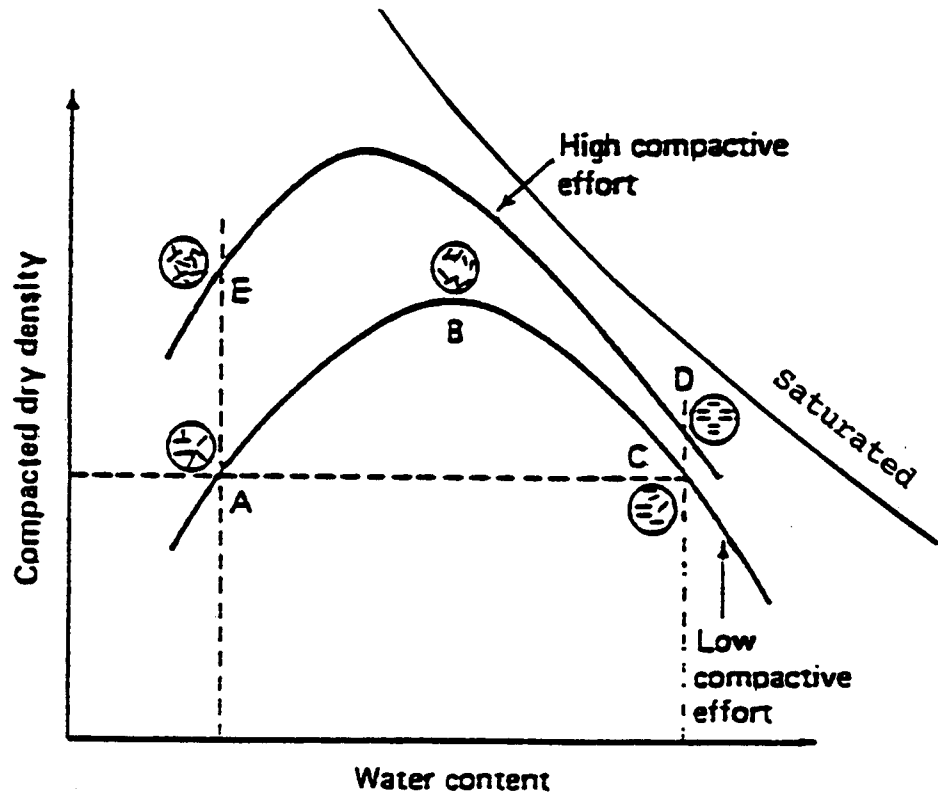


Figure 3-1. Effect of Compaction on Soil Structure
(After Lambe 1958)

The range of moisture contents required for ground clay to form a coherent mass (plasticity is demonstrated) is called Atterberg limits. The lower value of water content at which a thread of soil just begins to crack and crumble when rolled to a diameter of 1/8 inch is defined as plastic limit (P.L). The higher value of moisture content at which a 2-mm-wide groove in a soil pat will close for a distance of 0.5 inch is called liquid limit (L.L). The difference between the lower and the higher values is defined as the plasticity index (P.I).

3-4 Previous Studies of Scour or Erosion in Cohesive Soils

The phenomenon of scour or erosion of cohesive soils has been studied by many investigators. Some of the early efforts in attempting to understand the scour mechanism were made by Middleton in the early 1930's. He studied the effect of physicochemical properties on erodiability of cohesive soil. Based upon his observation, Middleton concluded that the clays with high amount of calcium and magnesium are more resistant to erosion than clays with high amount of sodium.

Lutz (1934) studied the effect of plasticity on erosion of clay. He stated that a soil with high plasticity, which contains a higher percentage of clay, is nonerosive and its suspension rapidly flocculated. While the lower plasticity soil is more erodible.

Another investigation was conducted by Dunn (1950) to determine the critical shear stress required to initiate the movement of soil particles. Dunn performed many experiments by applying a vertical jet impinging upon submerged soil samples. He concluded that the critical shear stress increases as the clay content increases in the soil. Furthermore, he stated that the grain size distribution of cohesive soil and plasticity index in the range of 5 to 16, are good parameters for predicting soil resistance to erosion. Dunn derived the following equations from his experiments using statistical analysis techniques:

$$\tau_c = 0.2 + \frac{S_v + 180}{1000} \times \tan (30 + 1.73 PI) \quad (3-21)$$

$$\tau_c = 0.02 + \frac{S_v + 180}{1000} \times \tan (0.06U_f) \quad (3-22)$$

where S_v is the vane shear strength, U_f is the percentage of clay particles less than 0.06 mm by weight, and P.I is the plasticity index.

Smerdon and Beasley (1959) performed several tests, in which cohesive soil samples were placed in the bottom of a flume and water was allowed to flow over the sample until bed failure was noted. They concluded that the tractive force based on the properties of soil such as plasticity index, mean particle size, and percentage of clay.

They derived the following equations:

$$\tau = \gamma D S \quad (3-23)$$

$$\tau_c = 0.0017 \times (PI)^{0.85} \quad (3-24)$$

where τ is the tractive force (lb/ft²), D is the mean depth of flow, S is the channel gradient, τ_c is the critical tractive force, and P.I is the plasticity index of soil.

Abdel-Rahman (1960) attempted to relate the soil characteristics to hydraulic shear stress by running water in a flume over a cohesive bed. The experiments were carried out using sandy-clayey mixture with a maximum sand diameter of 2.0 mm. He developed the following equation based on the dimensional analysis and the experimental results:

$$\frac{(\gamma_w R_m J_e)^2}{S} = P + b \gamma_w T_m \quad (3-25)$$

where $(\gamma_w R_m J_e)$ is the tractive stress of water, S is the final vane shear-strength of the bed soil (t/m²), T_m is the mean erosion depth, $P=0.2 \times 10^{-8} \gamma_w$ (t/m²), and $b=4.57 \times 10^{-6}$. The applicable range of this equation is stated to be for $\gamma_w R_m J_e$ between 0.746×10^{-4} and 4.4×10^{-4} t/m².

According to the developed equation, the critical tractive stress, at which T_m equal zero, can be expressed as:

$$\tau_c = \sqrt{S \times 0.2 \times 10^{-8} \gamma_w} \quad t/m^2 \quad (3-26)$$

Furthermore, he concluded from his experiments on purely cohesive beds, that the stability of such beds depends on the end flow conditions at which a certain mean bed roughness height is attained (Q_m). He derived the following equation by using the dimensional analysis technique:

$$\frac{\rho U_*^2}{S} = 0.83 \times 10^{-4} + 2.9 \times 10^{-6} \left(\frac{Q_m^2 \gamma J_s}{\mu U_*} \right) \quad (3-27)$$

where

Q_m = Absolute mean roughness of the bed.

U_* = Shear velocity ($g R J_s$)^{1/2} m/s

ρ = Density of water.

μ = Absolute viscosity of water.

J_s = Slope of the bed.

S = Final vane shear-strength of the bed material.

F_* = Friction Froude's number ($U_*^2/g Q_m$).

A study was carried out by Lyle and Smerdon (1965) to examine the relation between the soil properties and the critical tractive shear force.

They conducted a group of tests on sandy loams, silty clays, and clay materials in a hydraulic flume. They correlated the plasticity index (P.I), dispersion ratio, mean particle size, and clay percentage, to the critical tractive force.

The culmination of their study was the formation of the following equations:

$$T = 0.00771 + 0.0233(1.2 - e) + (0.00079 + 0.00035(e - 1.2))P.I \quad (3-28)$$

$$T = 0.0322 + 0.0086(1.2 - e)10^{-nDr} \quad (3-29)$$

$$T = 0.0141 + 0.00075(1.2 - e)10^{0.0062(pc)} \quad (3-30)$$

$$n = 0.00452 (10)^{0.32(e - 1.2)} \quad (3-31)$$

where T is the critical tractive shear force, e is the void ratio, P.I is the plasticity index, pc is the percentage of clay, and Dr is the dispersion ratio.

Moreover, they found that some other parameter such as percent organic matter, vane shear strength, cation exchange capacity (CEC), and calcium-sodium ratio, have a great influence on the erodibility of cohesive materials.

Partheniades and Paaswell (1970) stated that the vane shear strength and plasticity index parameters do not accurately describe the state of the soil at the surface.

Furthermore, the determination of the shear stress required to initiate erosion is still lacking because of the following parameters:

- 1) Lack of a technique to define the actual water stress at the soil surface.
- 2) The difficulties in predicting the soil properties that control erosion process.

Extending the identification of the soil properties that influence the erosion process, Paaswell (1973) reported that the erosion of soil particles due to motion of water is the result of external and internal forces. The external forces are due to physicochemical osmotic pressure developed due to difference in pore and eroding fluid. The internal forces depend upon many factors, such as type and amount of clay, pore fluid composition, temperature, soil structure, and physicochemical behavior of clays.

Christensen and Das (1973) conducted several experiments on group of samples tube with cohesive material. These samples were placed in horizontal flume and allowed water to flow. They concluded that :

- 1) The rate of erosion is a function of the shear stress, temperature, density, soil moisture content, clay type, percentage of clay, and cation concentration.
- 2) When the critical shear stress was significantly exceeded, large clusters of soils were removed from the tube.

Liou et al (1973) concentrated their efforts in studying the effect of physio-chemical parameters in the erosion of cohesive soils. They concluded that the sodium adsorption ratio(SAR) is a good parameter for prediction the erosion of cohesive soil. As the SAR decreases, the shear strength of the

soil will increase which in turn decreases the erosion rate. Furthermore, they concluded that calcium ions increase the critical shear stress of the soil than the sodium ions. This fact was also confirmed by Arulanandan.

Investigation of the basic properties of cohesive soil that may influence the critical shear stress was carried out by Alizadeh (1974). He used three kinds of artificial cohesive soils, Na-Montmorillonite (Volclay bentonite), Grundit Illite with uniform graded material, and Hydrite-R Kaolinite. He performed a group of experiments by using a modified rotating cylinder apparatus. Alizadeh stated that:

- 1) At low values of SAR (1-5) and high pore fluid concentration, the critical shear stress increases with increasing dielectric dispersion ($\Delta\epsilon$). Hence, Montmorillonite clay has a higher critical shear stress than both Illitic and Kaolinitic soils.
- 2) At low value of SAR, the critical shear stress increases as clay content increases up to 20%. If the clay content is more than 20%, the critical shear stress is independent of clay percentage.
- 3) At higher values of SAR (50-60), the kaolinite clay has higher critical shear stress than Montmorillonite clay.
- 4) At higher value of SAR, the critical shear stress is inversely proportional to the clay content in a mixture of sandy-clayey soil.

The culmination of this study was the formation of the following equations:

$$\tau_c = (\log C - C_1)(C_2 - \eta \log SAR) \quad (3-32)$$

$$\tau_c = \log C_p \left[1 - \frac{\log SAR}{1.74} \right] [0.2 \Delta\epsilon^{-14}] \quad (3-33)$$

where C is the total concentration of pore fluid, (C_1, C_2, η) are constants based on types of clay, $\Delta\epsilon^{-1}$ is the dielectric dispersion which based on the type and amount of mineral clays, and C_p is the percentage of clay. The constant η is computed as:

$$\eta = 10 - 0.07 \nabla\epsilon \quad \text{for } SAR < 20$$

$$\eta = 2.6 + 0.09 \nabla\epsilon \quad \text{for } SAR > 20$$

Moreover, Alizadeh investigated the effect of soil gradation on the rate of erosion. He used three soil mixtures with different grain size distribution. Two of the mixture contained uniform particle size with average grain sizes of 0.5 mm and 0.025 mm, the third mixture was considered as a well graded soil with D_{50} grain size of 0.085 mm. From the results, he stated that the rate of erosion of the well graded soil is higher than the uniform soil. The reason is that the finer particles in well graded soil are fitted between the coarser particles, and as a result, the exposed surface area subjected to erosion is larger than uniform soil mixture.

Arulanandan (1975) examined the effect of the soil pore fluid and the eroding fluid on surface erosion process. He used a rotating cylinder similar to that used by Alizadeh. Some of his resulting conclusion are:

- 1) The relation between the dielectric dispersion ($\Delta\epsilon$) and Cation Exchange Capacity (CEC) of clay is a linear relationship.
- 2) Calcium and Magnesium clays are bonded more firmly than Sodium clays.
- 3) At high SAR, repulsive forces between the particles are predominate, and thus increase the erodibility of such clay. The reverse is true for clay has a low SAR value.
- 4) The erodibility of a cohesive soil decreases as the salt concentration of the eroding fluid is equal to or higher than the salt concentration of the pore fluid. If the salt concentration of the eroding fluid is lower than the soil pore fluid, eroding fluid will move into the surface of clay particles causing swelling by osmosis process, and thus reduce the interparticle bonding forces.

Kuti and Yan (1976) continued the identification of the principle physical factor of the soil that affecting the critical shear stress. They conducted many experiments on the scour at the toe of a spillway using cohesive soils. The soil used comprised of from 20 to 80 percent clay. They concentrated on the time and scour parameters as a function of

the percent of clay mineral in the soil. Their conclusions can be summarized as follows:

- 1) Soil with high percentage of clay (by weight), takes a longer time to reach equilibrium scour than soil with low percentage of clay at the same void ratio.
- 2) The void ratio factor only affects time at which scouring reaches an equilibrium state.
- 3) At the same void ratio, increasing the amount of clay will decrease the scoured volume.

Abt (1980) examined the localized scour at culvert outlets in hopes of establishing a design criterion for quantifying scour hole in cohesive bed. He performed twelve experiments on soil comprised primarily of 58% sand and 27% clay yielding a plasticity index of 15.

He derived many equations based on the principle of dimensional analysis using Buckingham PI theory. Some of the resulting equations are:

$$\tau_c = 0.001 (S_{v_{sat}} + 180) \tan (30 + 1.73 PI) \quad (3-34)$$

$$S_{v_{sat}} = 10 \left[\frac{25 - W_c}{14.7} - \log S_v \right] \quad (3-35)$$

$$\frac{d_s}{D} = 3.46 \left(\frac{\tau_c}{\rho V^2} \right)^{0.34} \quad (3-36)$$

$$\frac{d_s}{D} = 2.18 \left(\frac{Q}{g^{0.5} D^{5/2}} \right)^{0.57} \quad (3-37)$$

$$\frac{V_s}{D^3} = 110.32 \left(\frac{Q}{g^{0.5} D^{5/2}} \right)^{1.42} \quad (3-38)$$

where D is the culvert diameter, S_v and $S_{v\text{sat}}$ are the initial and saturated shear strength, P.I is the plasticity index, W_c is the soil water content, d_s is the scour depth, V_s is the scour volume, V is the velocity of jet at culvert outlet, τ_c is the critical shear stress, and ρ is the fluid density.

Shaikh (1988) studied the erosion rate of dispersive and non dispersive clays. He conducted experiments on unsaturated compacted sodium and calcium Montmorillonite clays. Clays were pressed into sample containers and subjected to water in the flume. The results showed that the erosion rate of Ca-Montmorillonite was about two times the erosion rate of Na-Montmorillonite.

Shaikh treated the Ca-Montmorillonite with Calcium chloride and Sodium carbonate to study the effect of clay's pore-water chemistry on erosion rate, which can be controlled by the Sodium adsorption ration (SAR) and total dissolved salt (TDS= Ca+Mg+Na+k).

The results showed that when calcium Montmorillonite was treated with 0.88% by dry weight sodium carbonate, the erosion rate was reduced to the same order as sodium Montmorillonite.

Briefly, Shaikh derived the following equations based on analysis of experimental data for erosion rate:

$$E = 4.41 (SAR)^{-1.34} \tau \quad (3-39)$$

$$E = 4.41 (\%clay)^{-0.91} \tau \quad (3-40)$$

$$E = 0.157 (S_t)^{-1.338} \tau \quad (3-41)$$

where E is the erosion rate, S_t is Torvane shear strength, and τ is the tractive stress.

Another research conducted by Kamphuis (1989) investigated the abrasive effect of the granular material in the eroding fluid on the cohesive bed erosion. He conducted the experiments by adding sand to the water, at a concentration of about 0.1% by volume.

Kamphuis concluded that the initiation of erosion is determined by the initial movement of the granular material which was found over the cohesive soil. Therefore, Kamphuis concluded that the designer should take into account the sediment transport characteristics of the sand and gravel existing in the eroding fluid.

CHAPTER IV
EXPERIMENTAL FACILITIES AND TEST PROCEDURES

4-1 Introduction

An experimental program was conducted in the hydraulics laboratory at the Engineering Research Center of Colorado State University. Three Sets of flume experiments were performed to specify the effect of cohesion on pier scour.

Set 1 of test runs examines the effect of clay content in non-cohesive soil (sand). Set 2 of experiments investigates the effect of compaction of unsaturated cohesive soil. While Set 3 of test runs specifies the effect of initial water content (IWC) of saturated cohesive soil on pier scour.

A detailed description of the experimental facilities, soil selection and samples preparation, and testing procedures follows in the subsequent sections.

4-2 Experimental Facilities

4-2-1 Flumes

The experimental investigation was completed using three different flumes located at the Engineering Research Center of Colorado State University. The first of these flumes is a 17 feet wide by 100 feet long flume and will be referred to as the Seventeen-foot flume. The second flume is 8 feet wide by

200 feet long flume and will be referred to as the Eight-foot flume. The third flume is a 4 feet wide by 29 feet long flume and will be referred to as the Four-foot flume.

1) The Seventeen-foot flume

The flume is a recirculating end sill flume which is 17 ft wide, 100 ft long, and 3 ft deep with a constant slope of 0.2%. Water into the flume is supplied from a sump tank by a pump and a 18-inch pipeline. A headbox consisting of a mesh box of gravel which is placed at the upstream flume entrance, is to reduce the turbulent eddies induced at the flume entrance. The pump supplying water into the flume has a 75 HP capacity and can provide a maximum discharge of about 15 cfs.

For the purpose of collecting the eroded material, a 6-foot long sediment trap was placed at downstream end of the flume across the width of the flume.

A motorized instrument carriage runs longitudinally along the flume rails. The instrument carriage is designed to move a point gage with an accuracy of 0.005 ft laterally so that any place in the flume can be reached.

Six cylindrical clear plexiglass piers with 6 inches in diameter were placed in the flume. As shown in Figure 4-1, the distance between the piers were selected so that the disturbances generated by one pier would not affect the other piers .

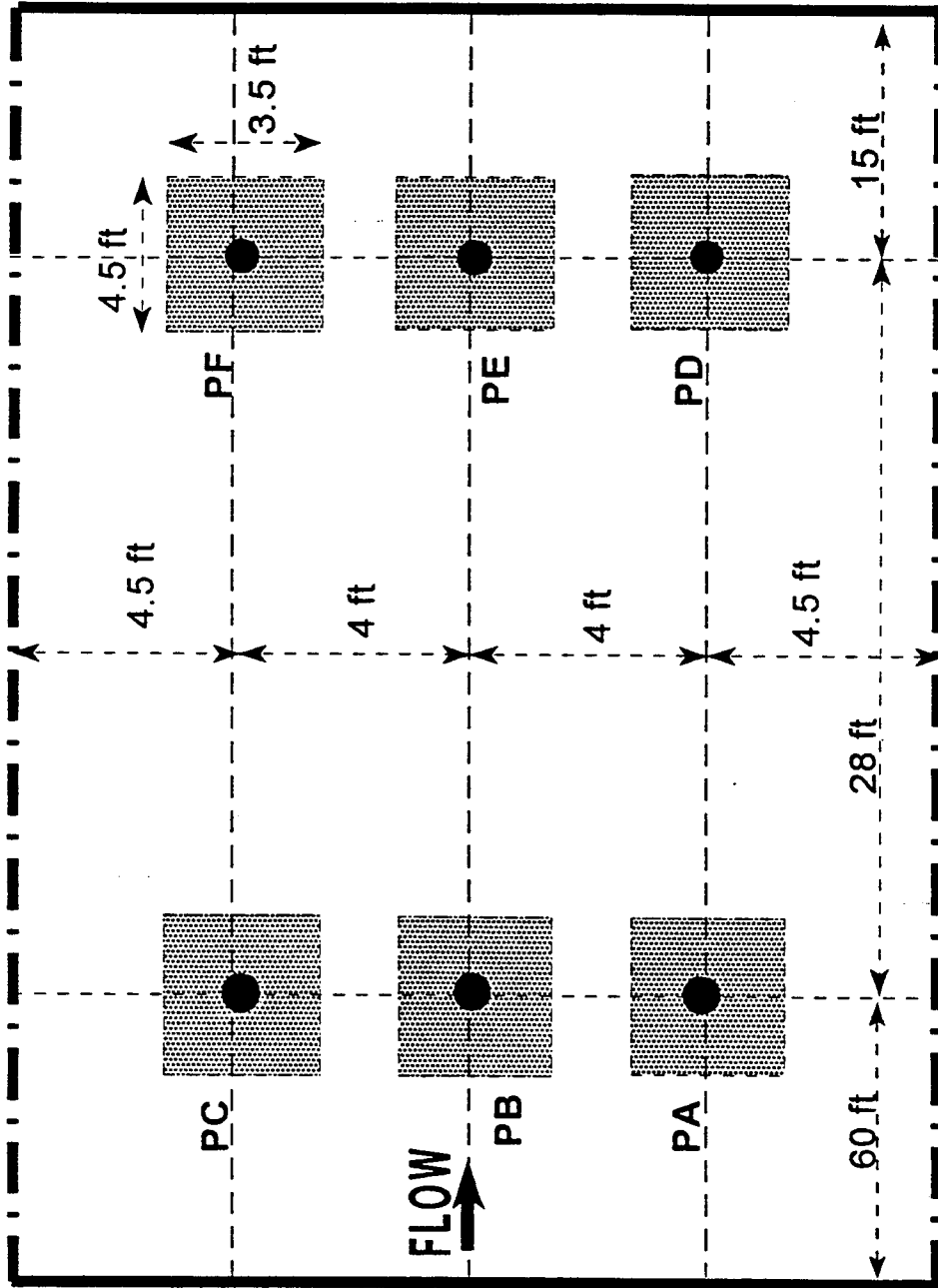


Figure 4-1. Plan View of the Seventeen-Foot Wide Experimental Flume

2) The Eight-foot flume

This flume is a recirculating tilting flume which is 8 ft wide, 200 ft long, and 4 ft deep with an adjustable slope. The side walls (except the test section for visual observations) of the flume are made of aluminum plates. The flume could be adjusted to any desired slope up to 3%. Water into the flume is supplied through three pipelines by three different pumps of 250 HP, 150 HP, and 125 HP. The three pumps can provide maximum discharge of 80 cfs. The discharge passing through the test flume is measured by a calibrated orifice meters placed in each of the pipelines.

At the entrance of the flume, a series of flow straighteners, a honeycomb, and a mesh box of gravel followed by a concrete ramp were used to reduce the turbulent eddies and to create a fully turbulent flow conditions in as short a distance as possible. A vertical adjustable tail gate was installed at the downstream end of the flume to control the water depth.

Rails placed along the top of each side wall of the flume support a motorized carriage. A point gage was mounted on the carriage for collecting water surface and bed elevation data and in order to support the probe of the magnetic current meter used for the velocity measurements.

As shown in Figure 4-2, three clear plexiglass piers with a diameter of 6 inches were installed along the centerline of

the flume. The distance between the piers was 40 feet and was selected such that the disturbances generated by any pier would not affect the other piers since they were 80 pier diameters apart.

3) The Four-foot flume

The flume is a recirculating tilting flume with working section of 4 ft wide, 35 ft long, and 3 ft deep. The side walls of the flume are made of 0.5 inch plexiglass. The slope of the flumes could be changed by means of an electrically driven tilting mechanism. Water into the flume is supplied from a sump tank through 6 inches pipeline by a 20-HP pump. A headbox of gravel is placed at the flume entrance to reduce the turbulent eddies induced at the flume head. The flow rate in the flume is adjusted by a valve on the pipeline.

An instrument carriage runs manually along the flume rails. The instrument carriage is designed to move a point gage, with an accuracy of 0.005 ft, laterally so that any place in the flume can be reached. This flume was used to produce higher Froude number ($Fr > 0.56$) for the experiments of saturated clay at 32% initial water content.

As shown in Figure 4-3, a single pier with a diameter of 4 inches was placed at 20 ft downstream of the flume head, equidistance from the flume side walls. Summary of the flumes used in this study is presented in Table 4-1.

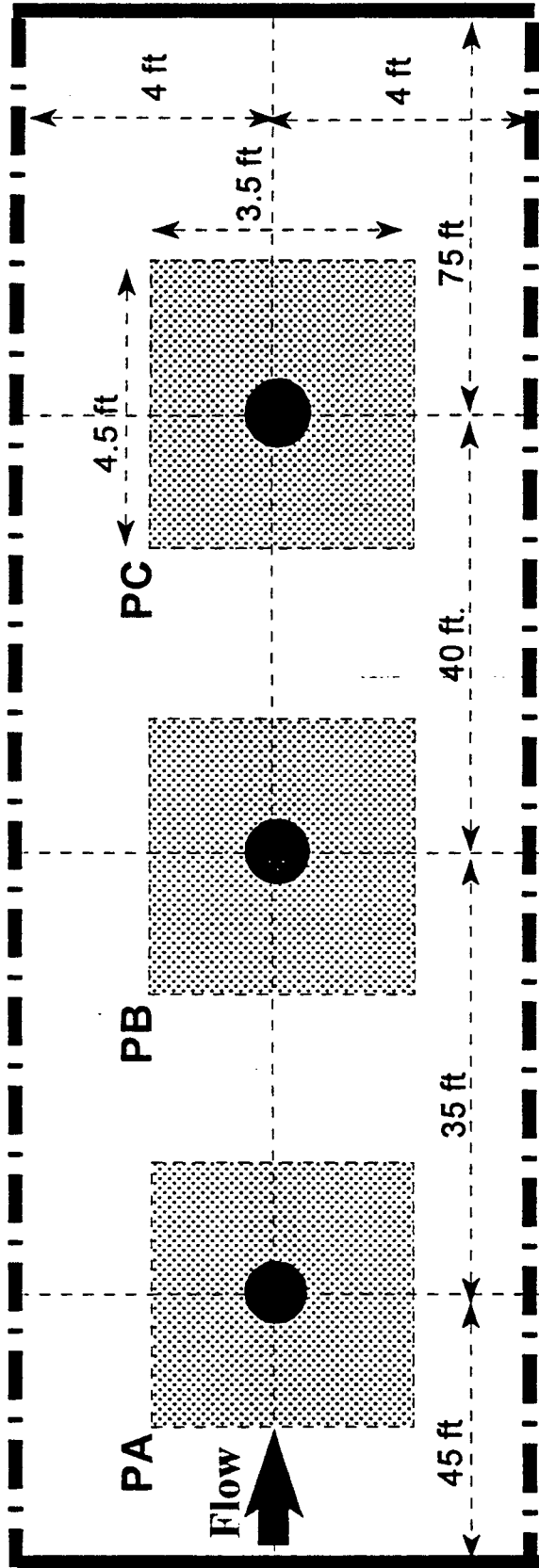


Figure 4-2. Plan View of the Eight-Foot Wide Experimental Flume

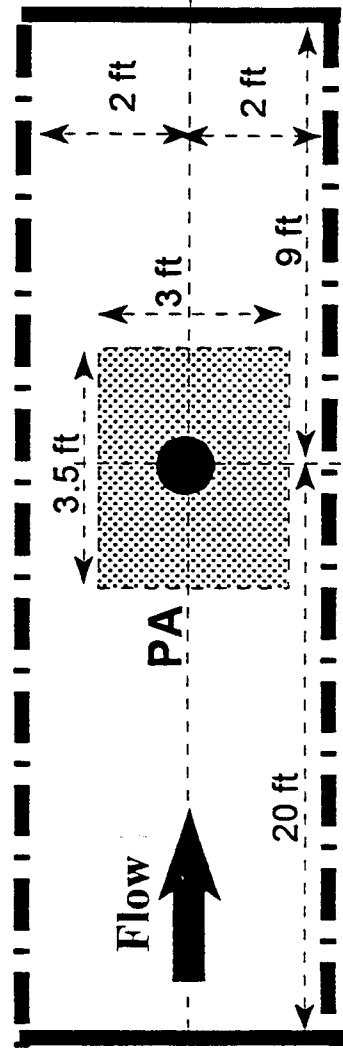


Figure 4-3. Plan View of the Four-Foot Wide Experimental Flume

Table 4-1. The Flumes Used in the Study

Flume	Width ft(m)	Length ft(m)	Depth ft(m)	Slope control	Pump power(HP)
F17	17(5.18)	100(30.5)	3(0.915)	End sill	75
F8	8(2.4)	200(61)	4(1.2)	Tilting	250
F4	4(1.2)	29(8.85)	2(0.61)	End sill	20

4-2-2 Piers

In all the experiments, cylindrical piers made of clear plexiglass pipes, 6 and 4 inches in diameter, and 40 inches long were used. Each pier was supported by a set of four pieces of iron angle, bolted to the flume bed for rigidity.

For the purpose of the rate of scour measurement, three measuring tapes were attached at the front, side, and back of the interior wall of each pier. The scour depth development around each pier was measured against time utilizing a small periscope manufactured by the use of an inclined mirror.

4-2-3 Current Meter

During each experiment, velocity measurements were carried out using a Marsh-McBirney magnetic velocity meter, mounted to read values in orthogonal direction in a plane parallel to the bottom of the flume. The current meter has an accuracy of $\pm 4\%$ of reading and its range from -0.5 to 19.99 ft/sec.

4-2-4 Point Gage

Measurements of scour hole configuration, water slope, bed slope, and water depth, were carried out using a point gage supported on the motorized instrument carriage.

The point gage with an accuracy of 0.005 ft, was mounted on a graduated scale and actuated by a slow-motion screw.

4-3 Soils Selection and Bed Material Preparation

In order to achieve the objectives of this study, it was necessary to procure a material that satisfies the requirements. It was decided to use a homogeneous soil containing clay, silt, and fine sand particles, in which cohesion plays a predominant role. The cohesive soil used in the experiments was obtained from the Agronomy experimental field of Colorado State University.

Utilizing the X-Ray diffraction test, the dominant clay mineral was found to be Montmorillonite. According to the unified soil classification system (USCS), the cohesive soil was also classified as medium plasticity clay and the texture is clay loam.

A series of laboratory tests were performed on the cohesive materials lead to the following properties as shown in Table 4-2.

Table 4-2, Properties of Cohesive Soil Used in the Study

Atterberg Limits		Chemical Properties	
Liquid limit	37.9%	Na	1.803 %
Plastic limit	19.6%	Ca	1.20 %
Plasticity index	18.3%	Mg	2.39 %
Soil Composition		K	3.18 %
Sand content	24%	P	1.347 %
Silt content	44%	Al	10.94 %
Clay content	32%	Fe	8.515 %
Optimum water content	20%	Mn	0.1 %
Optimum dry density	110 pcf	O.M.	2.9 %
Specific gravity	2.65	SAR	1.2
Bulk density	1.5 g/cm ³	pH	7.7

where Na is Sodium, Ca is Calcium, Mg is Magnesium, K is the Potassium, P is the Phosphorus, Al is Aluminum, Fe is the Iron, Mn is the Manganese, O.M is the Organic Matter, SAR is the Sodium Adsorption Ratio, and pH is the negative logarithm of the Hydrogen-ion Concentration (pH<7 is acidic, pH>7 is alkaline).

The sand used in set 1 of experiments is commercially labeled as Masonry sand with 0.55 mm mean grain size. The resulting grain-size distribution for the Masonry sand and Montmorillonite clay used in the experiments are presented in Figures 4-4 and 4-5.

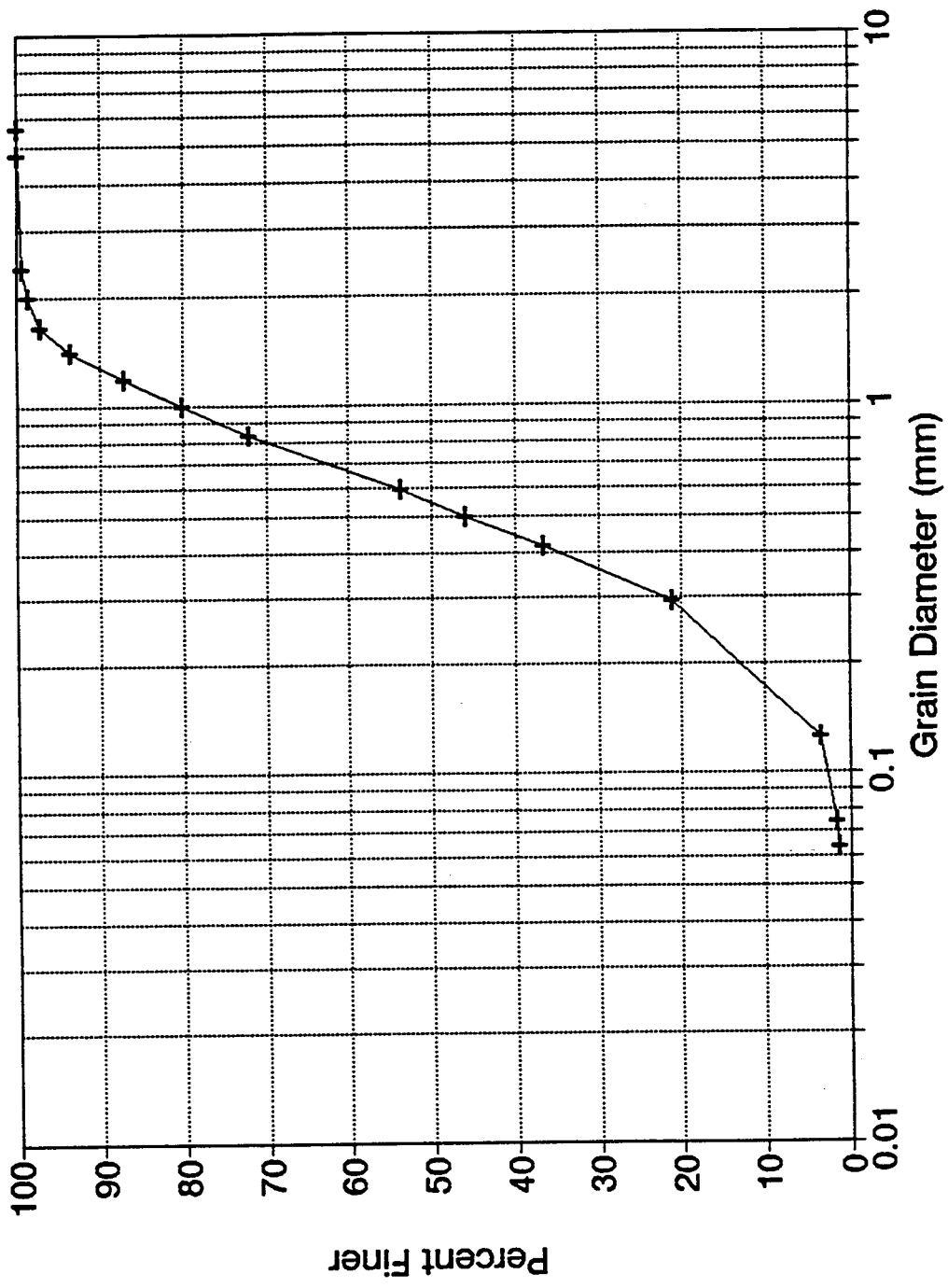


Figure 4-4. Grain Size Distribution of the Masonry Sand.

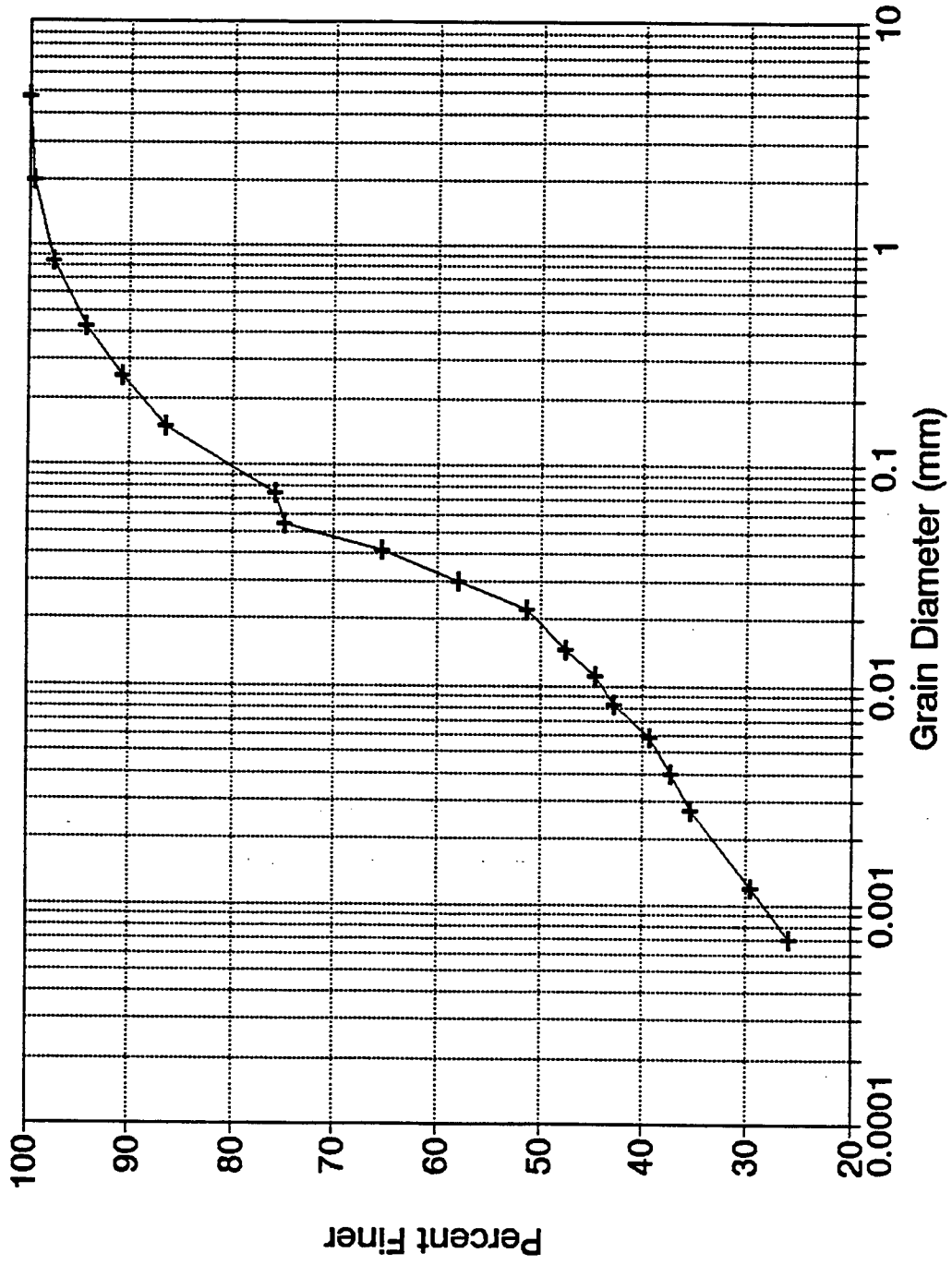


Figure 4-5. Grain Size Distribution of the Cohesive Soil

Prior to each experiment, the cohesive soil was first kept at a water content equal to 10-11%, and then sieved through a 5 mm Sieve to ensure the uniformity of compaction and in order to obtain a homogeneous material.

In this study, three sets of experiments identified as set 1, 2, and 3 were conducted. In set 1 of experiments, the amount of clay contents mixed with the sand were 0, 5, 10, 20, 30, and 40% by dry weight of mixture. The desired Mixtures were well mixed until homogenous materials at water content in the range of 10-11% were produced.

In set 2 of experiments, two subsets of experiments identified as subset 2.A and 2.B were conducted. In subset 2.A, the cohesive soil was prepared at an initial water content equal to the optimum water content (20%). While in subset 2.B, the clay soil was prepared at an initial water content equal to 15% (lower IWC case). Afterwards, the prepared clayey soil was laid out around the piers and compacted at 58, 65, 73, 80, 87, and 93% degree of compaction.

In set 3 of experiments, the sieved clay soil was placed in large dishes. The water content was measured and the additional water was added to achieve the desired initial water contents, which were 32, 35, 40, and 45%. The dishes were then covered with a plastic sheet for 5 day to prevent water losses and to achieve the maximum degree of saturation.

4-4 Experimental Procedures

Prior to each experiment, the flume bed was prepared in five stages as follows:

1) Laying out in the model

The prepared material was placed around the piers in an area of 3.5 ft wide by 3.5 ft long. The size of the area was selected to cover four times the expected maximum scour hole. The bed surface of each flume was leveled by hand using a staff gauge and surveying equipment. The regions around the piers, which were inaccessible with the blade, were leveled manually using a hand trowel.

2) Compaction process.

Since the compaction effect of unsaturated cohesive soil is the main interest of set 2 of experiments, the clay soil was placed around each pier and compacted under various degrees of compaction. The process of compaction was carried out by applying a specific mechanical energy, utilizing a hammer weighing 20 lb with base area of 11 inches by 7.2 inches, and a metal plate of 1/8 inch thickness and a surface area of 4 ft by 4 ft. The metal plate was constructed with a 6 inches in diameter semicircle.

The condition of applying the mechanical energy is a function of the mass of a hummer (W), the hammer base area (A), the height of drop (H), the numbers of drops or blows

(N), the number of layers of soil (N_1), and the thickness of soil layer (d_{co}), and is determined from the following relationship:

$$\text{Mechanical Energy} = \frac{W \times H \times N \times N_1}{A \times d_{co}} \quad \frac{\text{ft-lbf}}{\text{ft}^3} \quad (4-1)$$

In the compaction process, a 20 lb hammer weight was dropped from height 1 ft for all the experiments, while the number of blows (N), number of layers (N_1), and thickness of soil (d_{co}) were varied according to the desired compactions. The conditions of obtaining various degrees of compaction are listed in Table 4-3.

Table 4-3 Conditions of compactions

Comp.	Subset 2.A (IWC= 20%)				Subset 2.B (IWC= 15%)		
	N_1	N	d_{co} (ft)	energy ft-lbf/ft ³	N	d_{co} (ft)	energy ft-lbf/ft ³
87	3	6	0.4	19636	8	0.4	26181
80	2	4	0.6	5818	6	0.6	8727
73	1	3	1.0	1309	4	1	1745
65	1	1	1.0	436			
58	This compaction was obtained by dropping the soil around the piers under its weight .						

* The accuracy of the obtained compactions was $\pm 1.5\%$.

Once the compaction process has been completed, the degree of compaction was determined by measuring the wet unit density of the compacted soil using a copper cylinder tube of thickness 1.5 mm. The tube with sharp edges for inserting easily through the soil and has a dimension of 1.915 inches in diameter and 1.875 inches in height.

In order to determine the degree of compaction, the following procedures were carried out:

- a) The tube was immersed slowly into the leveled soil until the tube edge flattened with surface of bed.
- b) Next, the tube was extracted carefully without disturbing the soil sample.
- c) Afterwards, the soil sample was weighted (W_w), and placed in a microwave for ten minutes for drying and then weight it again (W_s).
- d) By knowing the tube volume ($3.079 \times 10^{-3} \text{ ft}^3$), the optimum dry unit density of the clay ($\rho_{\text{dopt.}} = 110 \text{ lb/ft}^3$), W_w , and W_s , the degree of compaction can be determined by using the following equations:

$$\text{wet unit density } (\rho_w) = \frac{W_w}{\text{tube volume}} \quad \text{gm/cm}^3 \quad (4-2)$$

$$\text{water content (W.C.)} = \frac{W_w - W_s}{W_s} \times 100 \quad \% \quad (4-3)$$

$$\text{dry unit density } (\rho_d) = \frac{\rho_w}{1 + \text{W.C.}} \quad \text{gm/cm}^3 \quad (4-4)$$

$$\text{Compaction (Comp.)} = \frac{\rho_d}{\rho_{d_{opt.}}} \times 100 \quad \% \quad (4-5)$$

In set 1 of test runs, the soil was compacted by applying the same energy for all the experiments. While in set 3 of experiments, there is no effect of applying any mechanical energy and the obtained compaction is based on the initial water content of saturated cohesive soil.

3) Soil shear strength measurements

Once the compaction process has been completed in Set 2 of experiments, the initial Vane shear strength (S) was measured directly by totally inserting a torvane shear vane into reasonably flat bed at a depth of 0.5 inch from the bed surface. Afterwards, the torvane knob was rotated while maintaining a constant vertical pressure.

At the moment of failure, the pointer showed the maximum shear strength at which the failure had taken place. The reported value of soil shear strength (S) around each pier was considered as the mean of five readings at different locations.

4) Initial bed elevation measurements

Once the degree of compaction and soil shear strength were measured, the initial bed elevation around each pier was measured by the point gage mounted on the motorized instrument carriage. The initial readings on the three tapes inside each pier were also taken.

5) Establishing flow conditions

When the previous four stages were completed, water was supplied into the flume by opening a valve on the pipeline very slowly until a pool was formed in the upstream reach of the flume between the headbox and the upstream end of the false floor. This filling process allowed the sediment bed to be wetted very slowly without causing any disturbance around the piers. Afterwards, the discharge was increased gradually with maintaining a large flow depth.

In the Seventeen and Four-foot flumes, the water depth is controlled by an end sill. While in the Eight-foot flume, the desired water depth was obtained by adjusting the tail gate. The flow rate into each flume was determined from a manometer readings at the orifice plate placed in a pipeline.

The discharge and the water depth were held constant during the entire experiment time, while the stream velocity was the only parameter that varied against the scour depth. All test runs were conducted under steady gradually varied flow conditions.

In the successive runs, the discharge and consequently the average velocity was increased in such a way to develop higher Froude numbers and the same previous steps were repeated for each test run.

4-5 Experimental Measurements

Once the desired flow conditions were verified, the carriage and the point gage were moved along the flume in such a way that any point could be reached with the measuring devices. Each experiment lasted for an average of 16-20 hours, based on the condition of each set, to ensure that the maximum scour depth has been reached.

The experimental measurements contain different issues and could be listed as follows:

- 1) Velocity distribution measurements.
- 2) Rate of scour measurements.
- 3) Water slope and water depth measurements.
- 4) Scour hole measurements.

In what follows each item of measurements will be discussed.

1) The velocity distribution measurements

When the steady gradually varied flow conditions at the requested discharge and flow depth have been established, the velocity measurements were carried out using a Marsh-McBirney magnetic velocity meter with an accuracy of $\pm 4\%$ of reading and its range from -0.5 to 19.99 ft/sec.

In the approach of each pier, velocities were measured at three cross sections, 3 ft, 5 ft, and 7 ft away from the piers. As shown in Figure 4-6, reference point grids provided the location of each vertical measurements with respect to the pier. Along each of these sections five vertical velocity profile measurements with at least eight points were taken.

The value of the approach velocity reported for each pier is the average of depth, width, and distance integrated average of at least 80 velocity measurements.

2) Rate of scour measurements

Once the desired discharge and flow depth were established, the scour around each pier was observed and readings from the tapes placed inside each of the piers were taken against time. The time interval between the readings was small during the first five hours of the experiment and it was bigger as the progression of scour became slow.

3) Measurements of water depth, water slope, and bed slope

The water surface elevations and corresponding bed elevation at the approach of each pier were measured at 3 approach cross sections and at 3 lateral locations at each of these sections by the use of point gage mounted on the flume carriage with an accuracy of 0.005 ft.

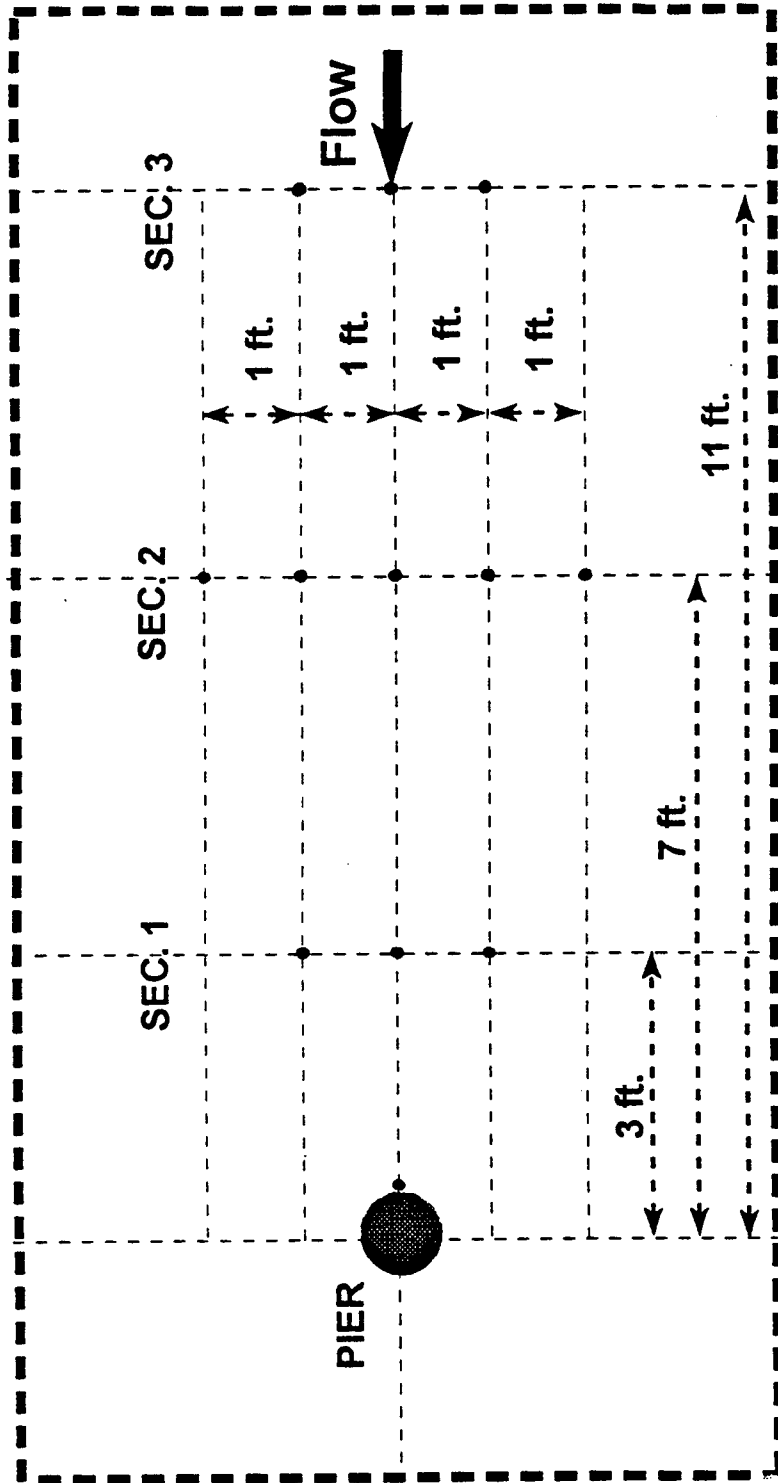


Figure 4-6. Velocity Measurements Grid

The approach water depth value of each pier was calculated and reported as the laterally and longitudinally averaged value of the difference between the water surface elevations and bed elevations at each pier approach. For high Froude numbers, the water surface readings were fluctuated significantly. Therefore, the minimum and maximum values at various points along the flume were averaged to obtain the actual value of water surface elevation.

For water slope value, linear regression was applied to the data to determine the best-fit line to the water surface slope in the approach of each pier.

For bed slope value, the same procedures were carried out along the centerline of the flume. Then a linear regression analysis was performed to determine the bed slope.

4) Scour hole measurements

At the end of each run, the flow into the flume was stopped with the tail gate in closed position, and water was drained gradually to avoid any disturbance. After sufficient water was drained allowing the bed material surface to be visible, the scour hole topographies were measured by the use of the point gage.

The measurements were carried out through an intensive grid. At least eight cross sections were taken in the region of the scour hole to determine the maximum scour depth and volume. Depending on the conditions of each scour hole, at

least eight points were measured along each of these cross sections. The maximum scour depth for each pier was calculated as the difference between the mean bed elevation at the upstream edge of the hole and the lowest measured point of scour.

In general, it was observed that the developed scour holes in the experiments of low compacted unsaturated clay and mixture of high clay content, were affected by the process of settlement and shrinkage during the drained time. Therefore, the scour hole measurements of these experiments were carried out once the scour hole could be visible.

Afterwards, photographic documentation was taken at the upstream, sides, and downstream of each scour hole to define the geometric shape of the scour. Finally, the scour hole volume was measured using a plastic sheet and water. The scour hole was first covered by a plastic sheet and calibrated water was dropped into the scour hole till the water flattened with the bed surface. The scour volume was considered as the volume of the dropped water into the developed scour hole.

CHAPTER V
ANALYSIS OF THE EXPERIMENTAL RESULTS

5-1 Introduction

In this Chapter, the available experimental data points are analyzed to predict the local scour at bridge pier placed in a mixture of cohesive and non-cohesive soil and in cohesive soil. Section 5-2 presents the dimensional analysis for the parameters affecting the pier scour. The data from the flume experiments for each set have been analyzed and the results are presented in Sections 5-3 through 5-5.

Section 5-3 presents the experimental results and analysis of pier scour in the mixtures of cohesive and non-cohesive soils. Section 5-4 introduces the experimental data for pier scour in compacted unsaturated cohesive soils.

Section 5-5 discusses the results of pier scour in saturated cohesive soils as well as the effect of dry-wet cycle on pier scour in cohesive materials. As a result of the analysis, a general equation for pier scour in both unsaturated and saturated cohesive soil is proposed.

The sensitivity analysis for the developed equations are presented in Section 5-6.

The complete experimental records of this study are presented as a part of the data supplement for the Project No. DTHF 61-91-c-0004 entitled "Effect of Sediment Gradation and Cohesion on Scour" for the U.S Federal Highway Administration. Therefore, only summary data Tables and pertinent summary information have been included in this dissertation.

All the experiments of the present study were carried out under steady gradually varied flow conditions. 14 test runs were conducted in the Seventeen-foot wide flume, 12 test runs were conducted in the Eight-foot wide flume, and 8 test runs were carried out in the Four-foot wide flume, for a total of 34 test runs and 111 data points. In each of the test runs up to 6 piers have been studied simultaneously to cover a wide range of flow and soil conditions.

5-2 Dimensional Analysis

The dimensional analysis in different forms has been used extensively for correlating the variables affecting the scour depth at bridge piers. The variables used in the analysis are parameters of soil, fluid, and model systems. These parameters are given below.

$$d_s = f(Y, b, V, d_{50}, \sigma_g, \phi, t, g, \rho, \nu, S, C, \text{Comp.}, IWC) \quad (5-1)$$

where d_s = scour depth; Y = depth of approach flow; b = pier width; V = velocity of approach flow; d_{50} = mean sediment diameter; σ_g = geometric distribution of sediment diameter about the mean; ϕ = pier shape factor; t = time; g = gravitational acceleration; ρ = fluid density; ν = fluid kinematic viscosity; S = soil shear strength; C = clay content; $Comp.$ = degree of compaction; and IWC = initial water content.

Applying the Buckingham-Pi Method and using b , V , and ρ as repeating variables, the following set of dimensionless parameters can be obtained.

$$\frac{d_s}{b} = f \left(\frac{Y}{b}, \frac{d_{50}}{Y}, \sigma_g, \phi, \alpha, \frac{Vt}{b}, \frac{V^2}{gY}, \frac{S}{\rho V^2}, C, Comp., IWC \right) \quad (5-2)$$

Since the parameters Y/b , ϕ , σ_g , d_{50}/Y , and α were kept constant during the study, these parameters will be eliminated from equation 5-2. For large experiment durations, the value of the term (Vt/b) had a very weak effect on the regression analysis, thus this term was also removed and equation 5-2 becomes:

$$\frac{d_s}{b} = f \left(F_r, \frac{S}{\rho V^2}, C, Comp., IWC \right) \quad (5-3)$$

in which

F_r = Froude number;

C = a parameter describing the amount of clay content in sandy soil (dry weight of clay/dry weight of mixture);

Comp.= degree of compaction of clayey soil;

IWC = initial water content of clayey soil; and

S = soil shear strength.

The parameters that were varied in the experiments have been evaluated for their effect on the scour depths obtained. The parameters that were varied were the stream velocity, the clay content in sandy soils, the compaction of unsaturated cohesive soils, and the initial water content of saturated cohesive soils.

The analysis of these parameters was presented in two separate ways. Firstly, the parameters were analyzed to determine general trends relating to the individual parameters involved. Secondly, the scour ratio, d_s/b , (scour depth/pier diameter) was regressed against the remaining dimensionless groups using multiple linear and non-linear regression analysis in the commonly available SAS statistical analysis package. The theory of this program is based on the least squares method.

5-3 Analysis of Pier Scour in Cohesive-Noncohesive Soil Mixtures

The first set of runs (39 experimental data points) was conducted to investigate the effect of clay content in sandy soils. Generally, the results from this set indicate that the scour depth decreases as the clay content in sandy soil increases up to 40%.

Summary of experimental conditions and results of this set of runs are presented in Table 5-1. Looking down the columns in Table 5-1, one can see that the scour depth decreases as the clay content increases for every condition tested. The relationship is in agreement with results of the previous research involving the rate of erosion of the mixtures. The reason is that, as the clay content increases in a mixture, the cohesion forces between the particles play an important part in controlling the scour process.

5-3-1 Geometry of Scour Hole in Mixtures

For all the experiments conducted in clay-sand mixtures, the maximum scour depth was observed to be occurring in front of the circular piers. This observation agrees with those of previous researchers conducting studies in sandy soils.

Generally the shape of the scour hole is conical in nature, with a smooth almost uniform half cone in front of the piers. The scour hole behind the pier is also a conical shape

Table 5-1. Summary of Experimental Conditions and Results for Set 1
(Effect of Clay Content on Pier Scour)

Run-Pier No.	Q (cfs)	Clay (% C)	Approach Y (ft)	Approach V (ft/s)	Fr	ds (in.)	(ds/b)	Vs (in. ^ 3)	(Vs/b ^ 3)
13-PA	11	0	0.776	0.920	0.184	3.468	0.58	494.3	2.288
13-PB	11	5	0.776	0.989	0.198	3.010	0.50	408.9	1.893
13-PC	11	10	0.776	1.020	0.204	3.630	0.61	610.3	2.825
14-PA	10	0	0.690	0.830	0.176	2.736	0.46	164.8	0.763
14-PB	10	5	0.690	0.925	0.196	3.020	0.50	400.0	1.852
14-PC	10	10	0.690	0.889	0.189	2.600	0.43	210.5	0.975
15-PA	12	0	0.735	0.900	0.185	3.492	0.58	494.3	2.288
15-PB	12	5	0.735	1.008	0.207	4.152	0.69	854.3	3.955
15-PC	12	10	0.735	1.028	0.211	3.600	0.60	549.2	2.543
16-PA	14.6	0	0.800	1.038	0.205	4.562	0.76	1013.0	4.690
16-PB	14.6	5	0.800	1.169	0.230	5.004	0.83	1196.1	5.537
16-PC	14.6	10	0.800	1.238	0.244	5.650	0.94	1220.0	5.648
17-PA	10	20	0.690	0.830	0.176	1.788	0.30	88.5	0.410
17-PB	10	30	0.690	0.925	0.196	2.050	0.34	166.6	0.771
17-PC	10	40	0.690	0.889	0.189	2.020	0.34	150.5	0.697
18-PA	12	20	0.735	0.900	0.185	2.280	0.38	188.5	0.873
18-PB	12	30	0.735	1.008	0.207	2.232	0.37	309.8	1.434
18-PC	12	40	0.735	1.028	0.211	2.352	0.39	250.5	1.160
19-PA	14.6	20	0.798	1.074	0.212	2.610	0.44	400.3	1.853
19-PB	14.6	30	0.798	1.175	0.232	3.780	0.63	890.0	4.120
19-PC	14.6	40	0.798	1.189	0.235	3.300	0.55	555.3	2.571
20-PA	13.5	20	0.756	1.045	0.212	3.096	0.52	387.5	1.794
20-PB	13.5	30	0.756	1.140	0.231	4.116	0.69	950.5	4.400
20-PC	13.5	40	0.756	1.145	0.232	3.780	0.63	690.6	3.197
21-PA	12	20	0.736	0.900	0.185	2.280	0.38	205.4	0.951
21-PB	12	5	0.736	1.008	0.207	4.152	0.69	854.3	3.955
21-PC	12	10	0.736	1.028	0.211	3.612	0.60	549.2	2.543
22-PA	10	20	0.701	0.857	0.180	2.124	0.35	88.5	0.410
22-PB	10	5	0.701	0.926	0.195	3.012	0.50	408.9	1.893
22-PC	10	10	0.701	0.892	0.188	2.664	0.44	310.5	1.438
30-PA	13	0	0.950	1.696	0.307	9.750	1.63	2929.1	13.561
30-PB	13	20	0.950	1.752	0.317	6.240	1.04	2318.9	10.736
30-PC	13	40	0.951	1.820	0.329	3.720	0.62	1708.7	7.910
31-PA	13	10	0.950	1.696	0.307	8.280	1.38	2831.5	13.109
31-PB	13	30	0.950	1.712	0.310	6.520	1.09	2400.4	11.113
31-PC	13	40	0.951	1.820	0.329	5.300	0.88	1900.3	8.798
32-PA	9	0	0.810	1.186	0.232	7.500	1.25	2002.6	9.271
32-PB	9	20	0.810	1.158	0.227	4.800	0.80	1000.0	4.630
32-PC	9	40	0.850	1.194	0.228	3.500	0.58	980.0	4.537

NOTES:

- * For all these runs, soils around the piers were compacted with the same energy.
- * The initial water content of the mixtures were kept in the range of 10-12%.
- * Runs 13 through 22 were conducted in the Seventeen-foot wide flume.
- * Runs 30 through 32 were conducted in the Eight-foot wide flume.

but it is much shallower and wider than the portion in front of the pier, similar to observations reported earlier.

The scoured material is deposited downstream of the scour hole and forms a mound. The volume of this mound decreases as the clay content in the mixtures increases. As the flow passes the mound, depth of flow suddenly increases causing a reduction in flow velocity. At this low velocity the fine materials settled around the mound's edge.

During this set of test runs, especially with runs of low clay content in the mixtures, the finer particles move out and the coarser grains concentrate in the top layer and start to rearrange themselves in a particular way to form an armor coat at the end of each run. This armor layer, once formed, acts as a coating or protection for the underlying and surrounding fine materials from being scoured.

The geometry of scour holes under different flow conditions and various clay contents are presented in Figures 5-1 through 5-4. These photographic documentation show that the scour volume around the piers decreases with increasing clay content.

The cross section geometry of the scour holes across the center line of the piers are plotted in Figures 5-5 through 5-10. These plots show that the slope of the scour hole steepens with decreasing clay content in sandy soils under different flow conditions.



Figure 5-1. View of the Scour Hole for Pier A (0% Clay)
at the End of Run R32, $Q = 9$ cfs

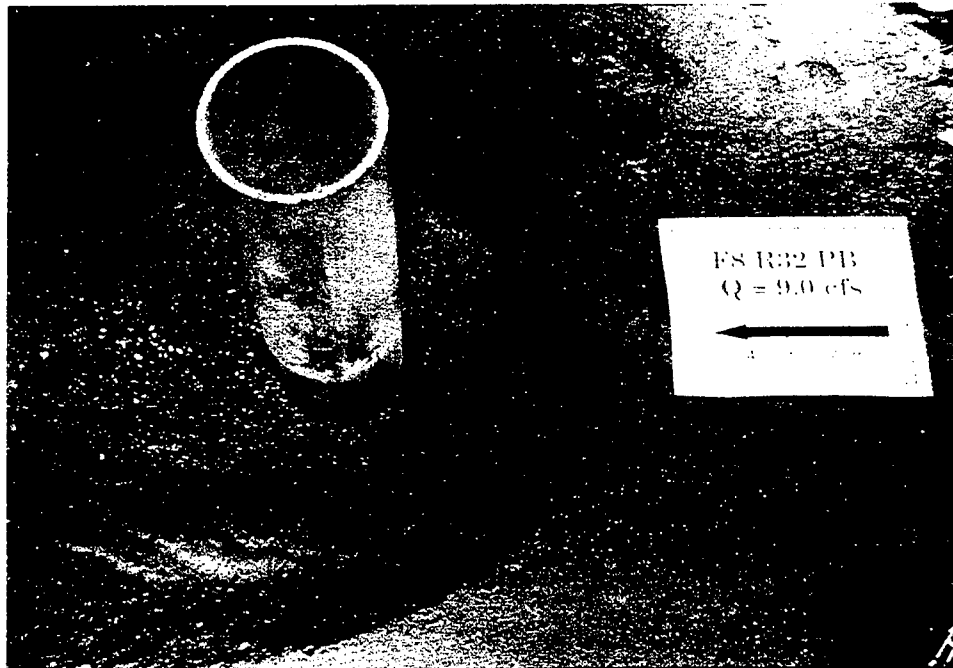


Figure 5-2. View of the Scour Hole for Pier B (20% Clay)
at the End of Run R32, $Q = 9$ cfs

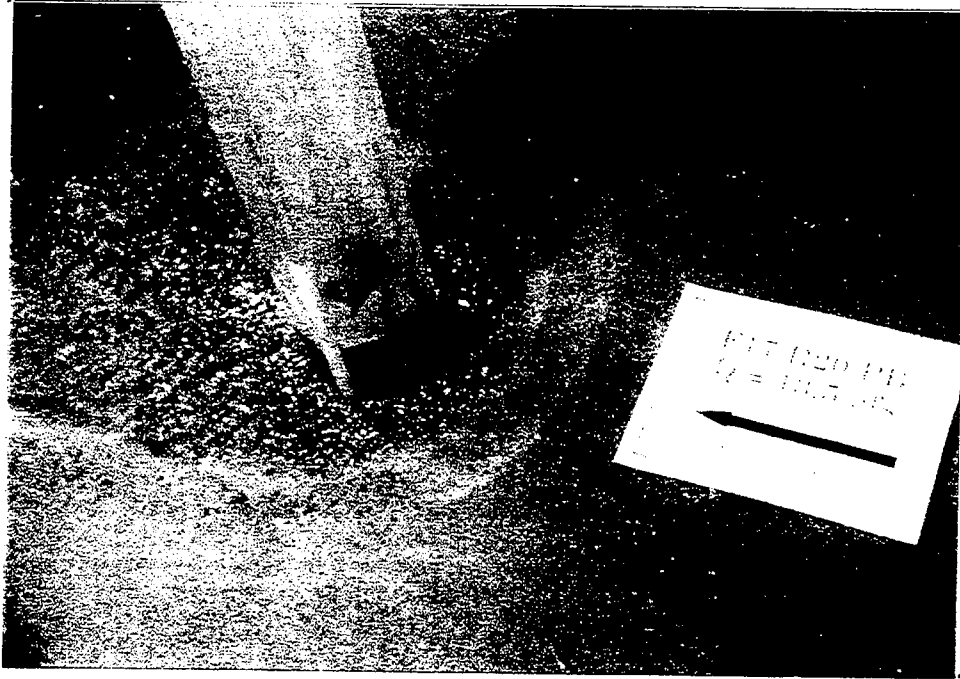


Figure 5-3. View of the Scour Hole for Pier B (30% Clay)
at the End of Run R20, $Q= 13.5$ cfs



Figure 5-4. View of the Scour Hole for Pier C (40% Clay)
at the End of Run R20, $Q=13.5$ cfs

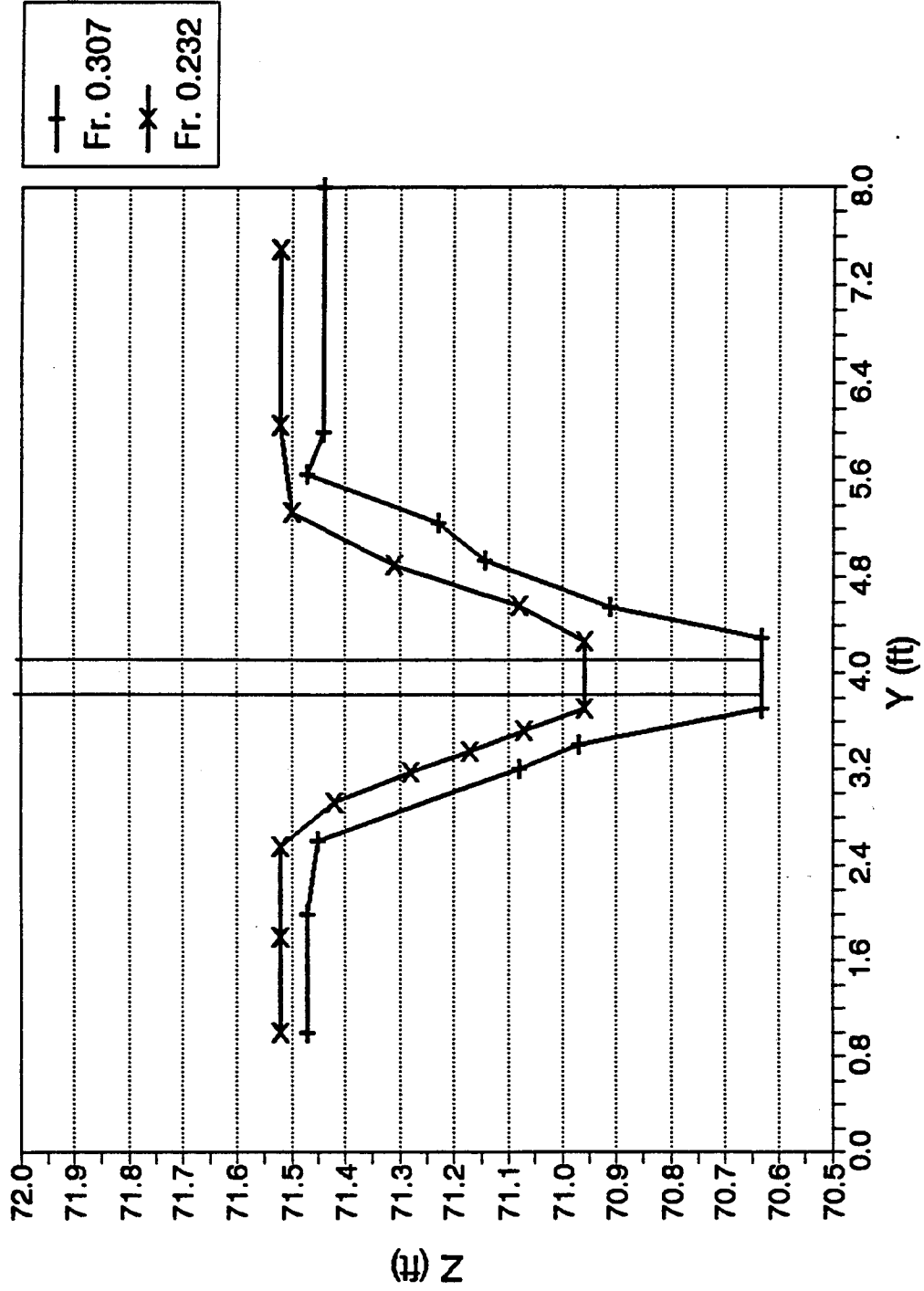


Figure 5-5. Effect of Clay Content on the Cross Section Geometry Along the Center Line of Pier PA for Runs R30 and R32 (0% Clay)

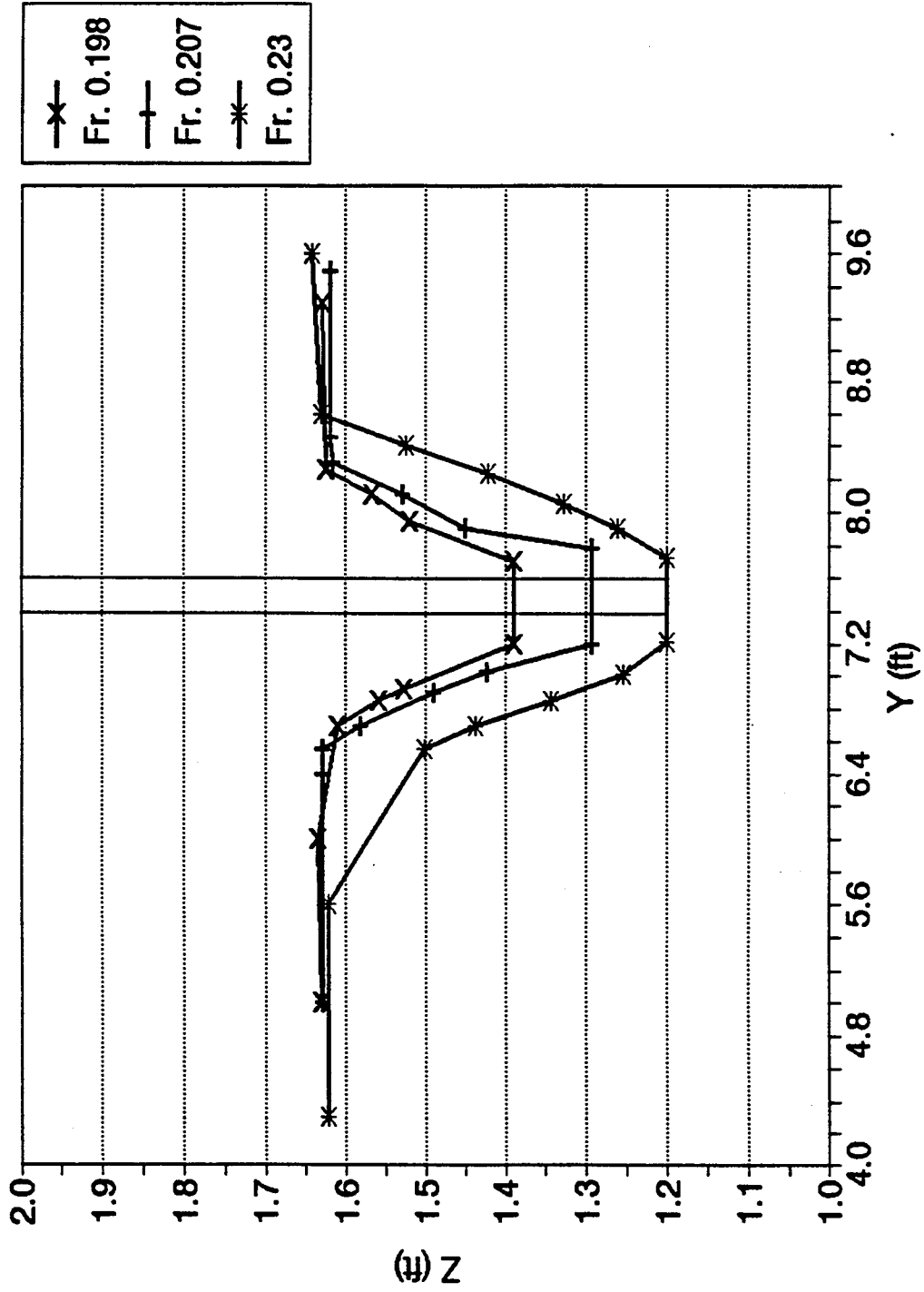


Figure 5-6. Effect of Clay Content on the Cross Section Geometry Along the Center Line of Pier PB for Runs R13, R16, and R21 (5% Clay)

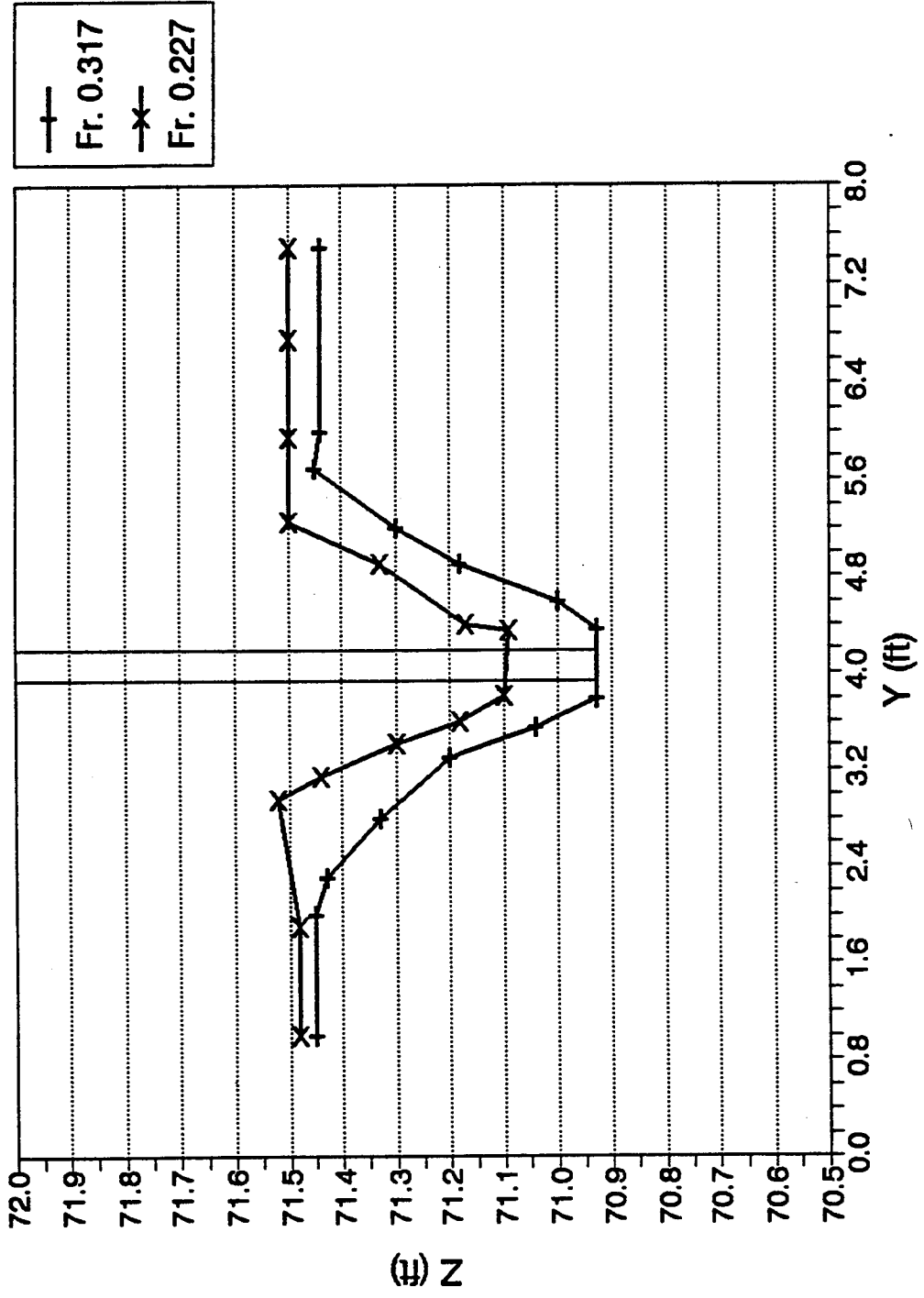


Figure 5-7. Effect of Clay Content on the Cross Section Geometry Along the Center Line of Pier PB for Runs R30 and R32 (20% Clay)

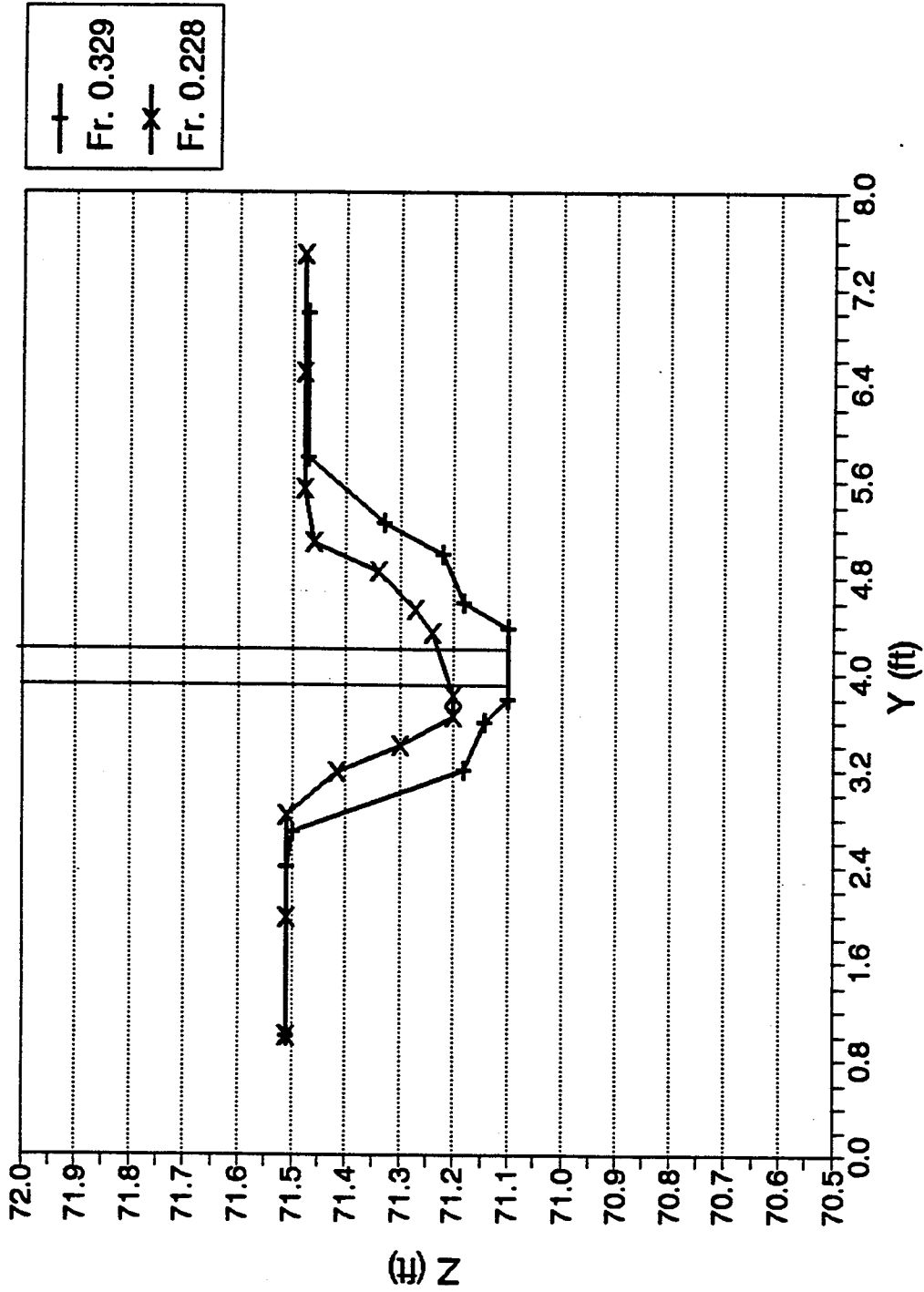


Figure 5-8. Effect of Clay Content on the Cross Section Geometry Along the Center Line of Pier PC for Runs R30 and R32 (40% Clay)

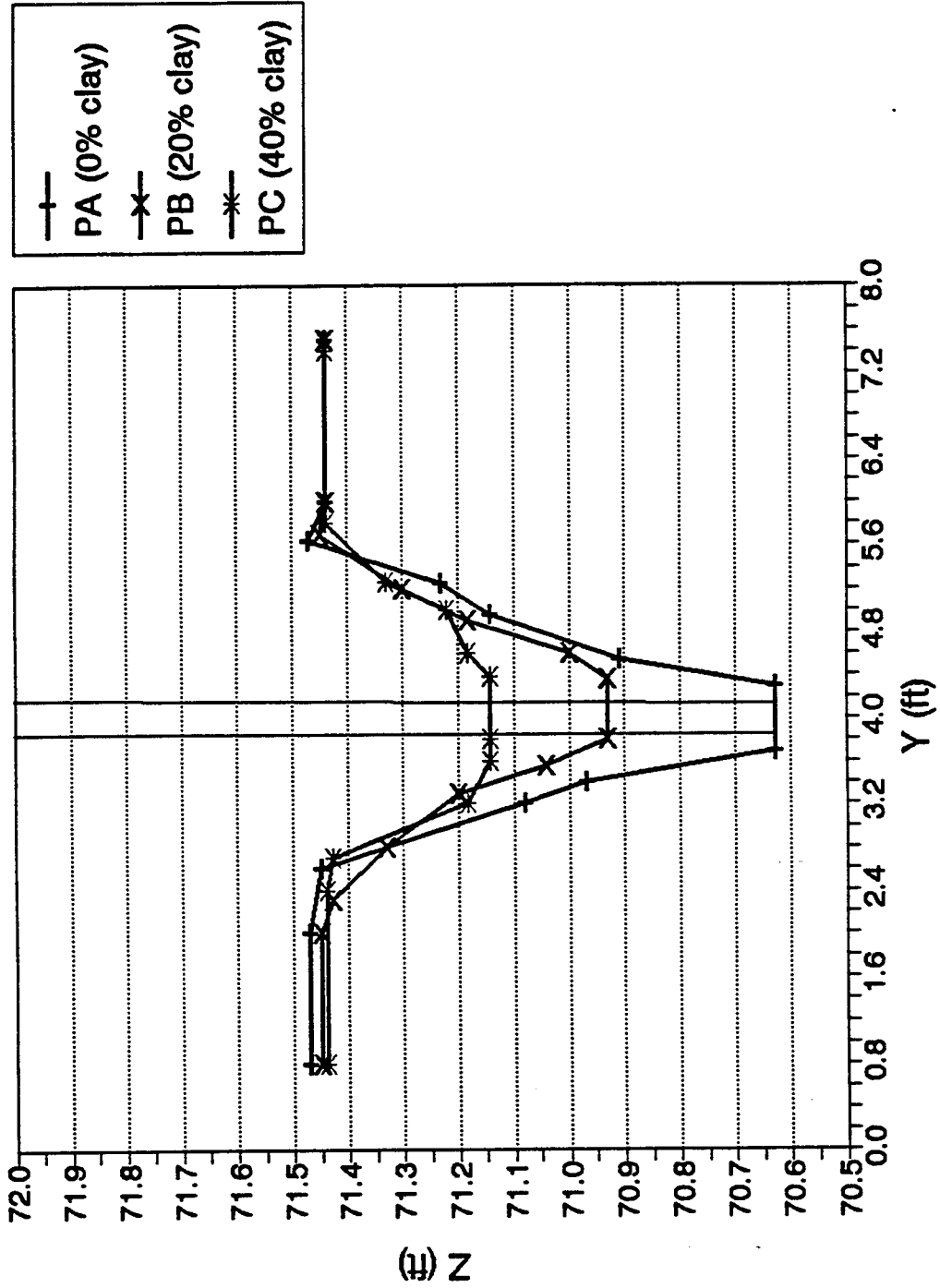


Figure 5-9. Effect of Clay Content on the Cross Section Geometry Along the Center Line of Piers PA, PB, and PC for Run R30

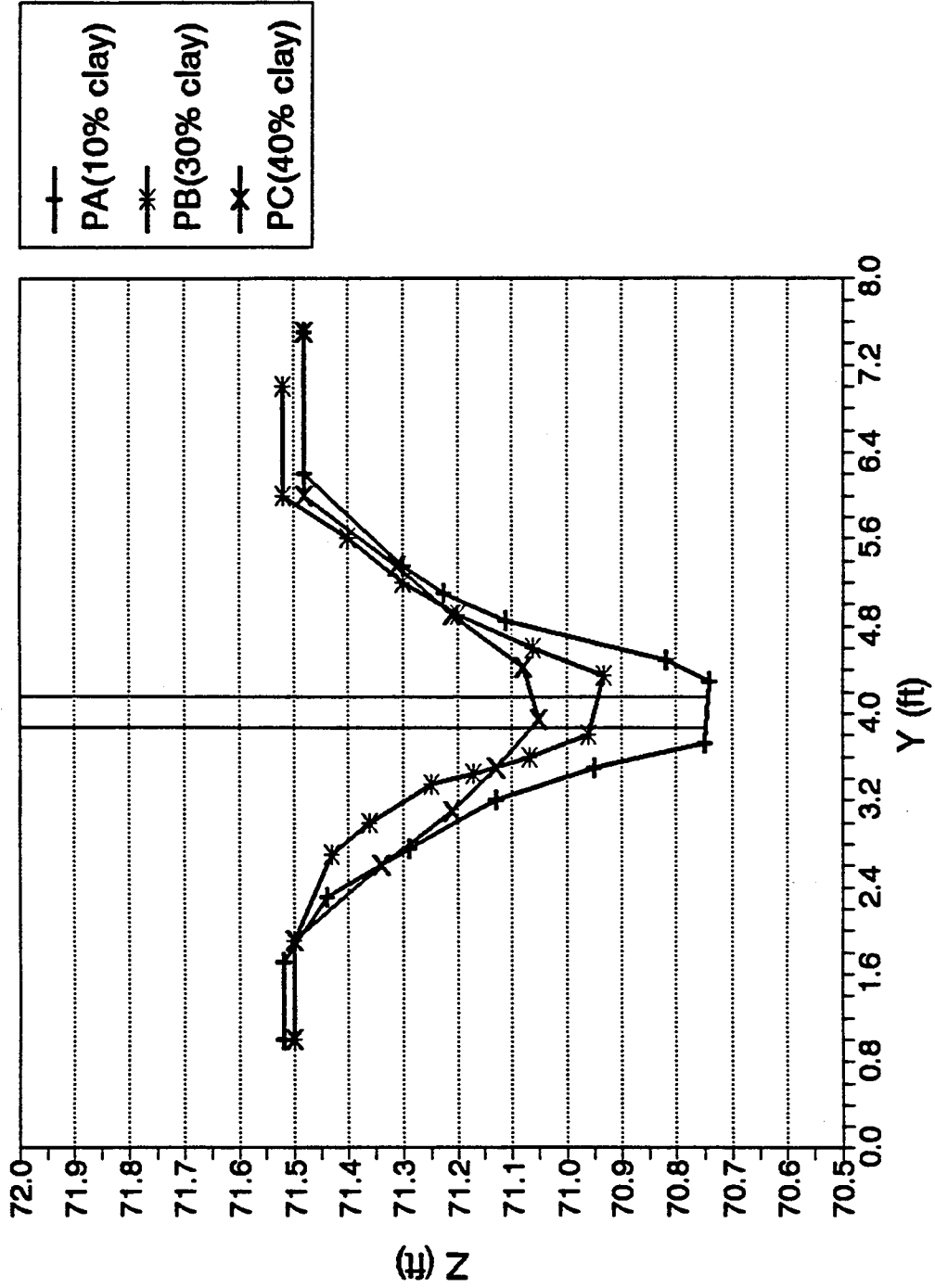


Figure 5-10. Effect of Clay Content on the Cross Section Geometry Along the Center Line of Piers PA, PB, and PC for Run R31

From the scour hole measurements a relationship between the side slope of the scour hole (Z) and the clay content (C) was developed as shown in Figure 5-11. By using the regression analysis, the following relationship is obtained:

$$Z = 1.422 + 0.06 (\% C) \quad (5-4)$$

Using equation 5-4, the diameter of the scour hole (B) region can be approximated by:

$$B = 2 b + 2 Z d_s \quad (5-5)$$

The relationship between the scour depth (d_s) and scour volume (V_s) in dimensionless form is shown in Figure 5-12 for all data points. By fitting the best line to the points plotted on Figures 5-12, the following relationship is obtained.

$$\left(\frac{d_s}{b} \right) = 0.4 \left(\frac{V_s}{b^3} \right)^{0.41} \quad (5-6)$$

In order to apply the results of the present study to any pier diameter size, a scour ratio is introduced. The scour ratio is defined as the maximum scour depth measured in each individual test run to the pier diameter.

The variation of the scour ratio with Froude number has been analyzed for different clay contents in sandy soil. Figure 5-13 is a plot of these variables for all data points.

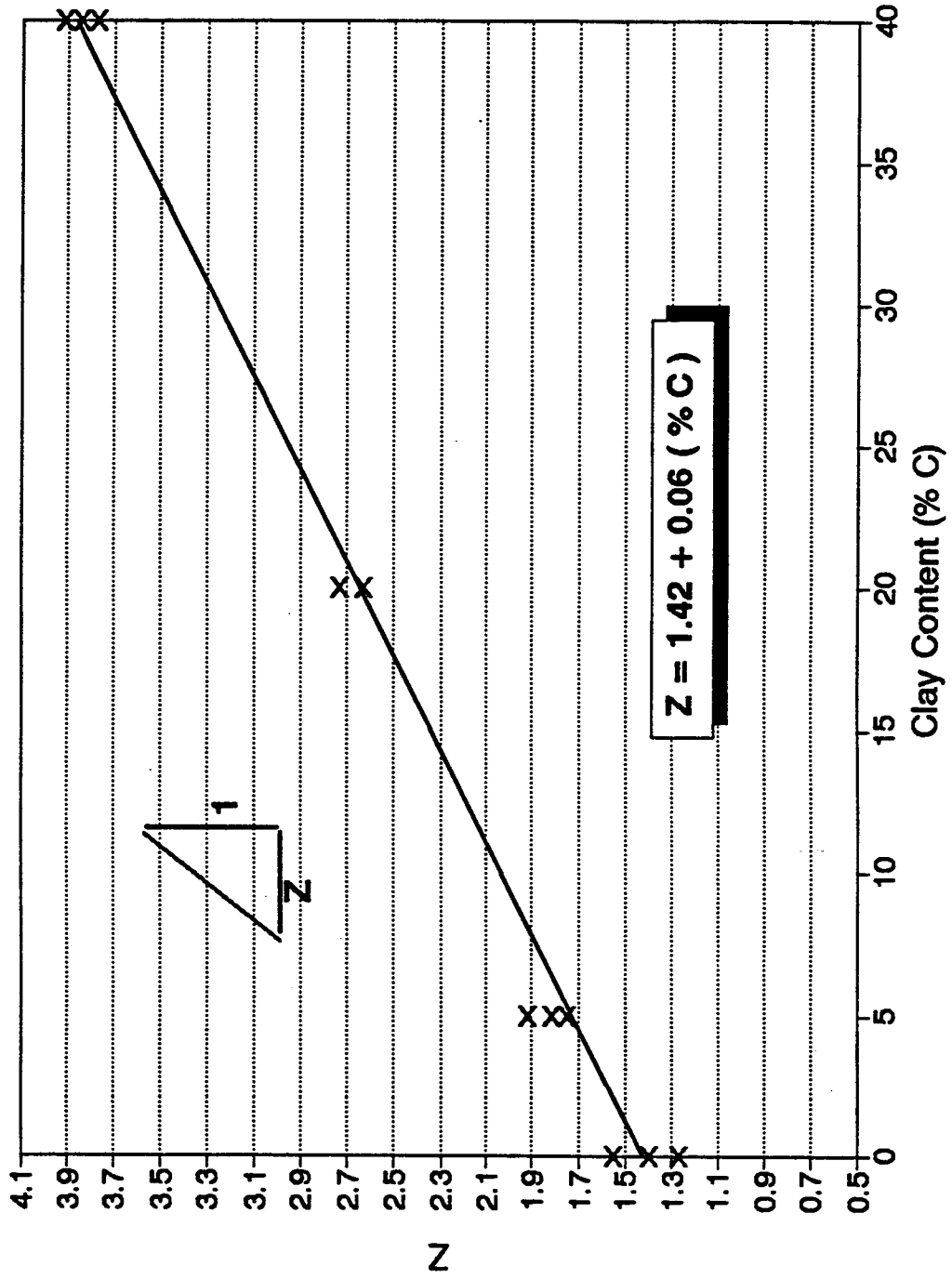


Figure 5-11. Effect of Clay content on the slope of the Scour Hole

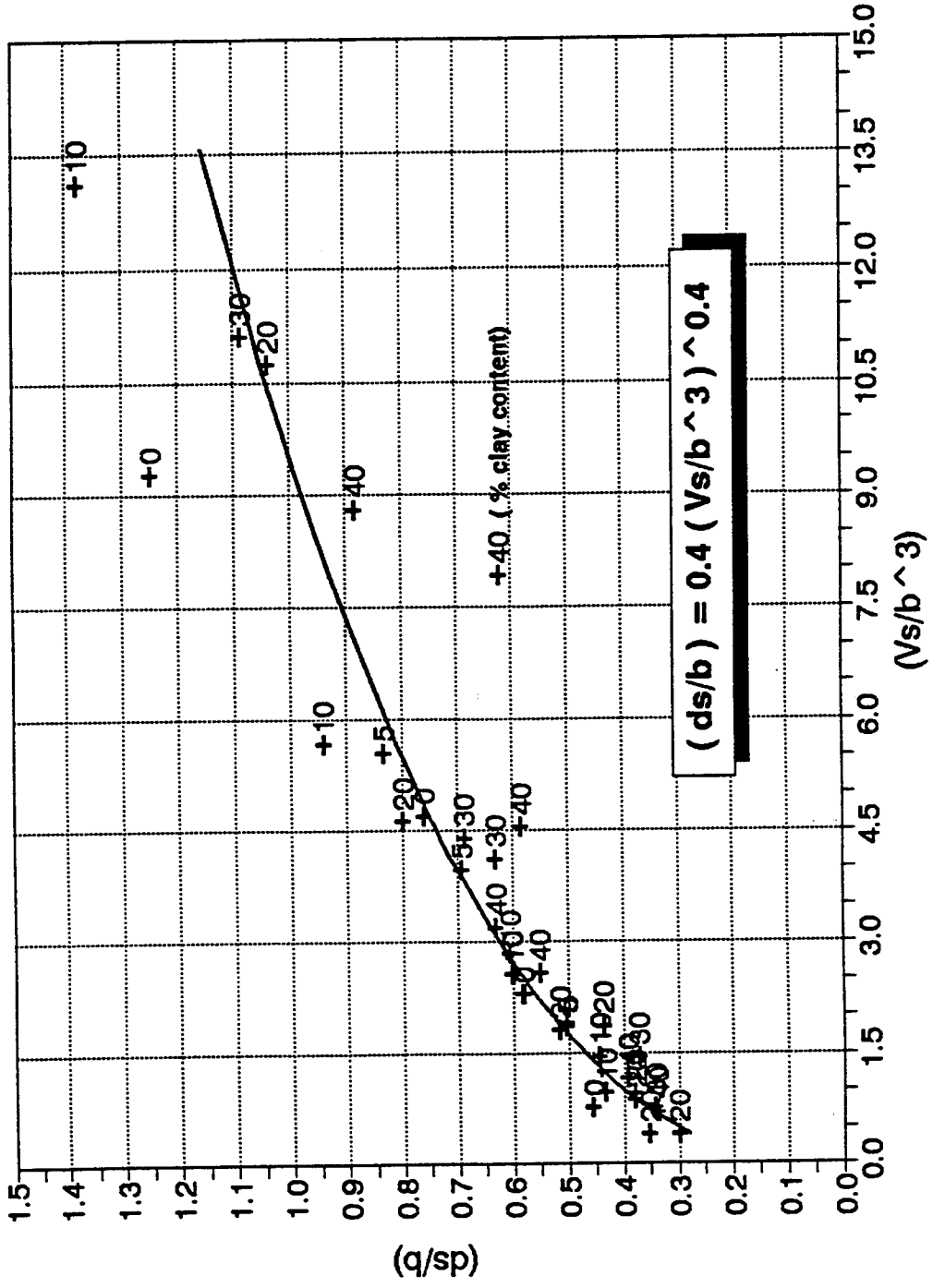


Figure 5-12. Effect of Clay Content in Sandy Soils on (d_s/b) versus (V_s/b^3) .

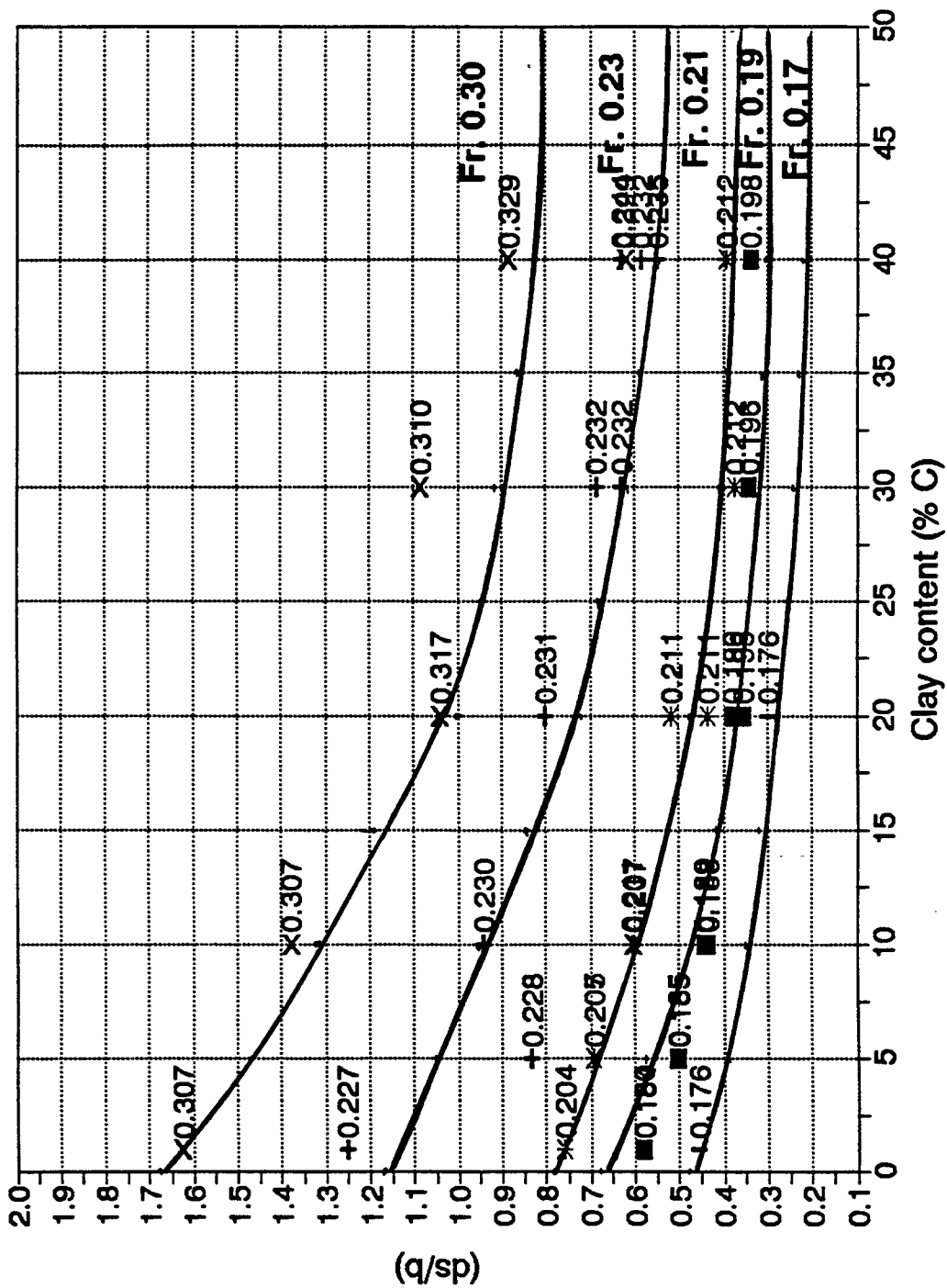


Figure 5-13. Effect of Clay Content in Sandy Soils on Pier Scour Ratio.

An analysis of these data points shows the trend as drawn on the graph. As the clay content increases up to 40%, the scour ratio decreases. The analysis can not be extended to clay content greater than 40 percent since beyond this amount of clay content, other cohesive parameters such as compaction, water content, etc. become dominant.

The conclusion that may be drawn as a result of these experiments is that the clay content in sandy soil can be represented in the form of a reduction factor which can be multiplied by the scour depth in sandy soil in order to obtain the scour depth in a mixture of sandy-clayey soil. This reduction factor can be defined as the ratio between the maximum scour depth in a mixture of sandy-clayey soil to that in sandy soil under the same flow conditions. Using this definition, the reduction factor would be 1 when the clay content is zero (all sand). The reduction factor can be applied to a wider range of conditions.

From Figure 5-13, the reduction factor (K) as a function of clay content in sandy soil is presented in Figure 5-14. A regression analysis of all data points in Figure 5-14 based on the assumption that the reduction factor is a power function of the clay contents, yielded:

$$K = \frac{1}{(1 + C)^{2.5}} \quad (5-7)$$

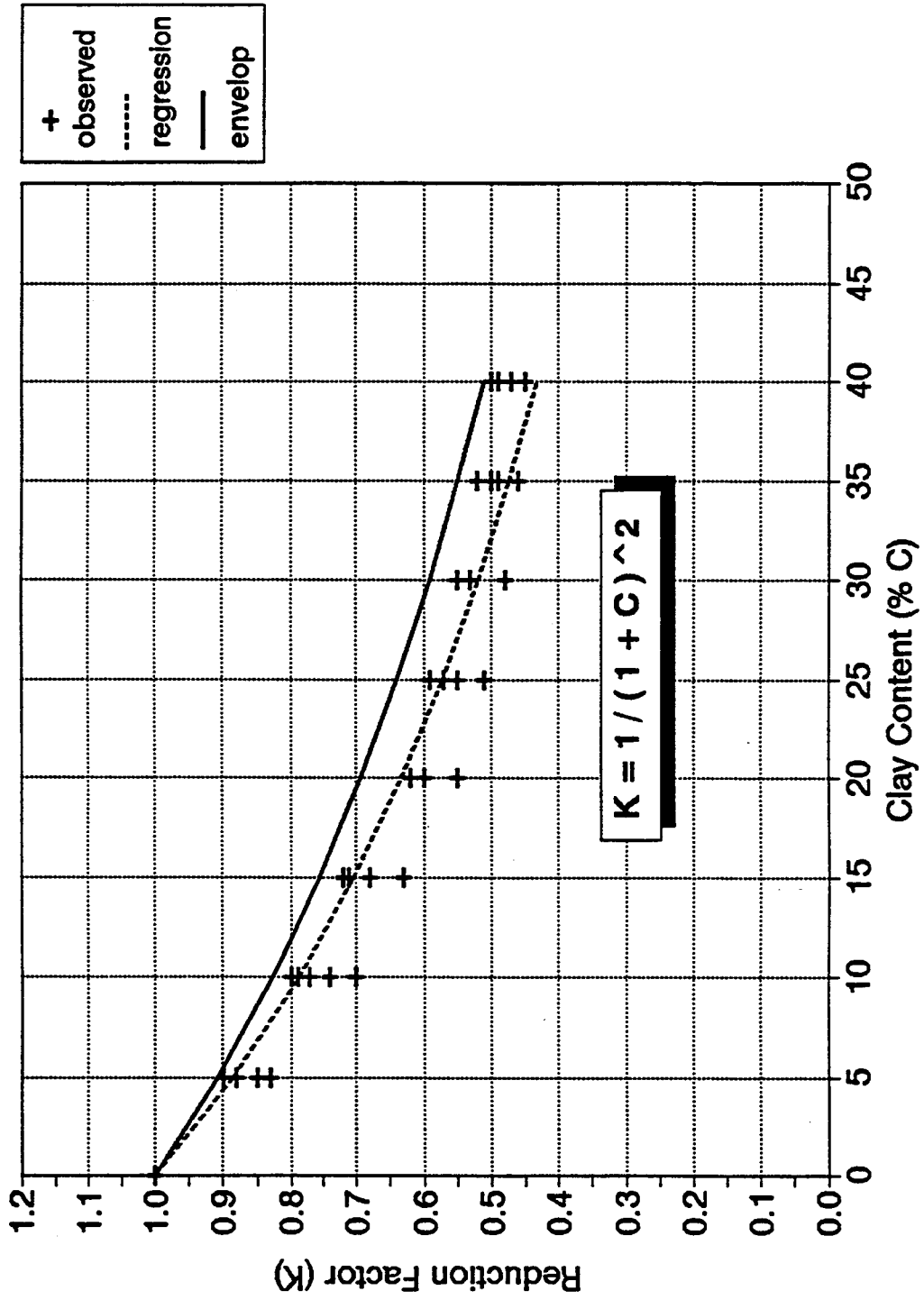


Figure 5-14. Effect of Clay Content in Sandy Soils on the Reduction Factor (K).

The value of linear correlation coefficient, $R=0.95$, between the observed and predicted reduction factor indicates how well the equation fits the data.

In order to form an envelope for all data, the exponent 2.5 in equation 5-7 was modified to 2, it resulted in

$$K = \frac{1}{(1 + C)^2} \quad (5-8)$$

The comparison between the observed and predicted reduction factor is shown in Figure 5-14.

5-3-2 Effect of Flow Intensity on Pier Scour in Mixtures

Generally, it was observed that the dimension of the scour hole increased with increasing the flow discharge. At the same water depth, the scour depth was varied only as a function of the approach velocity. Due to this fact, the stream velocity and Froude number are appropriate measures of the flow strength to analyze the behavior of scour depth in different mixtures. The approach velocity as cited in section 4-5 is the average of five vertical velocity profiles in the approach zone of each pier. Figures 5-15 through 5-18 show the distribution of velocities in the approach area for each pier.

The approach velocity and Froude number were plotted versus the scour ratio in Figures 5-19 and 5-20 respectively.

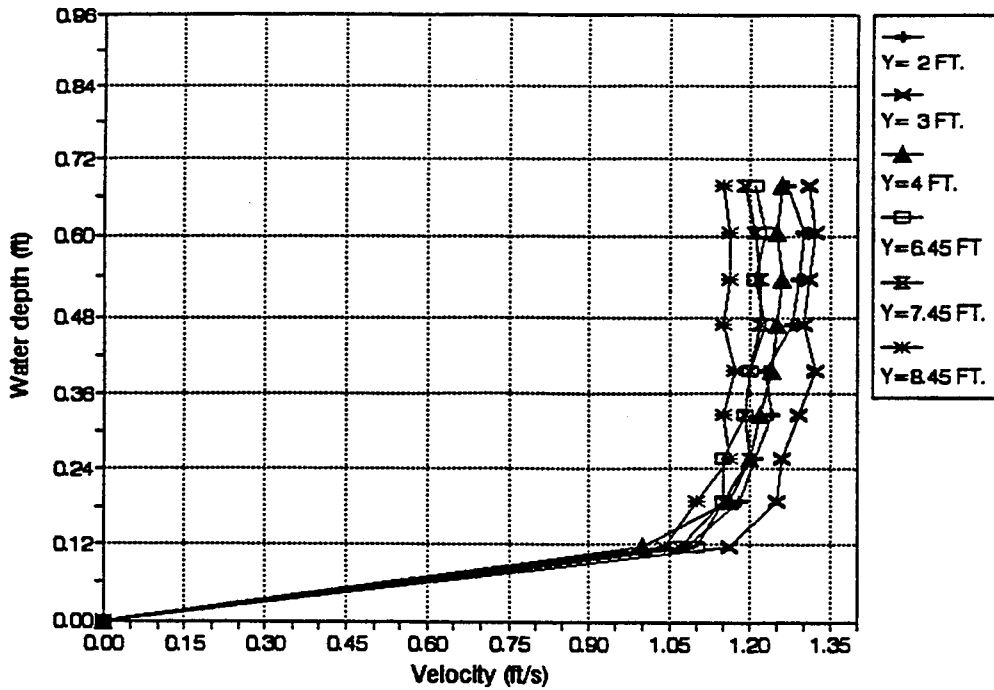


Figure 5-15. Vertical Velocity Distribution Across the Test Flume at the Approach of Piers PB and PC at Sec. 53 for Run R16

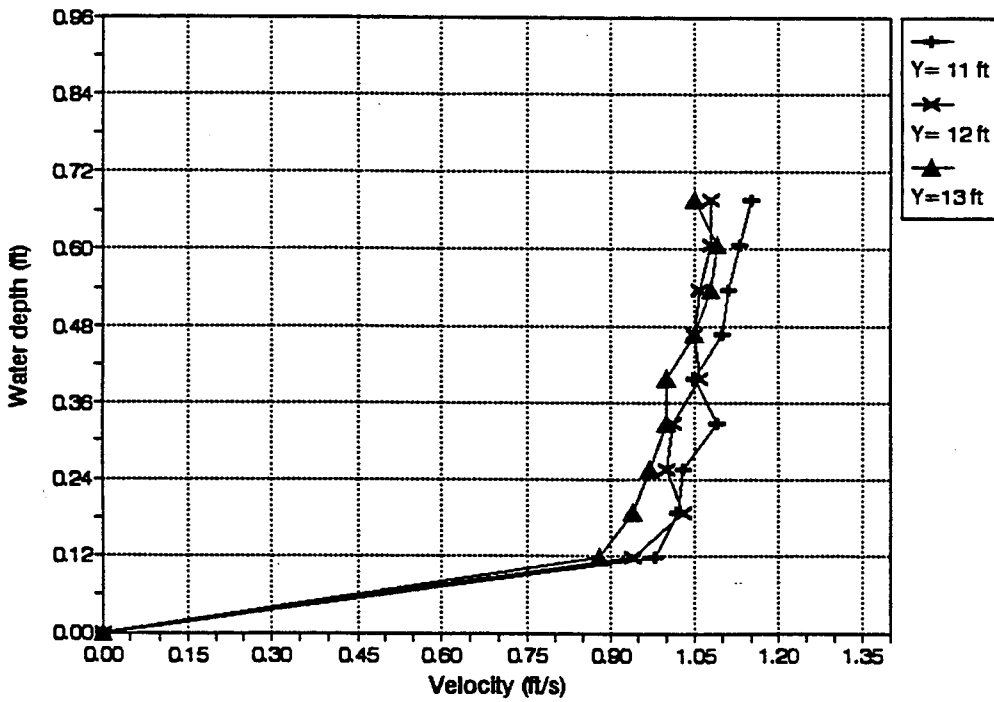


Figure 5-16. Vertical Velocity Distribution Across the Test Flume at the Approach of Pier PA at Sec. 53 for Run R16

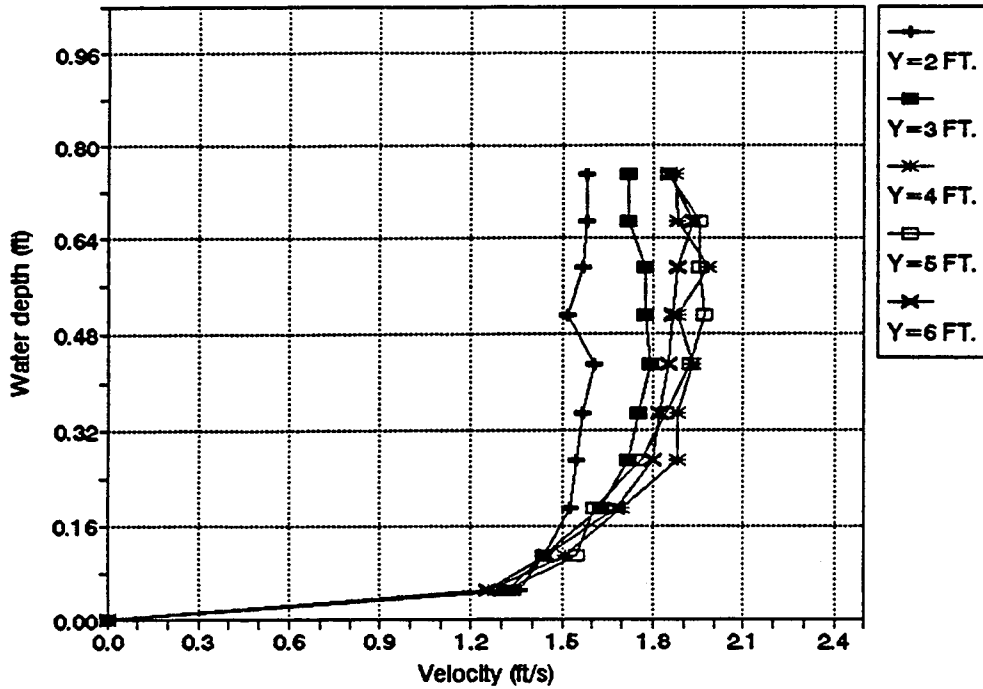


Figure 5-17. Vertical Velocity Distribution Across the Test Flume at the Approach of Pier PA at Sec. 37.6 for Run R30

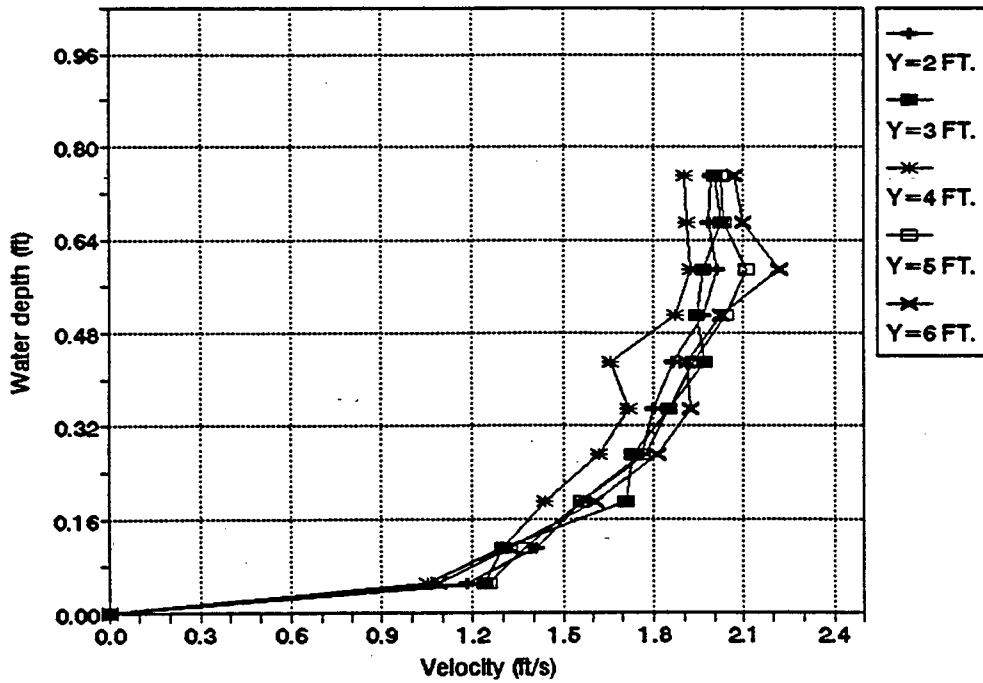


Figure 5-18. Vertical Velocity Distribution Across the Test Flume at the Approach of Pier PB at Sec. 73 for Run R30

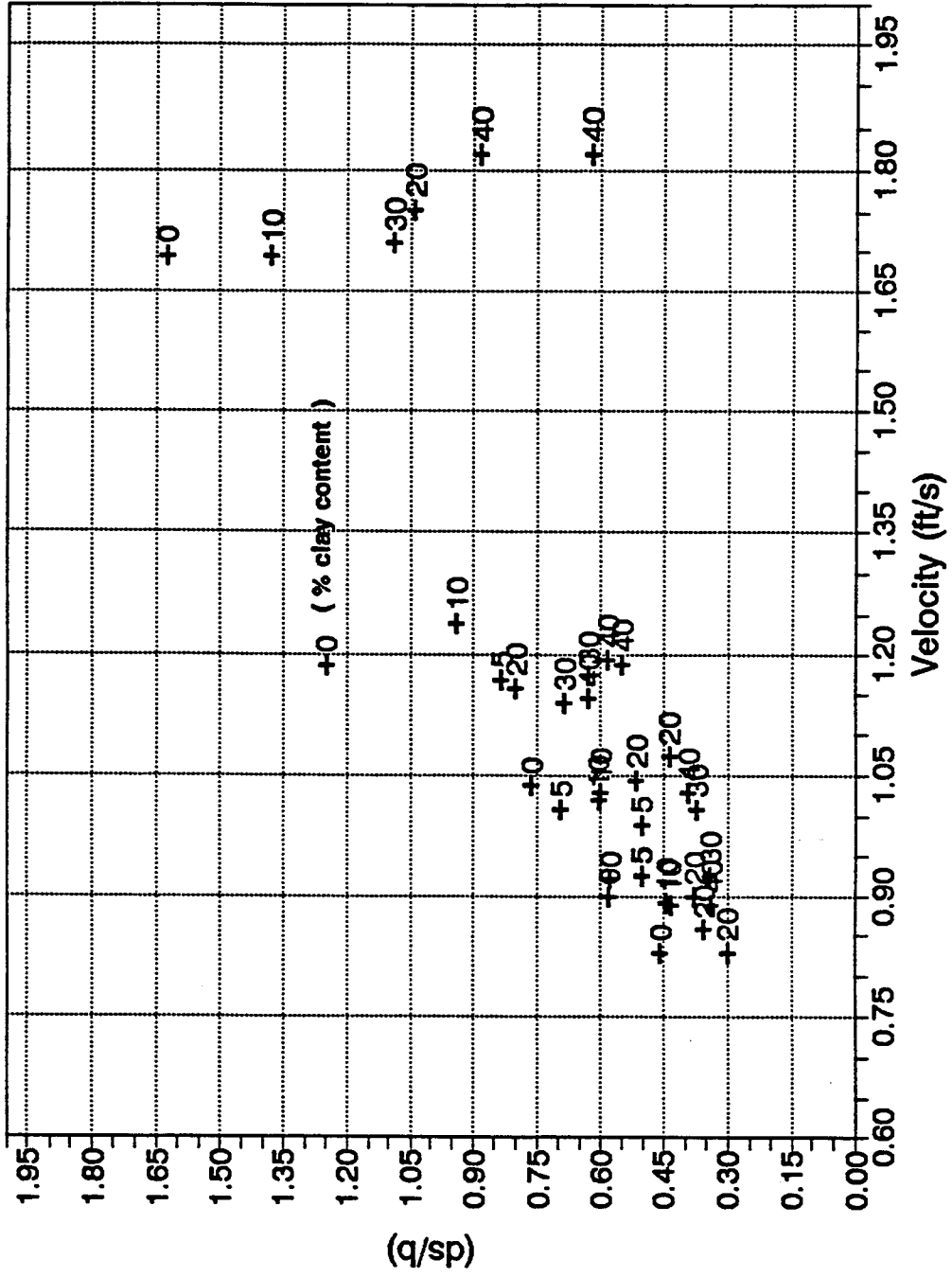


Figure 5-19. Effect of Clay Content on the Scour Ratio for Various Approach Velocities.

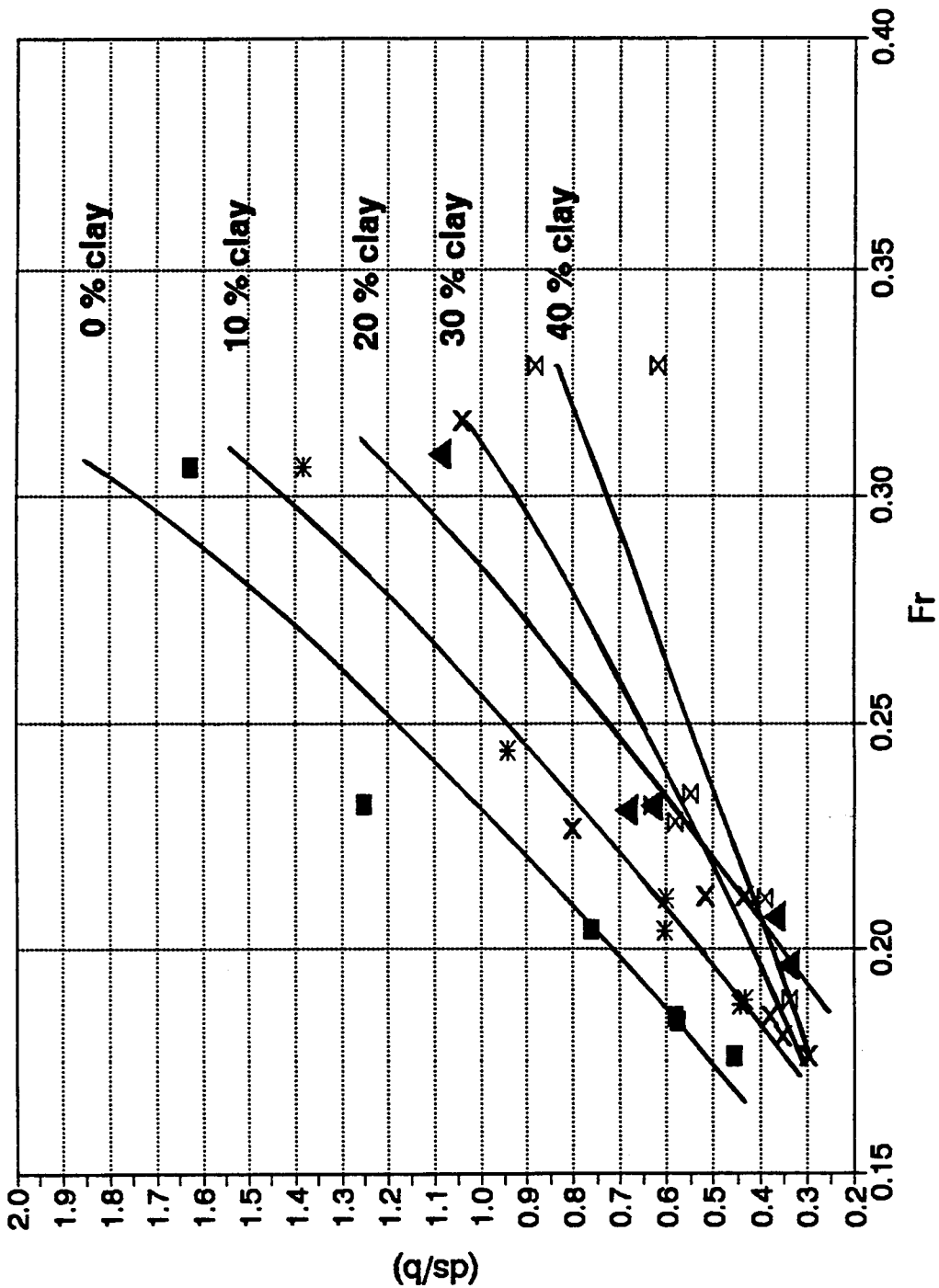


Figure 5-20. Effect of Clay Content on the Scour Ratio for Various Approach Froude Number

The lines on the graphs show the trend of the data for various clay contents in the mixtures. A definite trend in each of the curves is apparent. Generally, when the approach velocity or Froude number increases, more materials will be eroded from around the piers.

5-3-3 Effect of the Test Duration on Pier Scour in Mixtures

In this investigation, all test runs were conducted with 960 minutes test duration to insure the equilibrium scour depth was reached and became constant for a sufficient period of time. The development of scour depth with time was observed by the use of a mirror placed inside each of the plexiglass piers and by using a scale mounted on the walls of the piers.

Examples of the typical relationship between the scour depth and time of scour for various clay contents and different flow conditions are shown in Figures 5-21 and 5-22.

Approximately 90% of the scour occurred during the first 360 minutes of each test. As shown in Figures 5-21 and 5-22, the equilibrium scour depth was reached in a shorter time for a mixture of lower clay content compared to that in a mixture of higher clay content. This means that the higher the clay content in a soil, the longer the time it takes to reach the equilibrium scour depth.

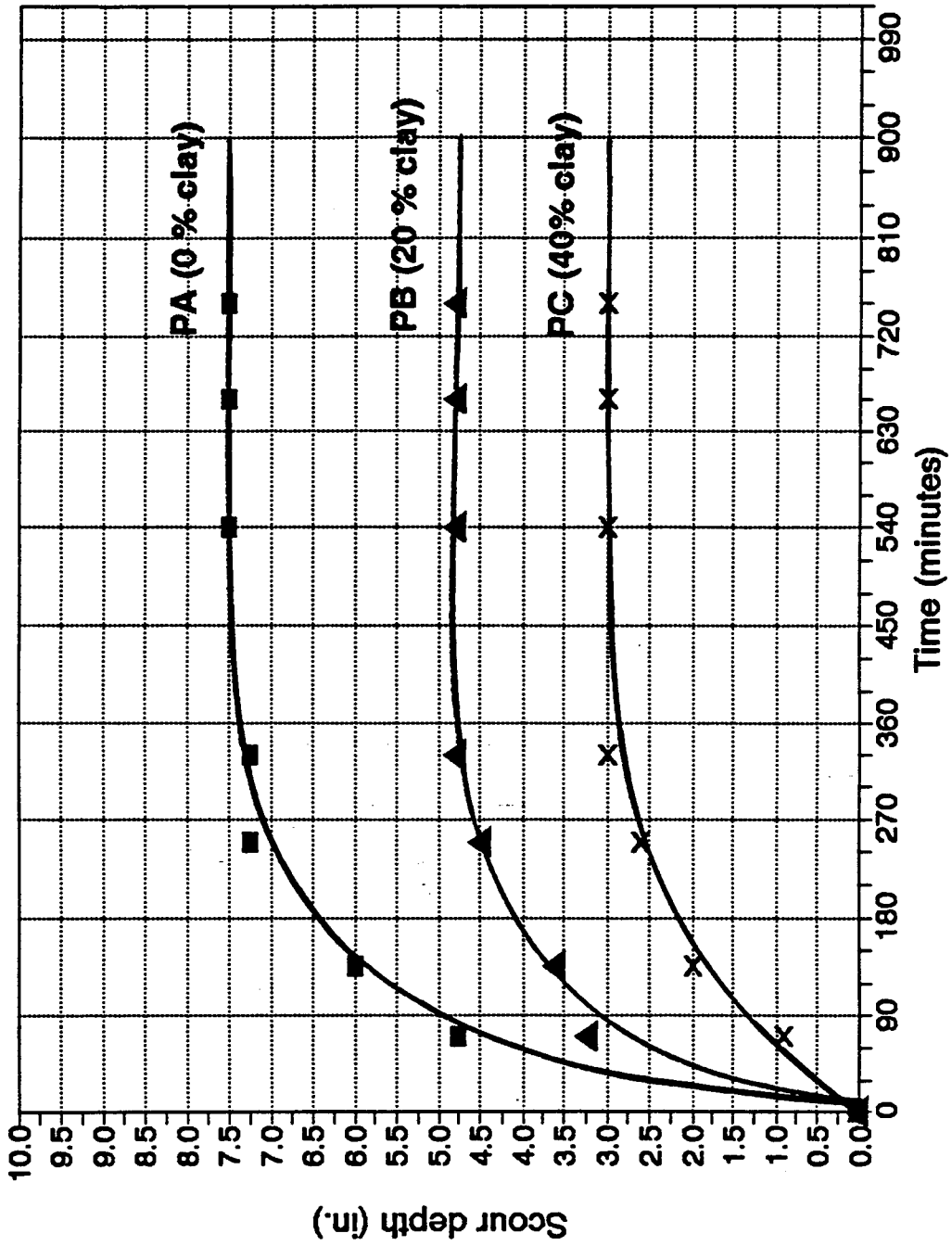


Figure 5-21. Effect of Clay content on Scour Development for Run R32

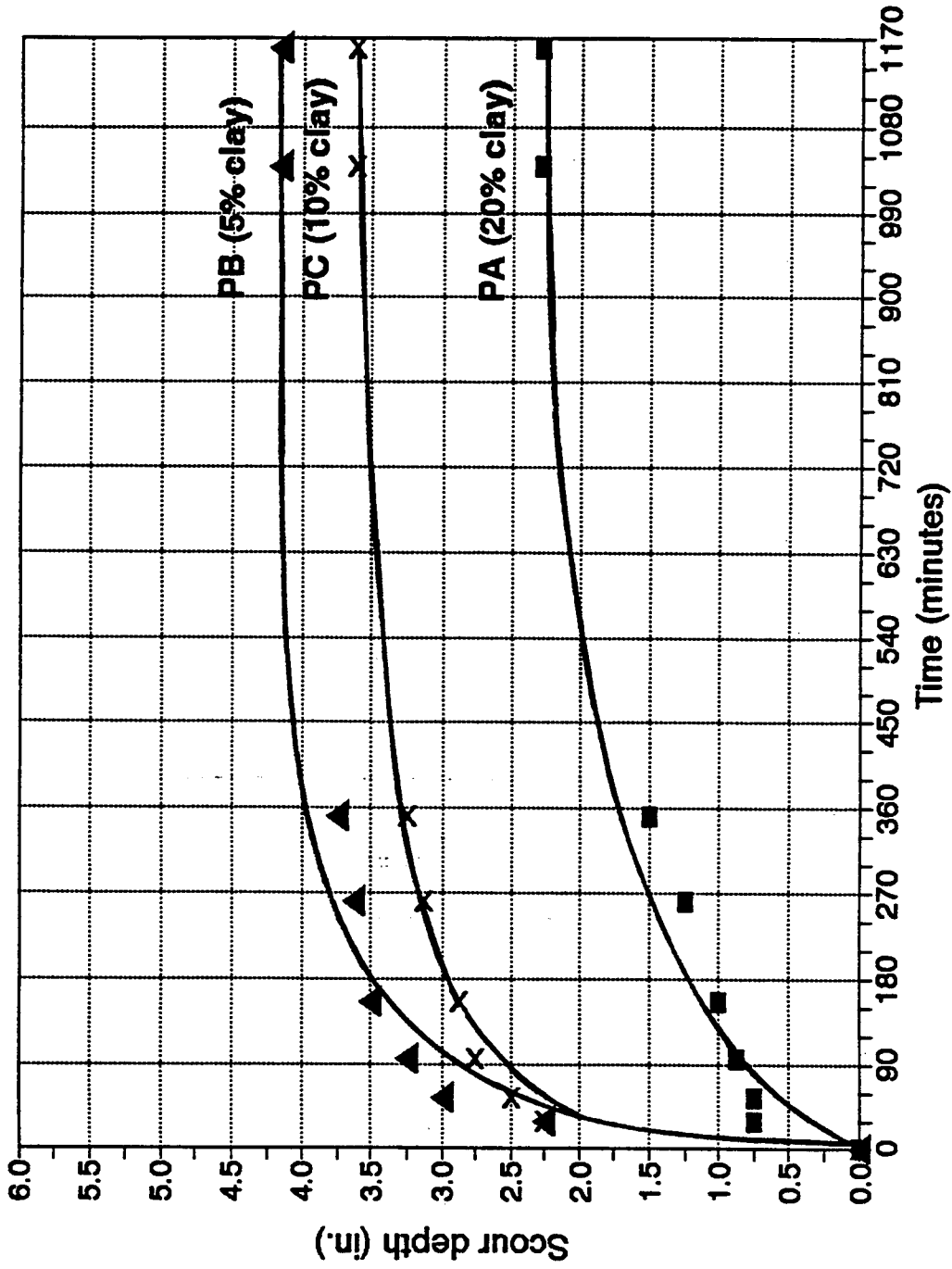


Figure 5-22. Effect of Clay Content on Scour development for Run R21

5-3-4 Regression Analysis for Pier Scour in Mixtures

Based on the dimensional analysis performed and the experimental data points, a stepwise regression analysis was used to develop a new clear water scour depth in a mixture of sandy-clayey soils.

During this set of test runs, the initial water content, compaction, and soil shear strength were kept constant, hence these parameters will be eliminated from Equation 5-3. For the purpose of using the scour depth predictor in sandy-clayey mixtures or in sandy soil, one was added to the clay content to allow for 0% clay content, thus equation 5-3 becomes:

$$\frac{d_s}{b} = f(F_r, 1+C) \quad (5-9)$$

The logarithmic values of (d_s/b) were regressed against the remaining dimensionless groups in equation 5-9 using the multiple linear regression form in the commonly used SAS statistical analysis package. The theory of this program is based on the least squares method. The best-fit regression equation which describes the data points given in Table 5-1 can be expressed as:

$$\frac{d_s}{b} = 18.92 \left(\frac{F_r^{2.06}}{(1+C)^{1.88}} \right) \quad (5-10)$$

in which C is the clay content in the sandy soil (C varies

between 0 and 0.4). This equation was developed for clear water scour and was tested for Froude numbers ranging from 0.18 to 0.33. The correlation coefficient, $R=0.85$, between the observed and predicted scour ratio indicates how well the equation fits the data points. The best-fit regression equation output from SAS program is presented in Table 5-2.

For the purposes of simplicity form, equation 5-10 was modified; it resulted in :

$$\frac{d_s}{b} = 18.9 \left(\frac{F_r}{1 + C} \right)^2 \quad (5-11)$$

The scour depth computed from this equation results in slightly larger values than those computed from equation 5-10. A comparison of equation 5-10 with the experimental data is shown in Figure 5-23. The dashed lines in this Figure represent ± 20 percent error boundaries. As shown in Figure 5-23 with the exception of 2 data points, all data represented by equation 5-11 with maximum error of ± 20 percent.

5-4 Analysis of Pier Scour in Compacted Unsaturated Cohesive Soils

In set 2, 17 test runs were carried out to investigate the behavior of pier scour in unsaturated clay soil at various degrees of compaction. All the concepts and the principal results obtained in this set of experiments are summarized in

Table 5-2. Regression Output from SAS Program for Set 1

Dependent Variable: LOG(ds/b)
Analysis of Variance

Source	DF	Sum of Squares	Mean Square	F value	Prob>F
Model	2	1.01218	0.50609	104.366	0.0001
Error	36	0.17457	0.00485		
C total	38	1.18675			

Root MSE	Dep Mean	C.V.	R-Square	Adj-R-Sq
0.06964	-0.22536	30.9004	0.8529	0.8447

Parameter Estimates

Variable	DF	Parameter Estimate	Standard Error	T for Ho: Parameter=0	Prob> T
INTERCEP	1	1.276727	0.1058265	12.064	0
Fr	1	2.085649	0.15100037	13.812	0
C	1	-1.883512	0.23058824	-8.168	0

CORRELATION

CORR.	Fr	C	(ds/b)
Fr	1.0000	0.2986	0.7618
C	0.2986	1.0000	-0.2709
(ds/b)	0.7618	-0.2709	1.0000

Regression Models for Dependent Variable: LOG(ds/b)

Number in Model	R-Square	Adjusted R-Square	C(p)	MSE	Variables in Model
1	0.58027283	0.56892886	67.72099	0.01346251	Fr
1	0.07336803	0.04832392	191.7772	0.0297212	C
2	0.85290078	0.8447286	3	0.0048918	Fr, C

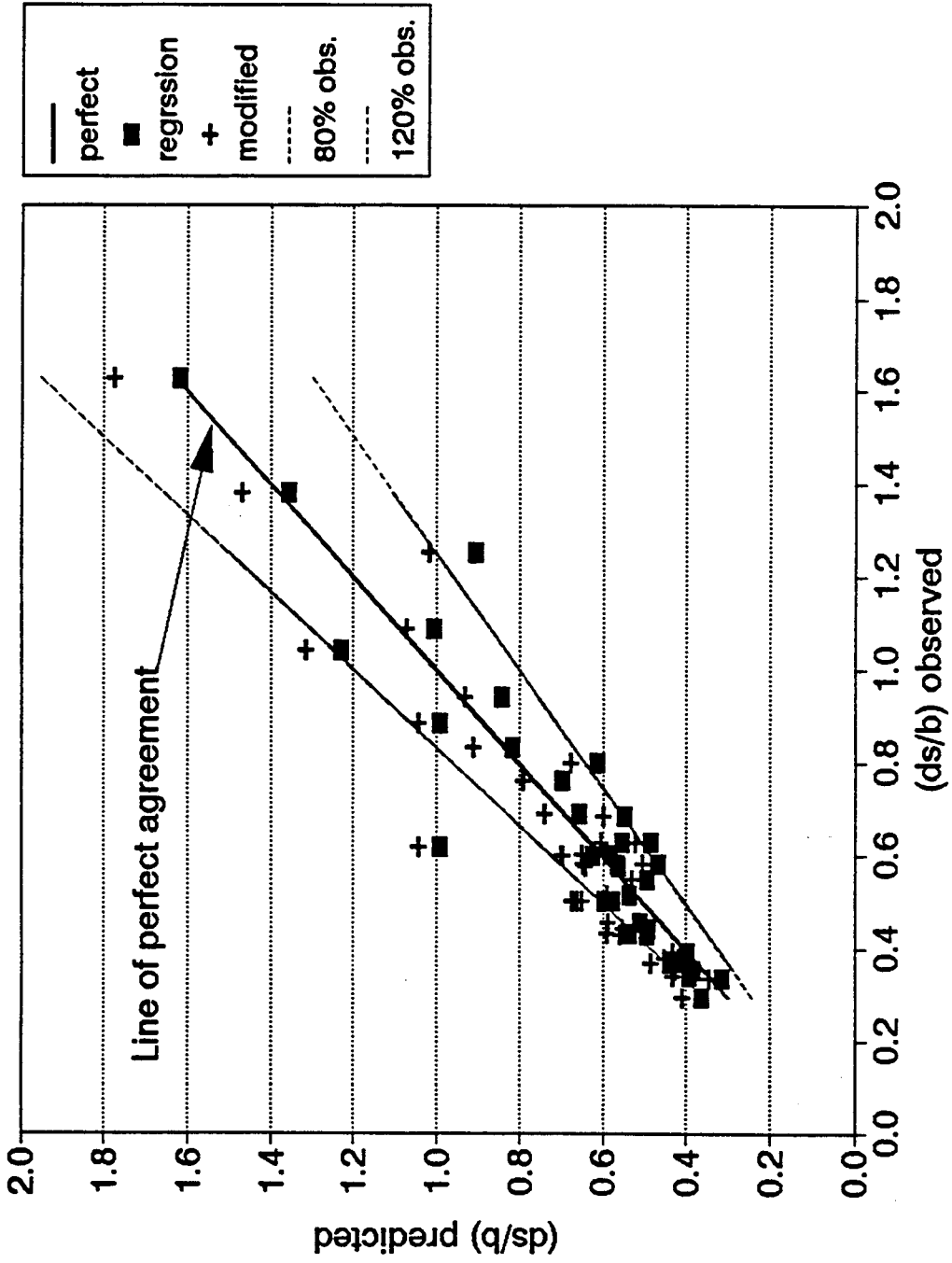


Figure 5-23 Comparison Between the observed and Predicted Scour Ratios in Sandy-Clayey Soil

Tables 5-3 and 5-4. In general, as expected, these Tables indicate that the scour depth decreases with increasing the degree of compaction. The less compacted clay material allows water to penetrate through the surface of clay particles causing swelling and resulting in the reduction of the interparticle bonding force which in turn increases the scour depth. This fact has been confirmed by many investigators in previous studies.

5-4-1 Geometry of Scour Hole in Unsaturated Cohesive Soils

The shape of the scour hole in cohesive soils is conical in nature with maximum scour depth occurring immediately upstream of the pier as in non-cohesive soils. But compared to non-cohesive soils, the slope of the scour hole was observed to be very steep and in some cases, approaching 90° (vertical). As expected, the results of experiments showed that the slope of the scour hole increases as the compaction of cohesive soil increases.

In cohesive soil erosion process, once the material eroded and removed from its environments, it remains in suspension. Therefore, there is no deposition upstream or downstream the scour hole compared to that in sandy soils.

The view of the scour holes for some runs are shown in Figures 5-24 through 5-27.

Table 5-3. Summary of Experimental Conditions and Results for Set 2
(Effect of Compaction of Clay Soil on Pier Scour)
Subset 2.A (IWC = 20%)

Run - Pier No.	Q (cfs)	S (kg/cm ²)	Wet Density (lb/ft ³)	Dry Density (lb/ft ³)	Comp. (%)	Approach Y (ft)	Approach V (ft/s)	Fr	ds (ft)	ds/b	Ve (ft/s)	(Ve/b ³)
13-PE	11	0.45	122.76	102.3	93.0	0.804	0.837	0.165	0	0.00	0.0	0.00
13-PF	11	0.38	114.84	95.7	87.0	0.804	0.854	0.168	0	0.00	0.0	0.00
14-PE	10	0.32	105.6	88	80.0	0.71	0.872	0.182	1.824	0.30	54.9	0.25
14-PF	10	0.26	96.36	80.3	73.0	0.71	0.865	0.181	2.231	0.37	64.1	0.30
15-PE	12	0.45	122.76	102.3	93.0	0.747	0.956	0.195	0	0.00	0.0	0.00
15-PF	12	0.38	114.84	95.7	87.0	0.747	0.992	0.202	0	0.00	0.0	0.00
16-PE	14.6	0.3	105.6	88	80.0	0.82	1.022	0.199	2.376	0.40	65.3	0.30
16-PF	14.6	0.25	96.36	80.3	73.0	0.82	1.128	0.220	2.88	0.48	170.5	0.79
17-PE	10	0.32	105.6	88	80.0	0.71	0.872	0.182	1.848	0.31	49.5	0.23
17-PF	10	0.26	96.36	80.3	73.0	0.71	0.865	0.181	2.088	0.35	75.1	0.35
18-PE	12	0.32	105.6	88	80.0	0.747	0.956	0.195	2.064	0.34	73.2	0.34
18-PF	12	0.2	96.36	80.3	73.0	0.747	0.992	0.202	2.54	0.42	92.3	0.43
19-PE	14.6	0.15	85.8	71.5	65.0	0.797	1.039	0.205	3.036	0.51	244.1	1.13
19-PF	14.6	0.07	76.56	63.8	58.0	0.797	1.082	0.214	3.912	0.65	448.5	2.08
20-PE	13.5	0.15	85.8	71.5	65.0	0.777	1.028	0.206	2.85	0.48	280.8	1.30
20-PF	13.5	0.1	76.56	63.8	58.0	0.777	1.067	0.213	3.756	0.63	398.7	1.85
21-PE	12	0.18	85.8	71.5	65.0	0.751	0.956	0.194	2.844	0.47	110.8	0.51
21-PF	12	0.09	76.56	63.8	58.0	0.751	0.992	0.202	3.96	0.66	209.7	0.97
22-PE	10	0.16	85.8	71.5	65.0	0.718	0.853	0.177	2.25	0.38	88.5	0.41
22-PF	10	0.09	76.56	63.8	58.0	0.718	0.855	0.178	2.76	0.46	143.4	0.66
27-PA	11	0.1	76.56	63.8	58	0.855	1.439	0.274	6.71	1.12	1281.5	5.93
27-PB	11	0.25	96.36	80.3	73	0.855	1.433	0.273	4.92	0.82	762.8	3.53
27-PC	11	0.35	105.6	88	80	0.855	1.47	0.280	4.44	0.74	213.6	0.99
35-PA	15	0.1	76.56	63.8	58	0.89	1.8	0.336	9	1.50	2203.0	10.20
35-PB	15	0.2	96.36	80.3	73	0.78	1.848	0.369	7	1.17	1226.6	5.68
35-PC	15	0.45	114.84	95.7	87	0.84	1.92	0.369	5.28	0.88	823.8	3.81

NOTES:

- * Runs 13 through 22 were conducted in the Seventeen-foot wide flume.
- * Runs 27 through 35 were conducted in the Eight-foot wide flume.
- * The accuracy of the Compactions 58, 65, 73, 80, and 87% is (+-1.5%).

Table 5-4. Summary of Experimental Conditions and Results for Set 2
(Effect of Compaction of Clay Soil on Pier Scour)
Subset 2.B (WC = 15%)

Run- Pier No.	Q (cfs)	S kg/cm ²	Wet Density lb/ft ³	Dry Density lb/ft ³	Comp. (%)	Approach Y (ft)	Approach V (ft/s)	Fr	ds (in.)	ds/b	Ve (in. ³)	(Ve/b ³)
23-PE	14.6	0.07	73.37	63.8	58.0	0.81	1.039	0.212	4.80	0.8	1067.9	4.944
23-PF	14.6	0.1	92.345	80.3	73.0	0.81	1.082	0.212	3.12	0.52	781.1	3.616
24-PE	13.5	0.07	73.37	63.8	58	0.777	1.028	0.206	4.596	0.77	872.0	4.037
24-PF	13.5	0.1	92.345	80.3	73	0.777	1.067	0.213	3.24	0.54	701.8	3.249
25-PD	12	0.15	101.2	88	80	0.751	0.931	0.189	2.352	0.39	192.2	0.890
25-PE	12	0.1	92.345	80.3	73	0.751	0.956	0.194	2.58	0.43	366.1	1.695
25-PF	12	0.07	73.37	63.8	58	0.751	0.99	0.201	4.464	0.74	469.9	2.175
26-PD	10	0.15	101.2	88	80	0.718	0.774	0.161	1.452	0.24	61.0	0.283
26-PE	10	0.1	92.345	80.3	73	0.718	0.853	0.177	1.836	0.31	88.5	0.410
26-PF	10	0.07	73.37	63.8	58	0.718	0.855	0.178	2.208	0.37	122.0	0.565
33-PA	11	0.07	73.37	63.8	58	0.85	1.439	0.275	7.38	1.23	1830.7	8.476
33-PB	11	0.1	92.345	80.3	73	0.85	1.433	0.274	5.1	0.85	1144.2	5.297
33-PC	11	0.18	110.055	95.7	87	0.855	1.47	0.280	3.72	0.62	610.2	2.825

NOTES:

- * Runs 23 through 26 were conducted in the Seventeen-foot wide flume.
- * Run 33 was conducted in the 8-foot wide flume.
- * The accuracy of the compactions 58, 73, 80, and 87% is (+-1.5%).

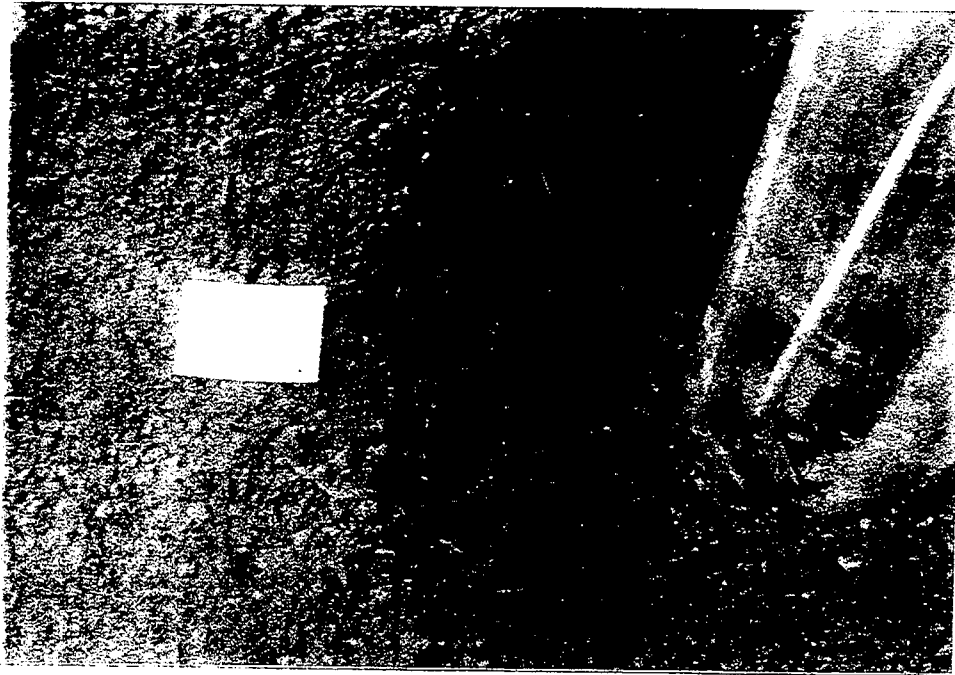


Figure 5-24. View of the Scour Hole for Pier A (58% Comp.)
at the End of Run R27, Q=11 cfs

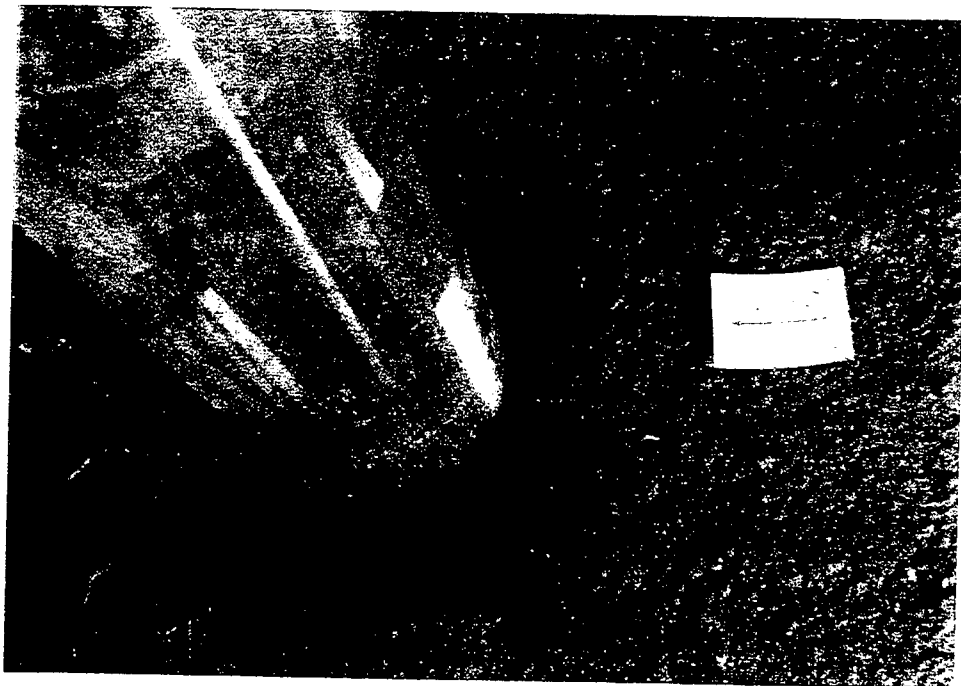


Figure 5-25. View of the Scour Hole for Pier C (80% Comp.)
at the End of Run R27, Q=11 cfs

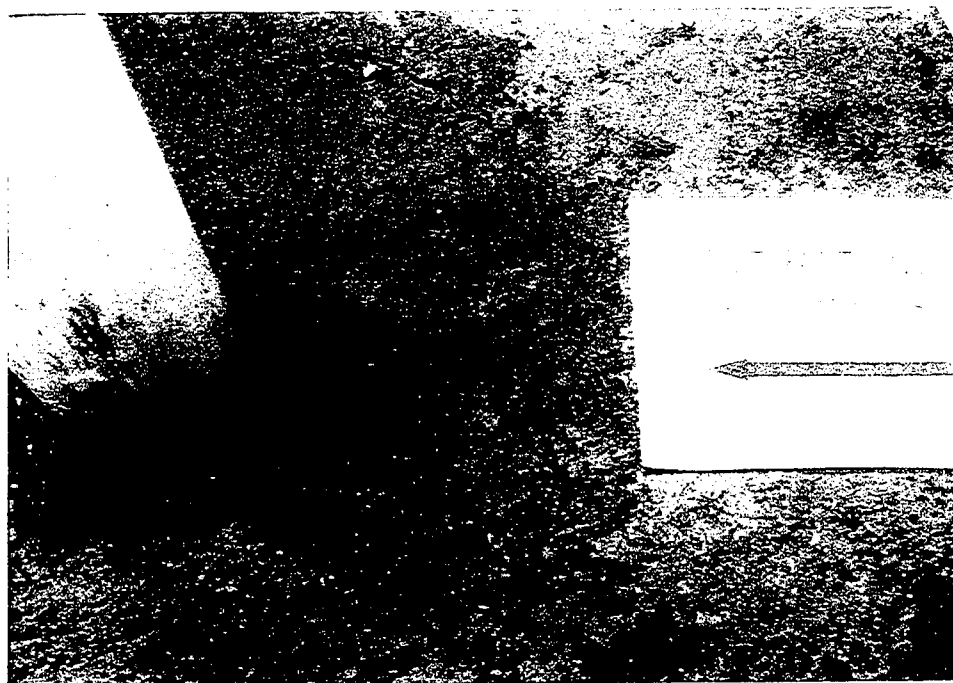


Figure 5-26. View of the Scour Hole for Pier E (80% Comp.)
at the End of Run R17, $Q=9.96$ cfs



Figure 5-27. View of the Scour Hole for Pier E (73% Comp.)
at the End of Run R26, $Q=10$ cfs

Examples of cross sections passing across the scour holes in cohesive soils at various degrees of compaction are presented in Figures 5-28 through 5-31 for various flow conditions.

For set 2 of test runs, the data points plotted in Figure 5-32 show the relationship between the scour ratio (d_s/b) and degree of compaction under different flow conditions. The results indicate that for a given flow condition, the scour depth decreases as the soil compaction increases.

The relationship between the scour depth and scour volume in dimensionless form is shown in Figure 5-33 for all data points. By fitting the best line to the points plotted on Figure 5-33, the following relationship is determined:

$$\left(\frac{d_s}{b} \right)_p = 0.5 \sqrt{\frac{V_s}{b^3}} \quad (5-12)$$

The conclusion that may be made is that the volume of scour hole (the inverted cone) is reduced significantly by increasing the degree of soil compaction. The time development of scour depth was also reduced significantly.

5-4-2 Effect of Flow Intensity on Pier Scour in Unsaturated Cohesive Soils

As was mentioned before, all test runs were conducted under steady gradually varied flow conditions. The approach flow depth was kept approximately constant and all other

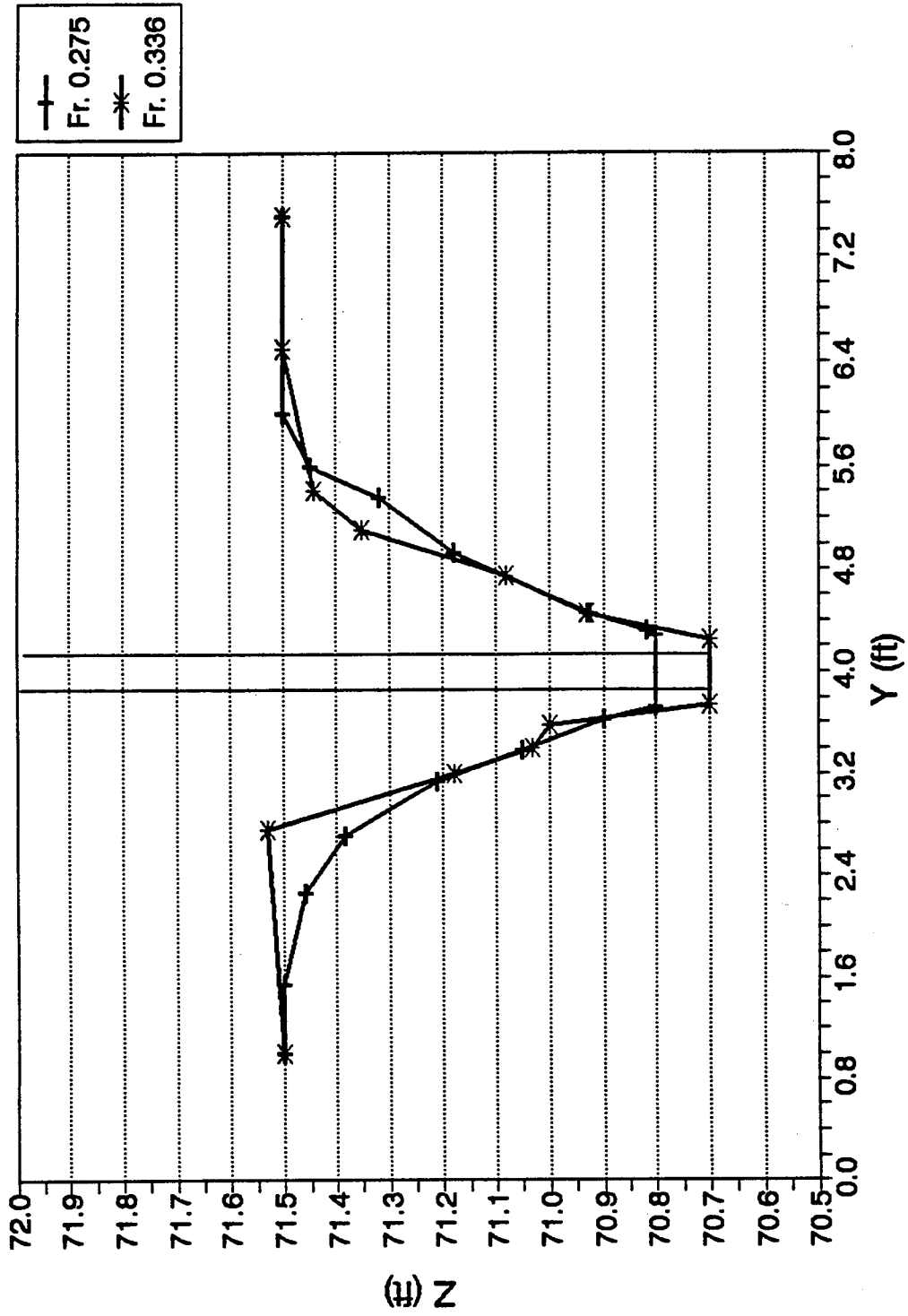


Figure 5-28. Effect of Compaction on the Cross Section Geometry Along the Center Line of Pier PA for Runs R33 and R35 (58% Comp.)

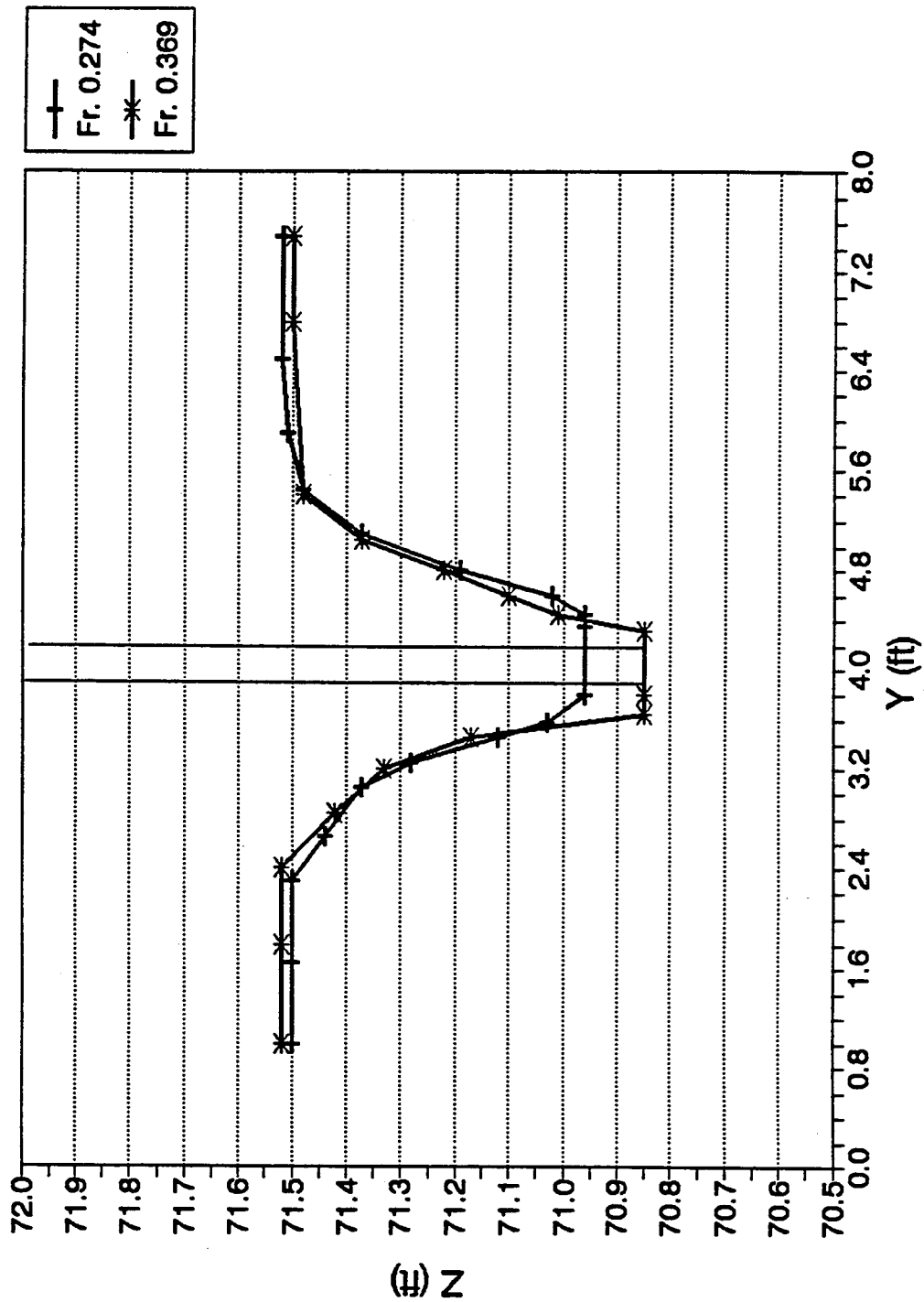


Figure 5-29. Effect of Compaction on the Cross Section Geometry Along the Center Line of Pier PB for Runs R33 and R35 (73% Comp.)

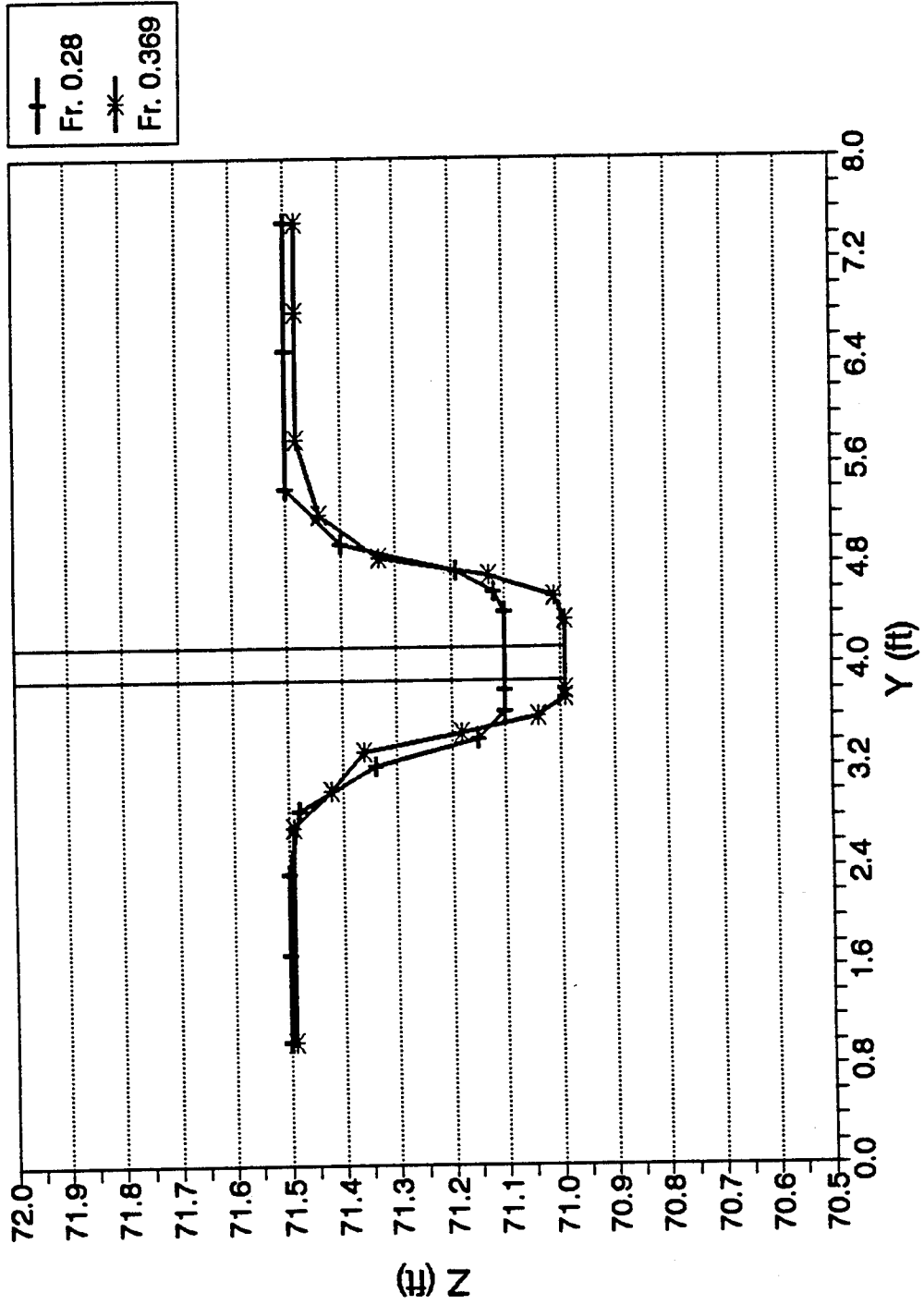


Figure 5-30. Effect of Compaction on the Cross Section Geometry Along the Center Line of Pier PC for Runs R33 and R35 (87% Comp.)

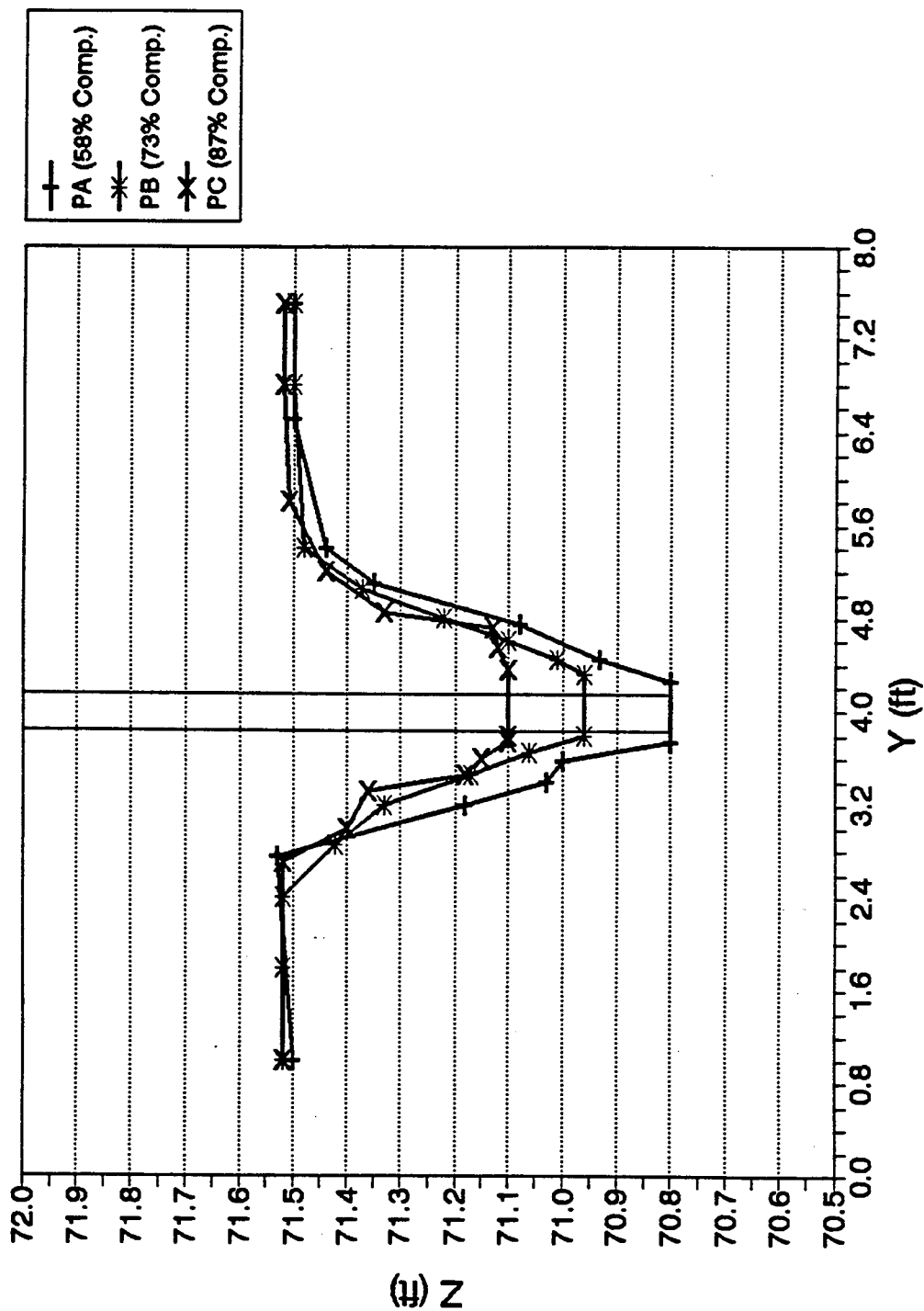


Figure 5-31. Effect of Compaction on the Cross Section Geometry Along the Center Line of Piers PA, PB, and PC for Run R35

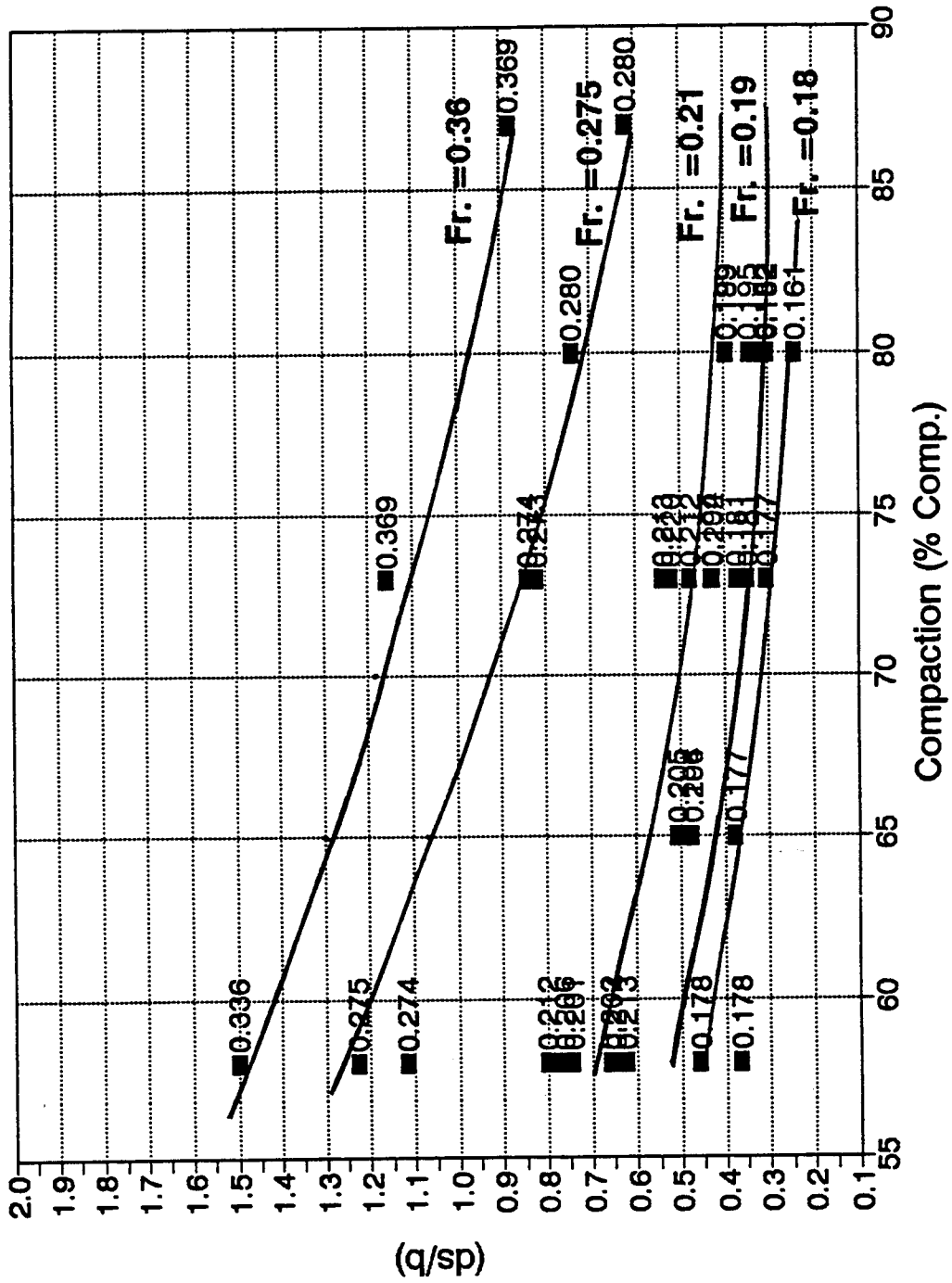


Figure 5-32. Effect of Compaction on the Scour Ratio.

parameters were constant, while the stream velocity was the only parameter that varied against the scour depth.

In general, the higher compacted clay required higher velocity or Froude number to initiate scour. Figures 5-34 and 5-35 demonstrate the effect of the approach flow velocity and Froude number on scour ratio. These Figures show an increase in scour ratio with an increase in the approach Froude number or velocity for various degrees of compactions. They also show that, at the same flow condition, the scour depth decreases with increasing the soil degree of compaction.

5-4-3 Effect of the Test Duration on Pier Scour in Unsaturated Cohesive Soils

As cited before, all test runs lasted 960 minutes to ensure that the maximum scour depth was reached and the rate of scour became very slow, almost zero to record. The obtained scour in cohesive soil is limited in time scale to the experimental laboratory times.

It was concluded that the development of scour depth with time is strongly affected by the degree of compaction of cohesive soils around the site of the piers.

The scour depths are plotted versus the time in Figures 5-36 and 5-37 as examples for some runs. The curves on the graphs show the trend of the data for these flow conditions. It was observed that for a cohesive soil at 58% compaction,

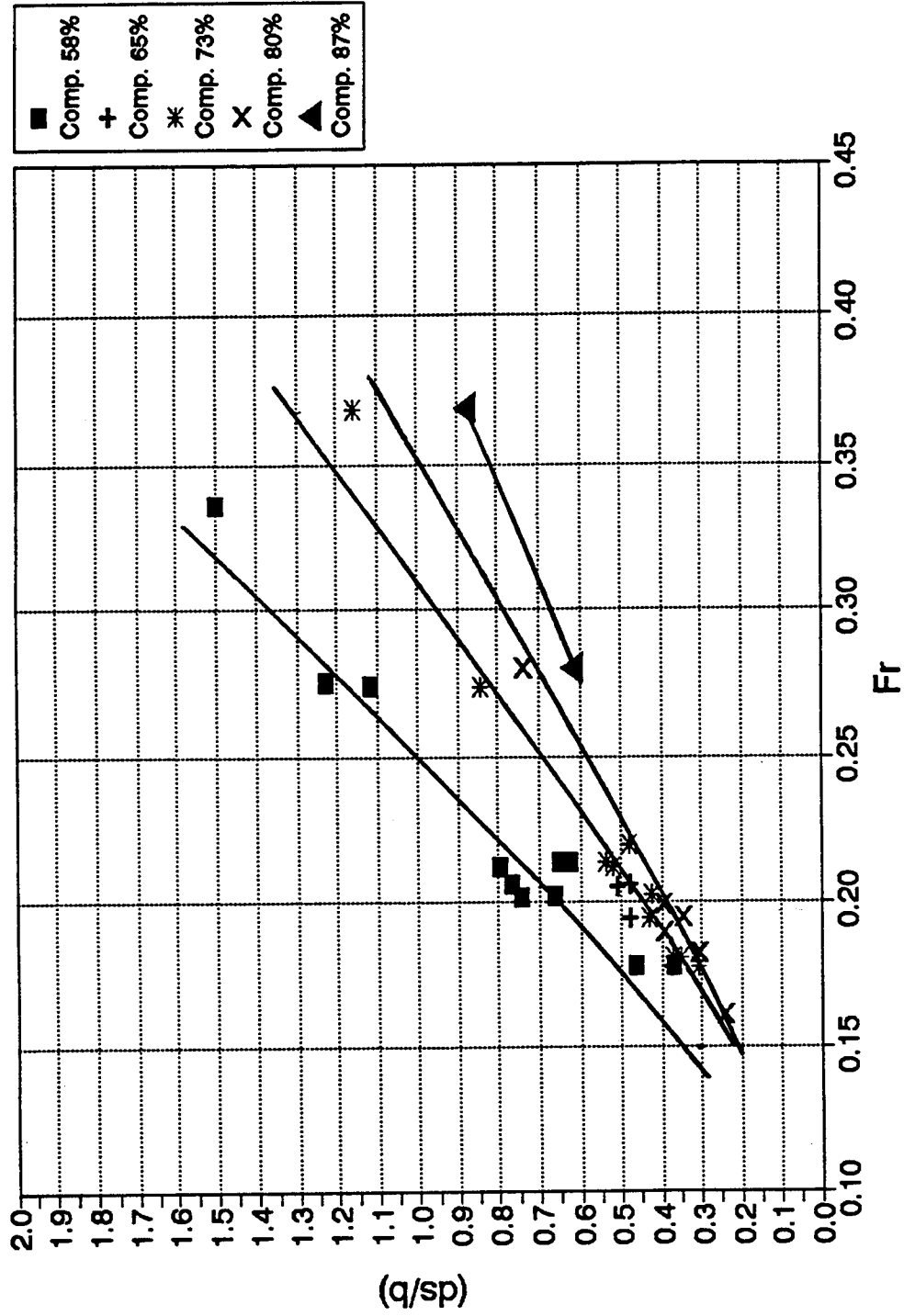


Figure 5-35. Effect of Compaction on the Scour Ratio for Various Froude Numbers

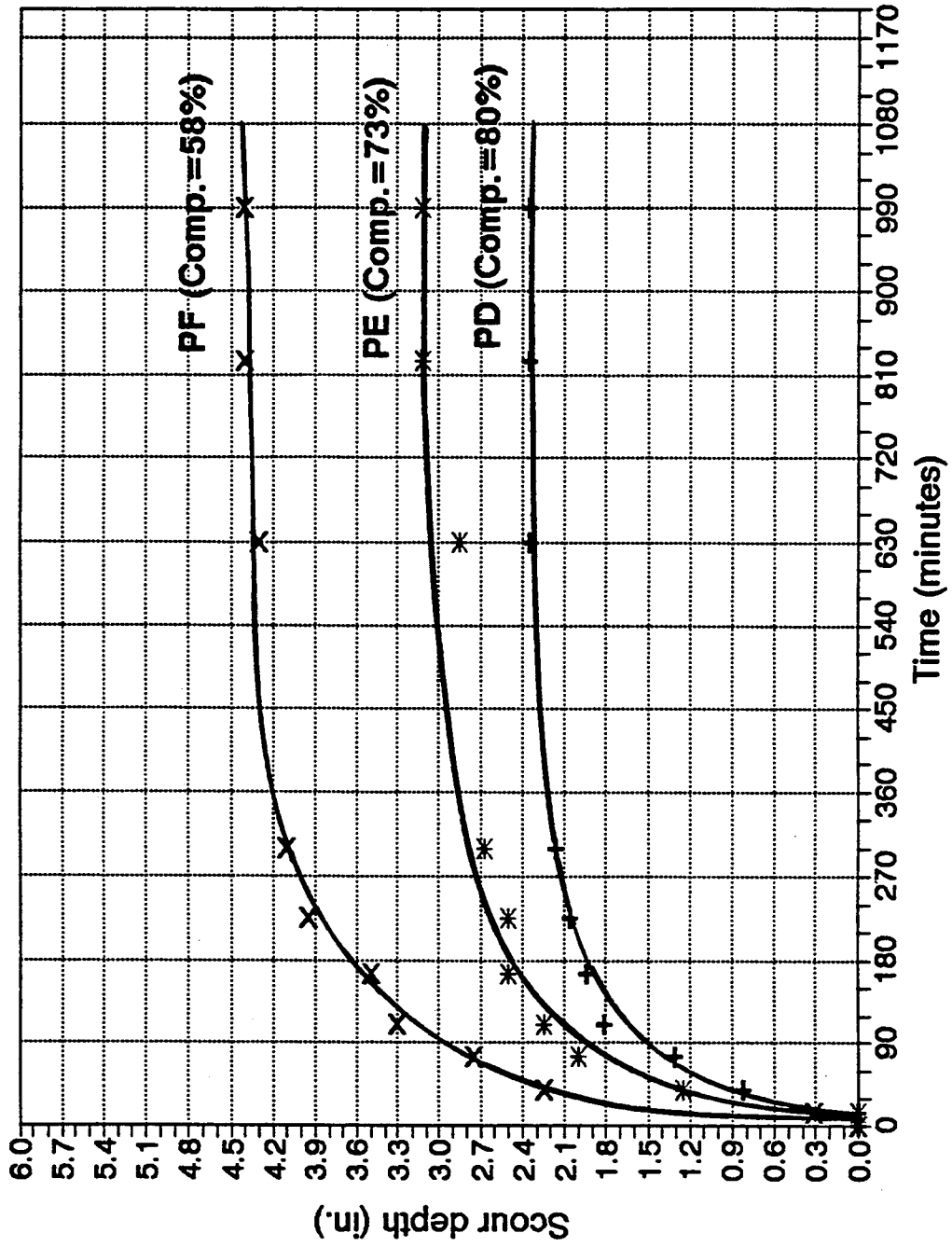


Figure 5-36. Effect of Compaction on Scour Development for Run R25

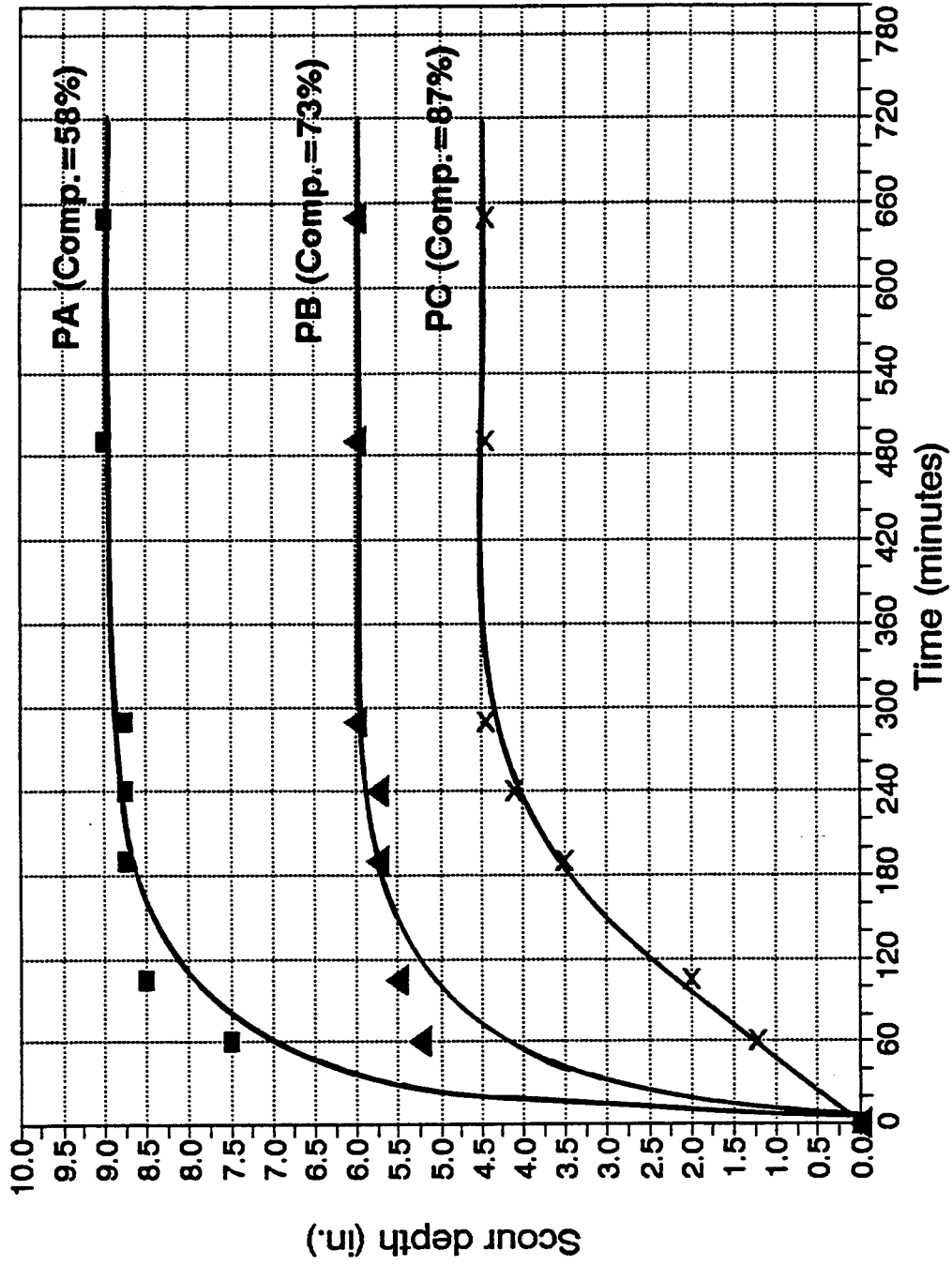


Figure 5-37. Effect of Compaction on Scour Development for Run R35

90% of the equilibrium scour depth is reached in the first 90 minutes, while the same percentage required the first 300 minutes for a cohesive soil at 80% degree of compaction.

5-4-4 Regression Analysis for Pier Scour in Unsaturated Cohesive Soils

Since many parameters affect the development of the scour depth, the experiments had been conducted by considering only the effect of flow conditions, initial water content, soil shear strength, compaction, and accepting the other parameter as constant during the study. Thus equation 5-3 becomes:

$$\frac{d_s}{b} = f \left(IWC, F_r, \frac{S}{\rho V^2}, Comp. \right) \quad (5-13)$$

The measured values of (d_s/b) were regressed against the remaining dimensionless groups in equation 5-13 utilizing the commercial SAS computer software. The theory of this program is based on the least-squares method. The best-fit regression equation resulting from the statistical analysis of experimental data is :

$$\left(\frac{d_s}{b} \right)_p = 2.71 (IWC)^{-0.36} F_r^{1.92} \left(\frac{S}{\rho V^2} \right)^{0.023} (Comp.)^{-1.62} \quad (5-14)$$

in which IWC is the initial water content ranging from 0.15 to 0.5, Comp. is the compaction of soil ranging from 0.5 to 1, V

is the approach velocity (m/sec.), S is the soil shear strength (kg/m^2), and ρ is the water density ($\rho=\gamma/g=102 \text{ kg}\cdot\text{sec.}^2/\text{m}^4$). This equation was tested in Froude numbers ranging from 0.18 to 0.37.

The best-fit regression equation output from SAS program is presented in Table 5-5. The higher value of the correlation coefficient, $R=0.95$, between the observed and predicted scour ratio indicates the strong correlation between measured scour depths and the parameters selected for defining flow and sediment properties.

From practical considerations, a simpler form of equation 5-14 was adapted. This new equation results in slightly larger scour depth values than the best-fit equation (e.g. more conservative) and is given as:

$$\left(\frac{d_s}{b}\right)_p = 3.3 (IWC)^{-1/3} F_r^2 \left(\frac{S}{\rho V^2}\right)^{1/40} (Comp.)^{-3/2} \quad (5-15)$$

The comparison of equations 5-14 and 5-15 with the observed data is presented in Figure 5-38. The data from experiments with no scour were not used in the correlation analysis since there are not enough experimental data available for highly compacted cohesive soil under a wide range of approach flow conditions.

Table 5-5. Regression Output from SAS Program for Set 2

Dependent Variable: LOG(ds/b)
Analysis of Variance

Source	DF	Sum of Squares	Mean Square	F value
Model	4	1.23638	0.3091	59.909
Error	30	0.05799	0.00193	
C total	34	1.29437		

Root MSE	Dep Mean	C.V.	R-Square	Adj-R-Sq
0.04397	-0.26153	-16.81114	0.9552	0.9492

Variable	DF	Parameter Estimate	Standard Error	T for Ho: Parameter=0	Prob> T
INTERCEP	1	0.42925	0.31346494	1.369	0.1
IWC	1	-0.364999	0.26717511	-1.366	0.1
Fr	1	1.928244	0.25404583	7.59	0
SROHV2	1	0.024526	0.1060258	0.231	0.8
Comp.	1	-1.622395	0.36316943	-4.467	0

CORRELATION

CORR.	IWC	Fr	SROHV2	Comp.	ds/b
IWC	1.0000	0.1274	0.3722	0.0208	-0.1608
Fr	0.1274	1.0000	-0.5925	0.0692	0.6526
SROHV2	0.3722	-0.5925	1.0000	0.5882	-0.4190
Comp.	0.0208	0.0692	0.5882	1.0000	-0.8805
ds/b	0.0068	0.8503	-0.8423	-0.4120	1.0000

Regression Models for Dependent Variable: LOG (ds/b)

Number in Model	R-Square	Adjusted R-Square	C(p)	MSE	Variables in Model
1	0.72299266	0.7145985	154.49358	0.01086517	Fr
1	0.70949114	0.70068785	163.53466	0.01139475	SROHV2
1	0.16977837	0.14462014	524.94478	0.03256412	Comp.
1	4.621E-05	-0.0302554	638.60324	0.0392215	IWC
2	0.94578789	0.94239963	7.30228	0.00219283	Fr, Comp.
2	0.89956602	0.89328889	38.25403	0.00406247	Fr, SROHV2
2	0.82860161	0.81788921	85.77422	0.006932	IWC, SROHV2
2	0.73344621	0.71680351	149.48287	0.01078123	IWC, Fr
2	0.72011337	0.7026421	158.40801	0.01132035	SROHV2, Comp.
2	0.17001489	0.11814082	526.7864	0.03357218	IWC, Comp.
3	0.95511951	0.95077624	3.05351	0.00187394	IWC, Fr, Comp.
3	0.95241231	0.94780705	4.86634	0.00198676	Fr, SROHV2, Comp.
3	0.92539662	0.91817693	22.95698	0.00311499	IWC, Fr, SROHV2
3	0.86916698	0.85650572	60.61026	0.00546279	IWC, SROHV2, Comp.
4	0.95519942	0.94922601	5.00000	0.00193295	IWC, Fr, SROHV2, Comp.

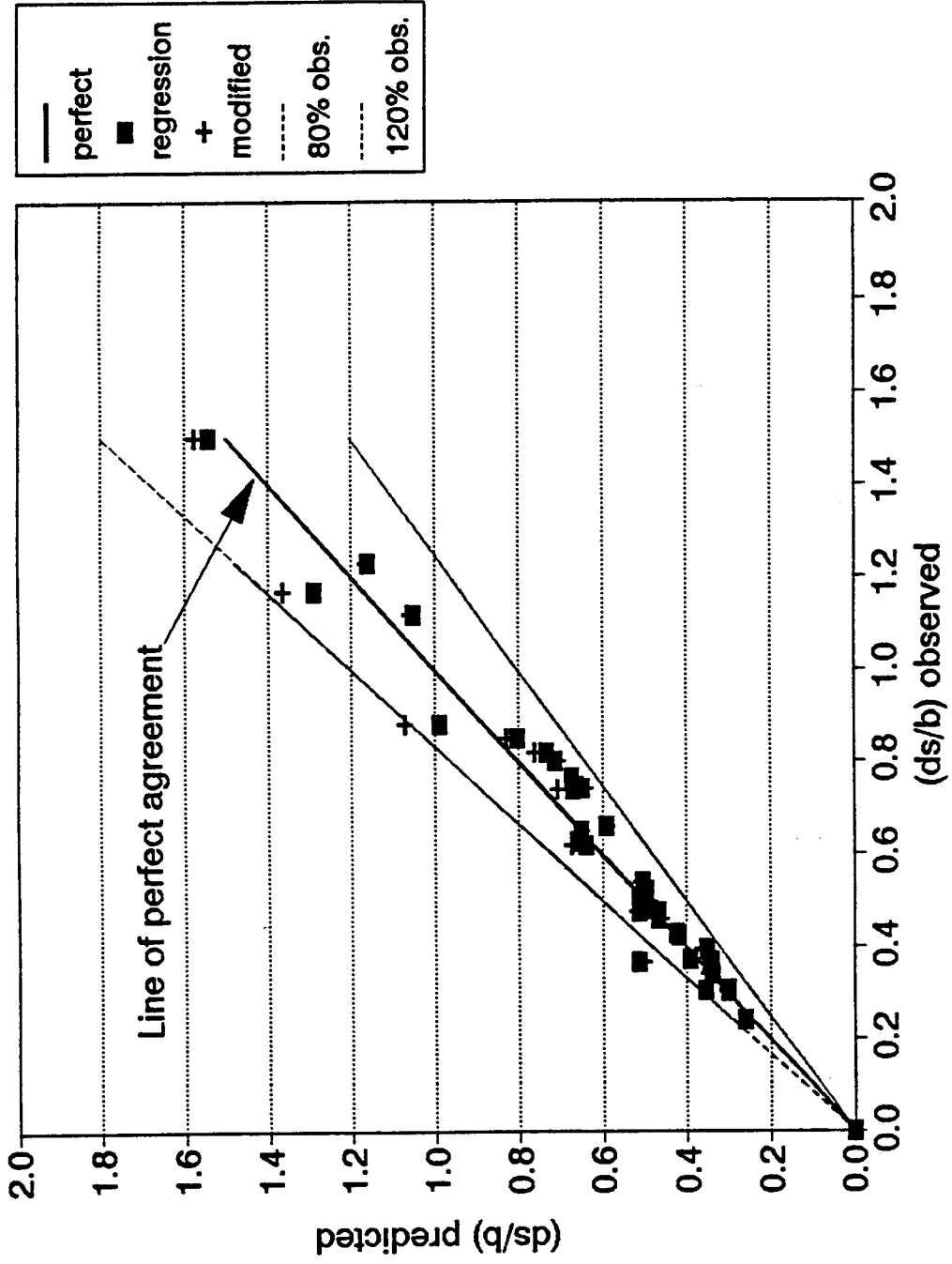


Figure 5-38 Comparison Between the Observed and Predicted Scour Ratios in Unsaturated Cohesive Soil

For the range of flow conditions considered for this experimental study, the predicted scour depth should be taken zero in case of ($F_r \leq 0.2$ and Compaction $\geq 85\%$).

5-5 Analysis of Pier Scour in Saturated Cohesive Soils

This section discusses the effect of the initial water content of saturated cohesive soils on pier scour. To specify this effect, 24 test runs were conducted, of which 6 test runs were conducted with supercritical approach conditions ($F_r > 1.0$). The experimental conditions and results of set 3 are presented in Table 5-6.

5-5-1 Geometry of Pier Scour in Saturated Cohesive Soils

As was mentioned before, the geometry of the scour hole is conical in nature with maximum scour depth occurring immediately in the front of the pier. In general, the slope of the scour hole in saturated cohesive soil was observed to be steeper than that in sandy soils and sandy-clayey mixtures. This slope increases as the initial water content decreases.

The configuration of scour holes in saturated cohesive soil are presented in Figures 5-39 through 5-42. This photographic documentation shows that the scour depth and volume decrease by decreasing the initial water content.

Table 5-6. Summary of Experimental Conditions and Results for Set 3
(Effect of Initial Water Content (IWC) of Saturated Clay on Pler Scour)

Run- Pier No.	Q (cfs)	IWC %	Wet Density lb/ft ³	Dry Density lb/ft ³	Comp. (%)	Approach Y (ft)	Approach V (ft/s)	Fr	ds (in.)	ds/bs	Ve (in. ^3)	(Ve/bs ^3)
13-PD	11	32	124.87	94.8	86.0	0.804	0.738	0.145	0	0.00	0.0	0.000
14-PD	10	35	121.77	90.2	82.0	0.71	0.788	0.165	0	0.00	0.0	0.000
15-PD	12	35	121.77	90.2	82.0	0.747	0.866	0.177	0	0.00	0.0	0.000
16-PD	14.8	35	121.77	90.2	82.0	0.82	0.988	0.192	0	0.00	0.0	0.000
17-PD	10	40	115.5	82.5	75.0	0.71	0.788	0.165	0	0.00	0.0	0.000
18-PD	12	42	110.9	78.1	71.0	0.747	0.866	0.177	0	0.00	0.0	0.000
19-PD	14.8	45	105.27	72.6	66.0	0.797	0.997	0.197	0	0.00	0.0	0.000
23-PA	14.8	48	102.56	69.3	63.0	0.798	1.07	0.211	5.77	0.98	299.0	1.384
24-PA	13.5	40	115.5	82.5	75.0	0.756	1.045	0.212	2.24	0.37	61.0	0.283
25-PA	12	48	102.56	69.3	63.0	0.736	0.914	0.188	0	0.00	0.0	0.000
26-PA	18.3	32	124.87	94.8	86.0	0.98	2.06	0.367	0	0.00	0.0	0.000
26-PB	18.3	38	119.9	86.9	79.0	0.96	2.078	0.374	2.52	0.42	54.9	0.254
28-PC	18.3	43	111.68	78.1	71.0	0.96	2.214	0.398	4.08	0.68	164.8	0.763
29-PB	28	38	119.9	86.9	79.0	1.01	2.846	0.499	5.28	0.88	170.9	0.791
29-PC	28	43	111.68	78.1	71.0	1.01	2.876	0.504	6.5	1.06	598.5	2.771
34-PA	15	35	121.77	90.2	82.0	0.89	1.8	0.336	2.28	0.36	67.1	0.311
34-PB	15	40	115.5	82.5	75.0	0.87	1.848	0.349	3	0.50	100.7	0.466
34-PC	15	45	105.27	72.6	66.0	0.84	1.92	0.369	4.55	0.76	188.7	0.874
36-PA	17.7	35	121.77	90.2	82.0	0.95	2.032	0.367	1.92	0.32	69.5	0.322
36-PB	17.7	40	115.5	82.5	75.0	0.92	2.188	0.402	3.98	0.66	210.6	0.975
36-PC	17.7	45	105.27	72.6	66.0	0.86	2.34	0.445	6.48	1.06	340.4	1.576
37-PA	26	35	121.77	90.2	82.0	1.04	2.49	0.430	2.75	0.533	201.4	0.932
37-PB	28	40	115.5	82.5	75.0	1.03	2.718	0.472	5.7	0.95	488.2	2.26
37-PC	28	45	105.27	72.6	66.0	1.04	2.93	0.506	7.56	1.26	680.3	3.150
38-PA	33.5	35	121.77	90.2	82.0	1.4	2.844	0.424	3.2	0.458	110.5	0.512
38-PB	33.5	40	115.5	82.5	75.0	1.32	3.002	0.460	4.5	0.75	244.1	1.13
38-PC	33.5	45	105.27	72.6	66.0	1.24	3.172	0.502	7.56	1.26	793.3	3.673
39-PA	3.41	32	124.87	94.6	86.0	0.194	4.4	1.76	3.948	0.99	178.5	2.7890625
40-PA	2.774	32	124.87	94.6	86.0	0.188	3.569	1.45	3.792	0.95	155.6	2.43125
41-PA	1.95	32	124.87	94.6	86.0	0.166	3.145	1.36	2.56	0.65	80.5	1.2578125
42-PA	2.28	32	124.87	94.6	86.0	0.18	3.25	1.349	2.7	0.68	76.8	1.23125
43-PA	3.15	32	124.87	94.6	86.0	0.191	4.13	1.66	3.816	0.95	210	3.28125
44-PA	2.77	32	124.87	94.6	86.0	0.369	2.25	0.66	1.452	0.36	45.76	0.715

NOTES:

- * Runs 13 through 25 were conducted in the Seventeen-foot wide flume with pier of diameter 6 inches.
- * Runs 28 through 38 were conducted in the Eight-foot wide flume with pier of diameter 6 inches.
- * Runs 39 through 44 were conducted in the Four-foot wide flume with pier of diameter 4 inches.

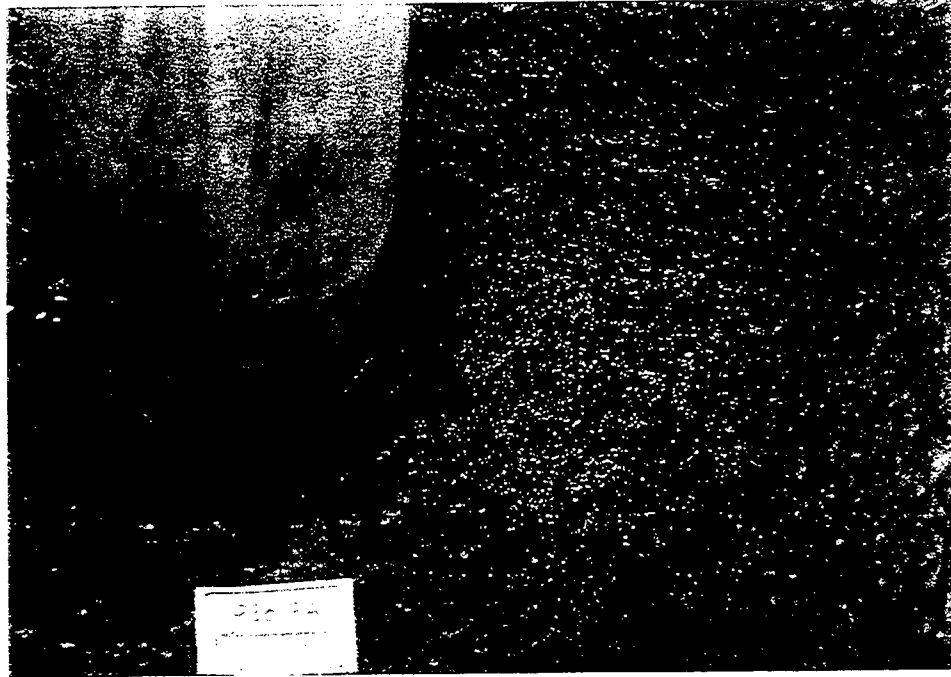


Figure 5-39. View of the Scour Hole for Pier A (35% IWC)
at the End of Run R36, $Q=17.7$ cfs

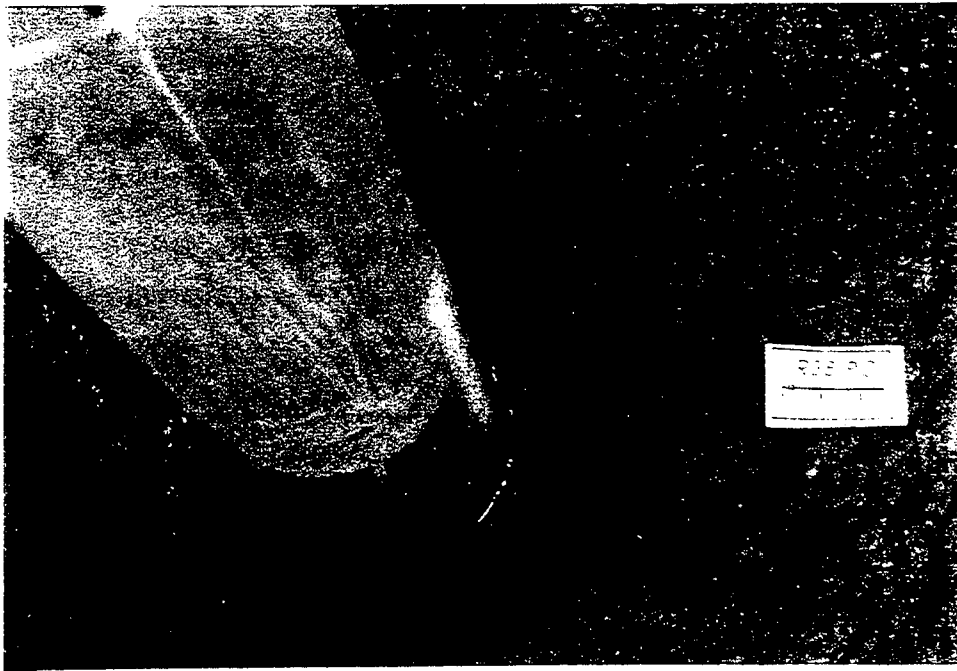


Figure 5-40. View of the Scour Hole for Pier C (45% IWC)
at the End of Run R36, $Q=17.7$ cfs



Figure 5-41. View of the Scour Hole for Pier B (40% IWC)
at the End of Run R36, $Q=17.7$ cfs



Figure 5-42. View of the Scour Hole for Pier A (32% IWC)
at the End of Run R41, $Q=1.95$ cfs

Examples of cross sections passing through the scour holes at various initial water contents are plotted in Figures 5-43 through 5-47 for different flow conditions. From these Figures, it appears clearly that the volume of scour hole increases as the initial water content (IWC) of the saturated cohesive soil is increased.

The relationship between the scour depth and the scour volume in dimensionless form is plotted in Figure 5-48. With the same procedure, the best-fit regression equation is:

$$\left(\frac{d_s}{b}\right)_p = 0.719 \sqrt{\frac{V_s}{b^3}} \quad (5-16)$$

5-5-2 Effect of the Approach Flow and IWC on Pier Scour in Saturated Cohesive Soils

Generally it can be concluded from this set of test runs that the scour depth is strongly affected by the initial water content of saturated clay and the approach Froude number.

In light of the dimensional analysis and choosing the initial water content and Froude number as independent variables, the variation of scour ratios is plotted in Figure 5-49. The curves on the graph show the trend of the data for these flow conditions. For a given IWC, scour depth increases as the approach flow conditions are augmented. As the IWC is increased for a given flow condition, the scour depth increases.

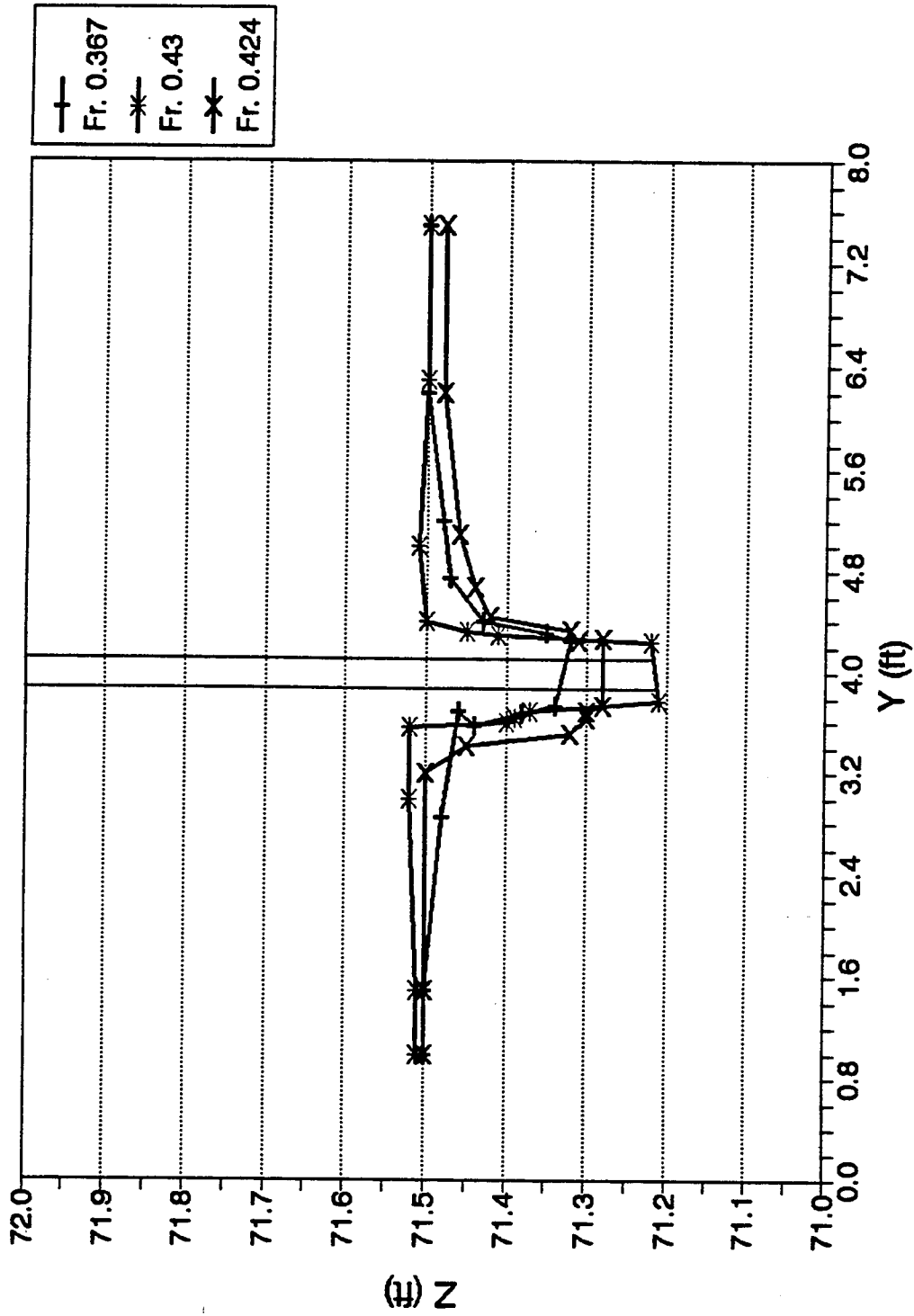


Figure 5-43. Effect of IWC of Saturated Clay on the Cross Section Geometry Along the Center Line of Pier PA for Runs R36, R37, and R38 (35% IWC)

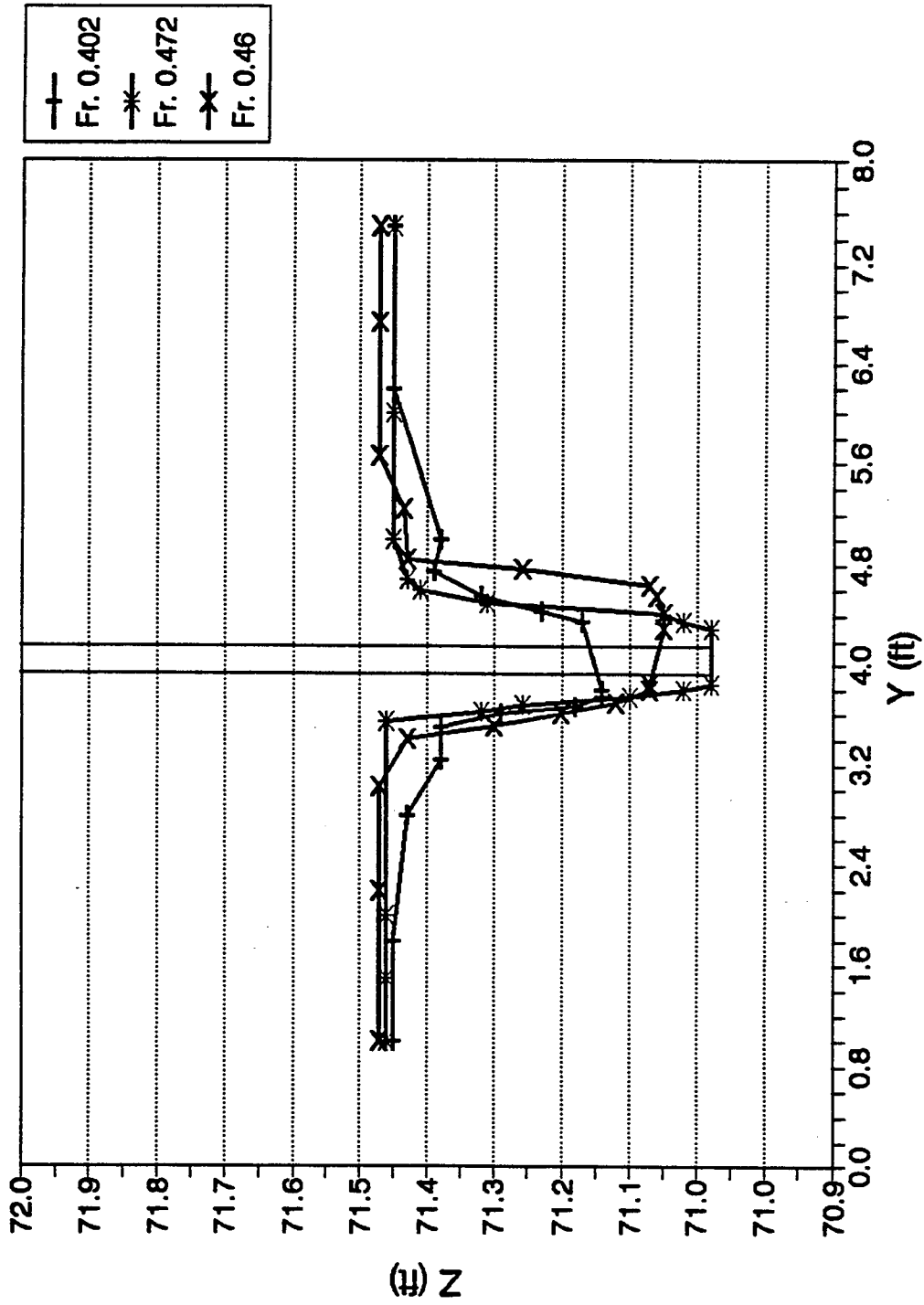


Figure 5-44. Effect of IWC of Saturated Clay on the Cross Section Geometry Along the Center Line of Pier PB for Runs R36, R37, and R38 (40% IWC)

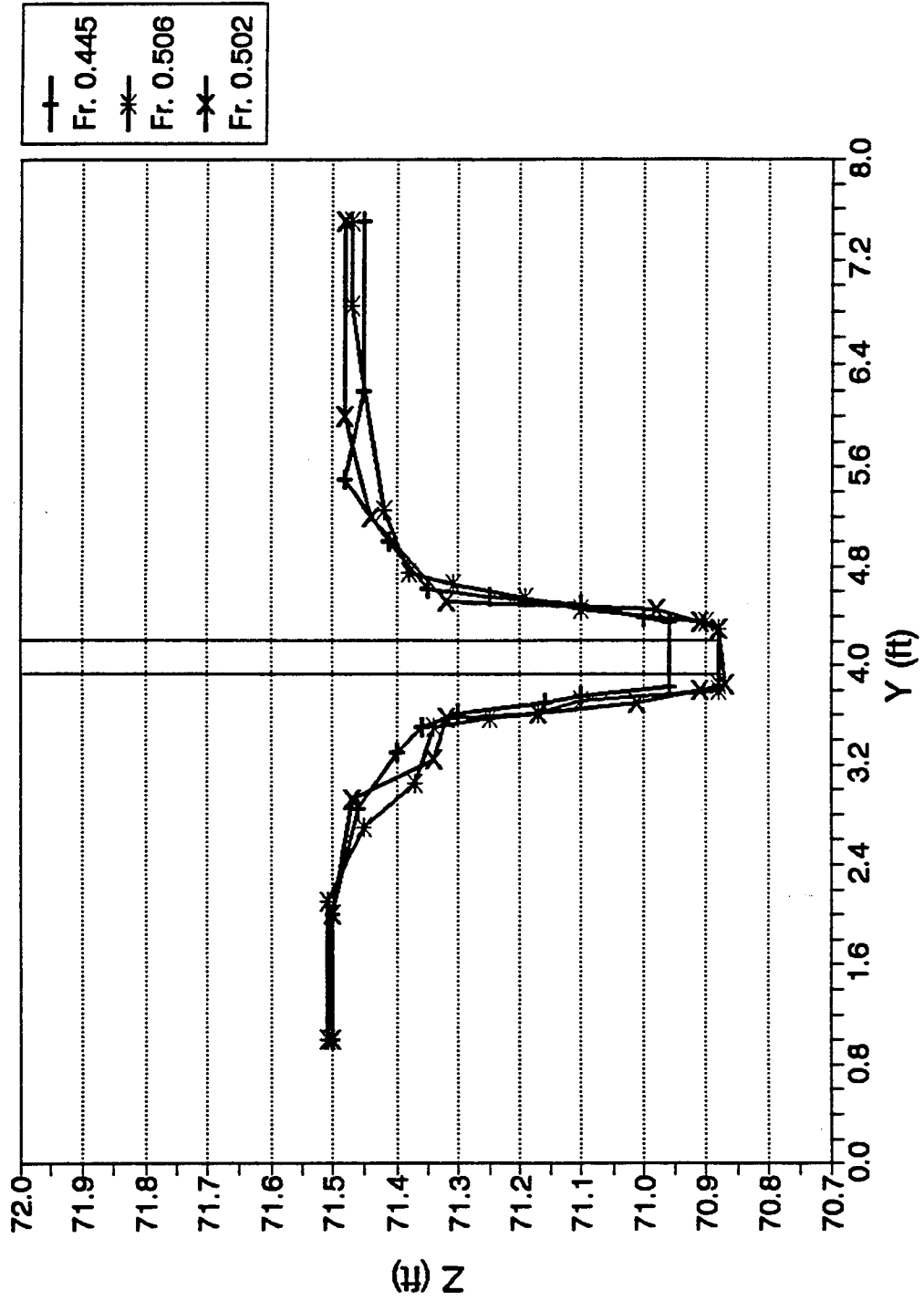


Figure 5-45. Effect of IWC of Saturated Clay on the Cross Section Geometry Along the Center Line of Pier PC for Runs R36, R37, and R38 (45% IWC)

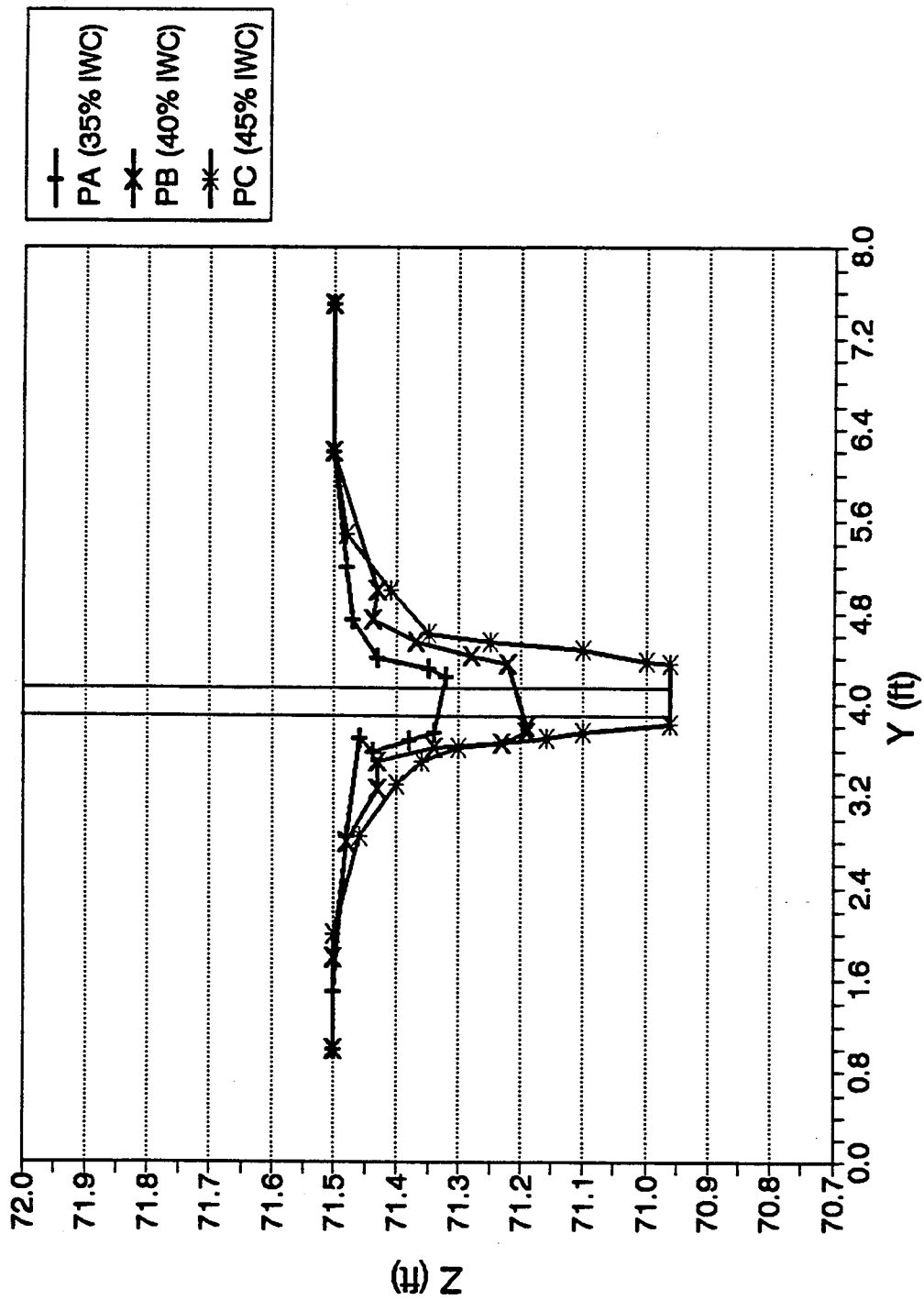


Figure 5-46. Effect of IWC of Saturated Clay on the Cross Section Geometry Along the Center Line of Piers PA, PB, and PC For Run R36

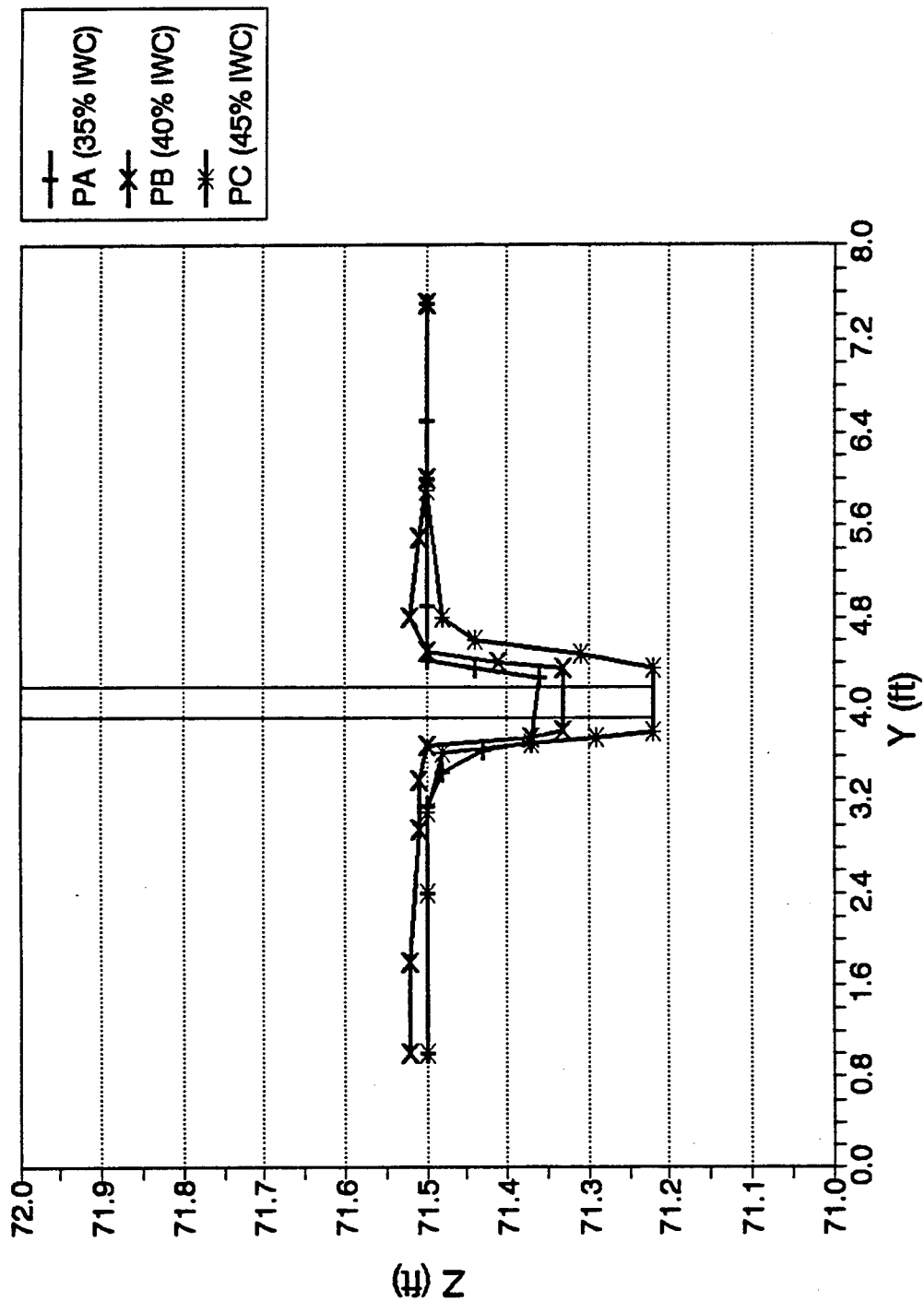


Figure 5-47. Effect of IWC of Saturated Clay on the Cross Section Geometry Along the Center Line of Piers PA, PB, and PC for Run R34

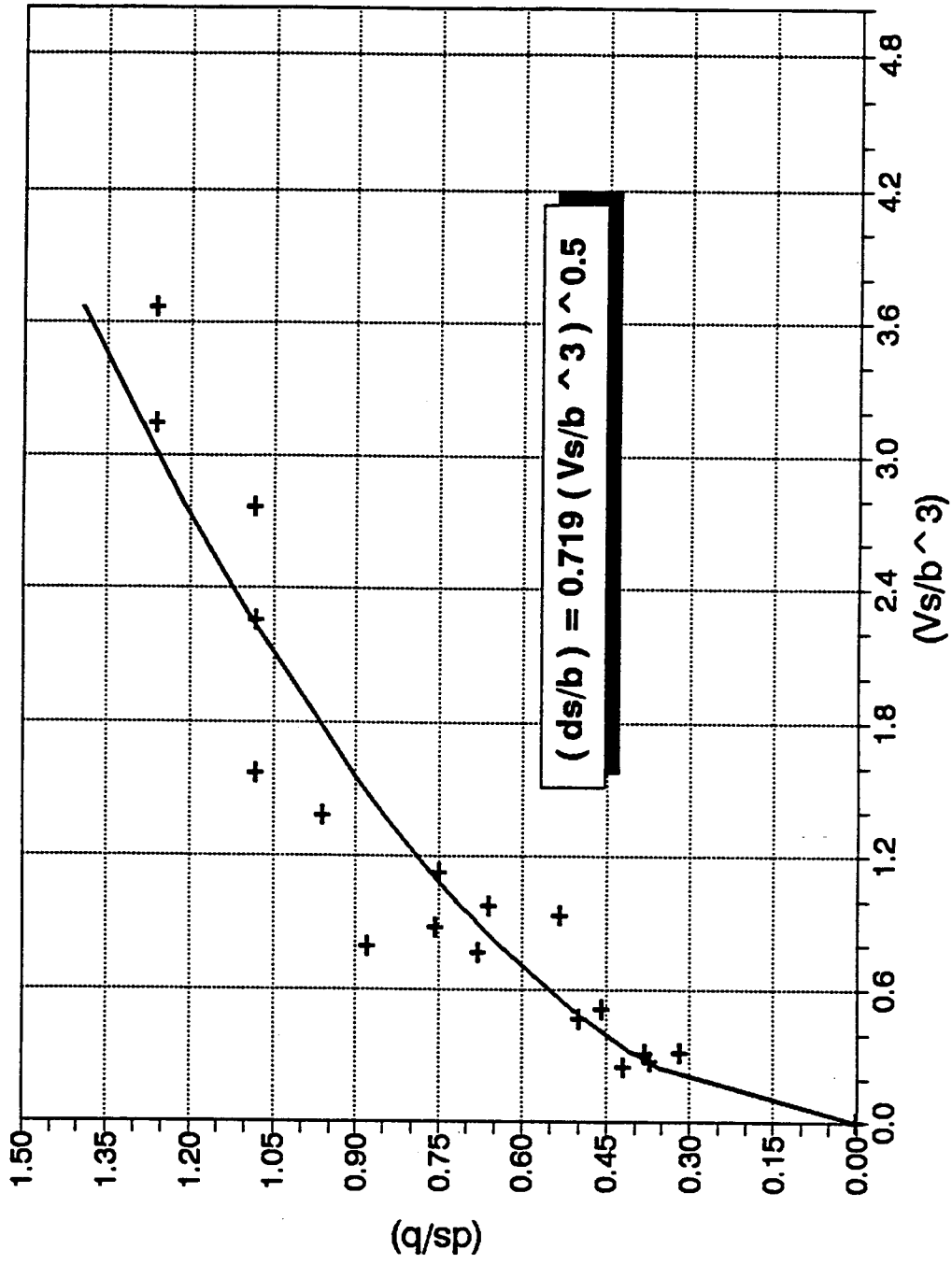


Figure 5-48. Effect of IWC of saturated clay on (d_s/b) versus (V_s/b^3)

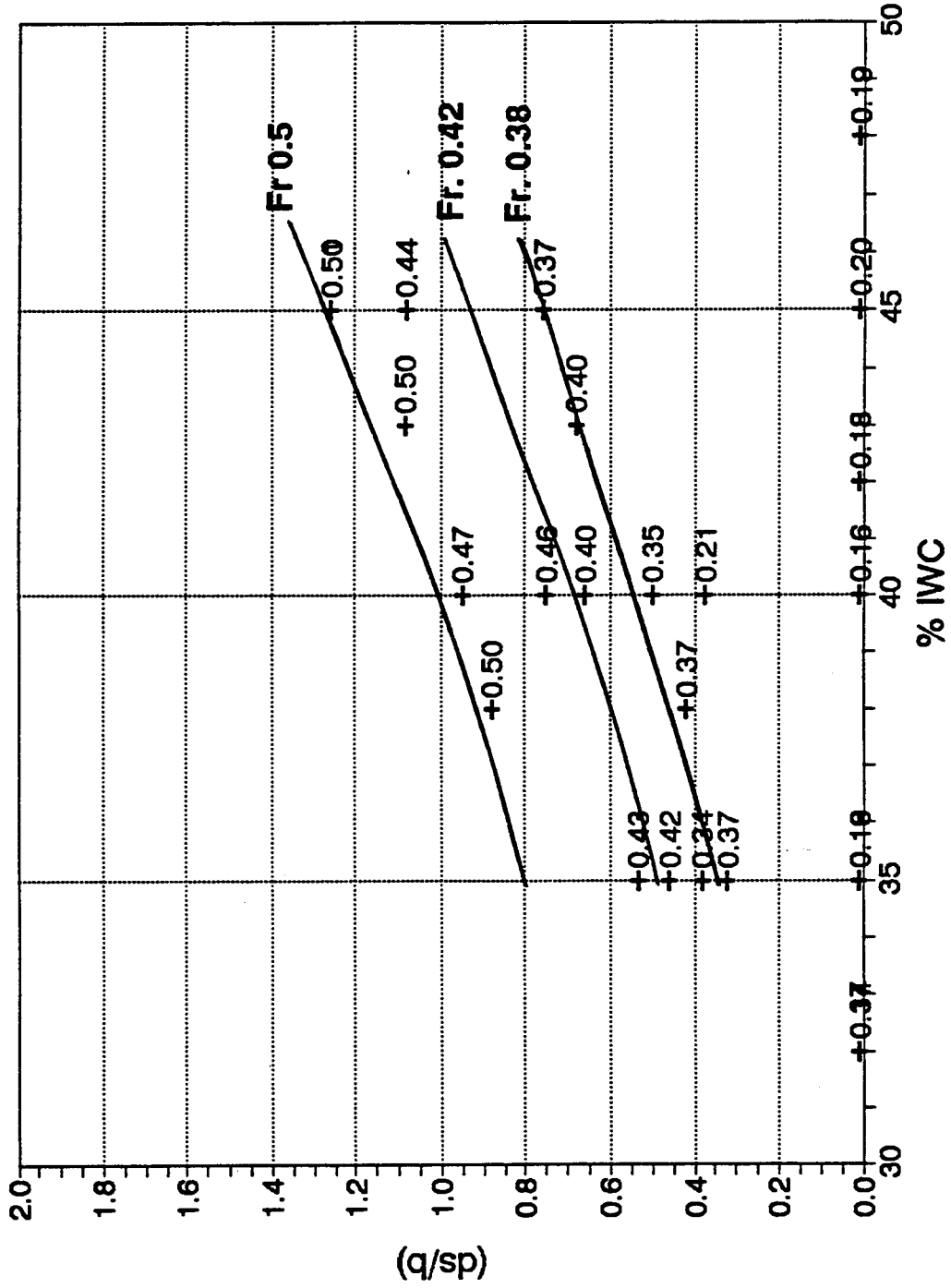


Figure 5-49. Effect of the IWC of saturated clay on the Scour Ratio

For the range of IWC's tested, it can be seen that the scour rate of increase appears to be constant. Next, the approach velocities are plotted versus the scour ratios in Figure 5-50.

It was observed that the saturated cohesive soil at 32% initial water content did not indicate any scour at Froude numbers less than 0.56. Therefore, 6 additional test runs were conducted at supercritical flow conditions and the results are presented in Table 5-6 and plotted in Figure 5-51.

The conclusion which can be made from this set of runs is that the water content of saturated cohesive soil as well as the magnitude of the approach flows govern the scour process. The IWC of saturated clay performs a very important part in the cohesive forces between the particles which in turn control the behavior of scour around the piers.

5-5-3 Effect of Test Duration on Pier Scour in Saturated Cohesive Soils

As pointed out in previous sections, all runs were conducted with 960 minutes to reach the equilibrium scour. The scour depth variations with time at different initial water contents are presented in Figures 5-52 and 5-53 for some runs as examples. The obtained scour depth is limited in time scale to the experimental laboratory times.

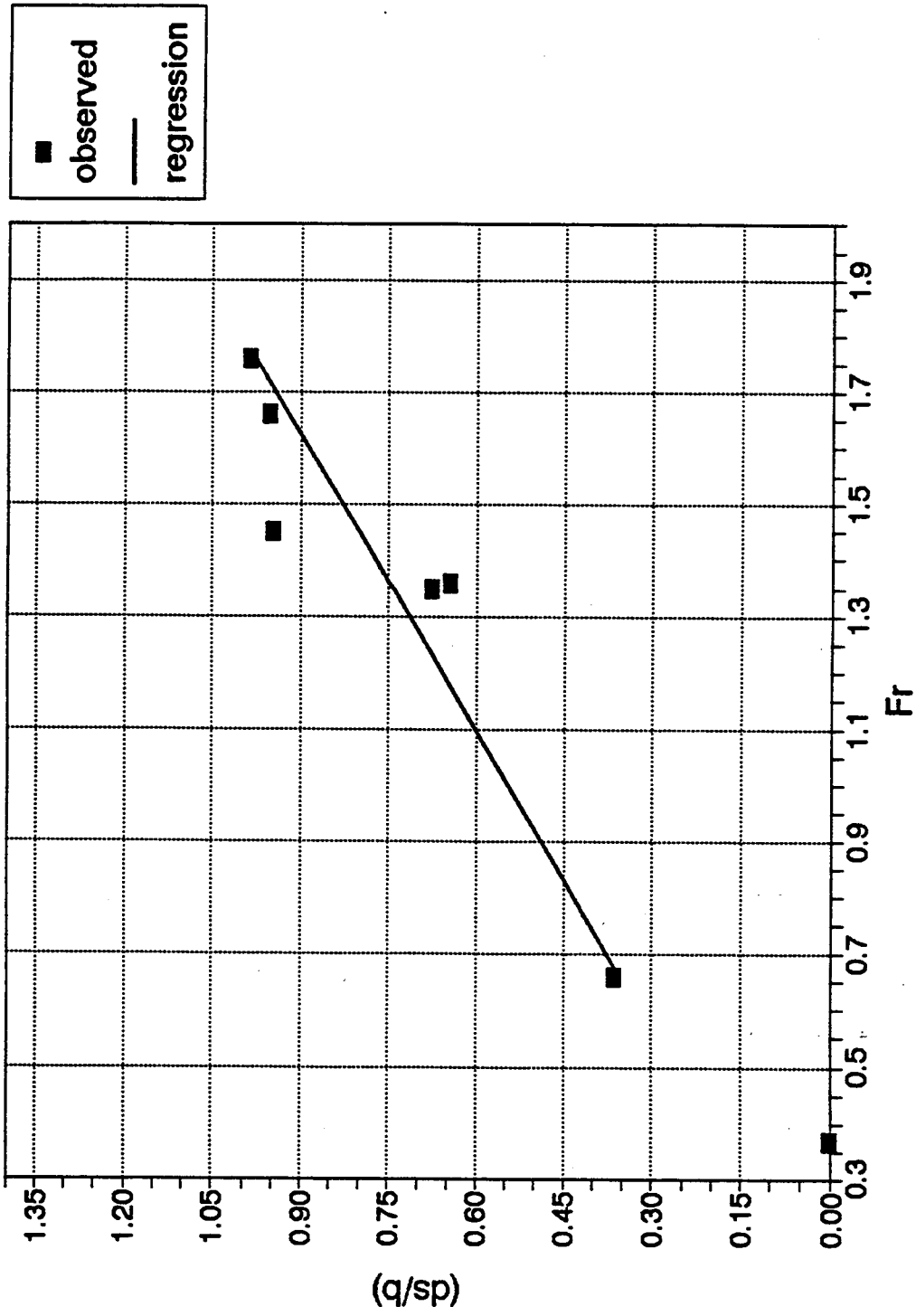


Figure 5-51. Effect of Froude Number on the Scour Ratio for Saturated Clay at 32% IWC

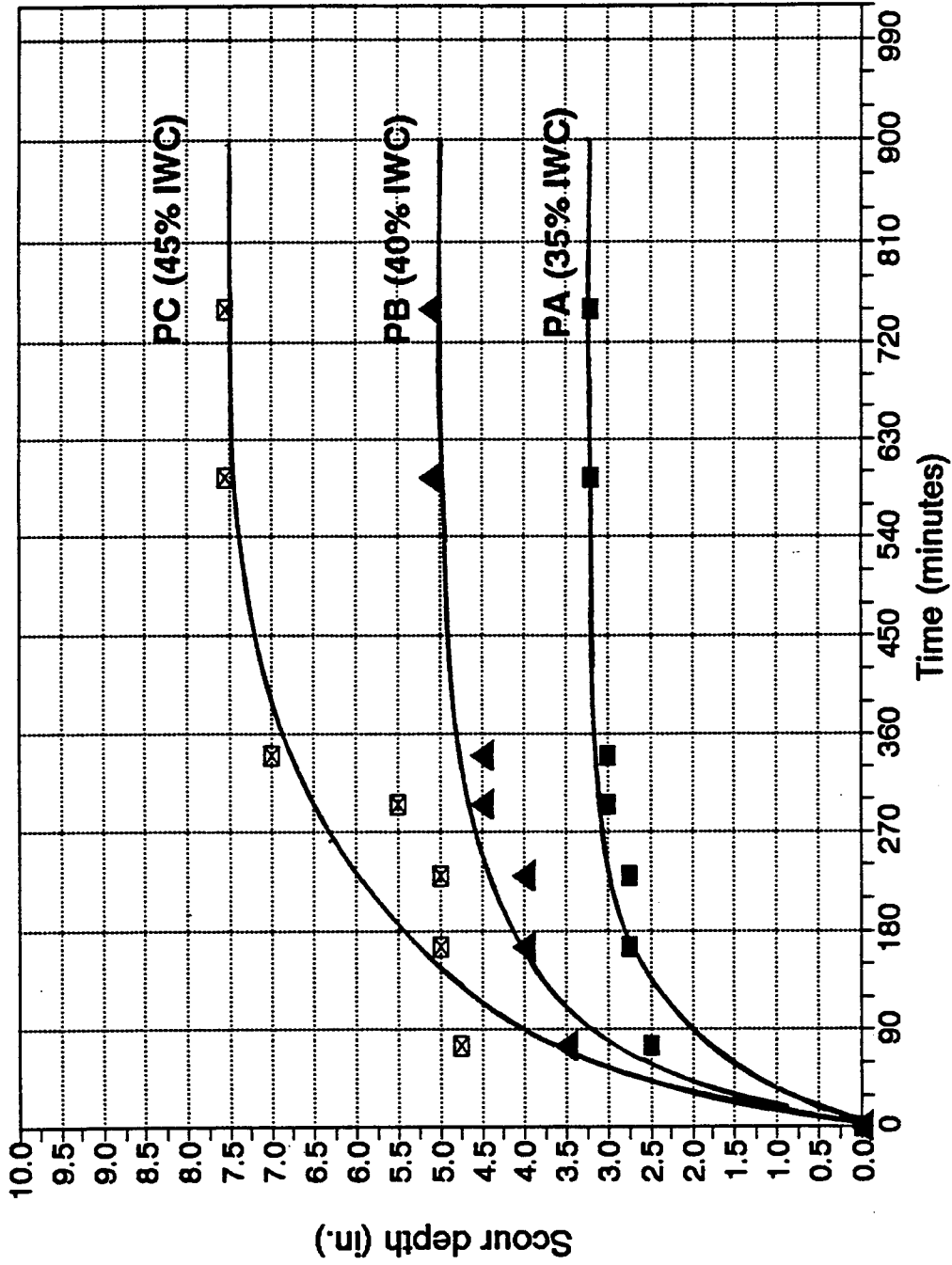


Figure 5-52. Effect of the IWC of Saturated Caly on Scour Development for Run R38

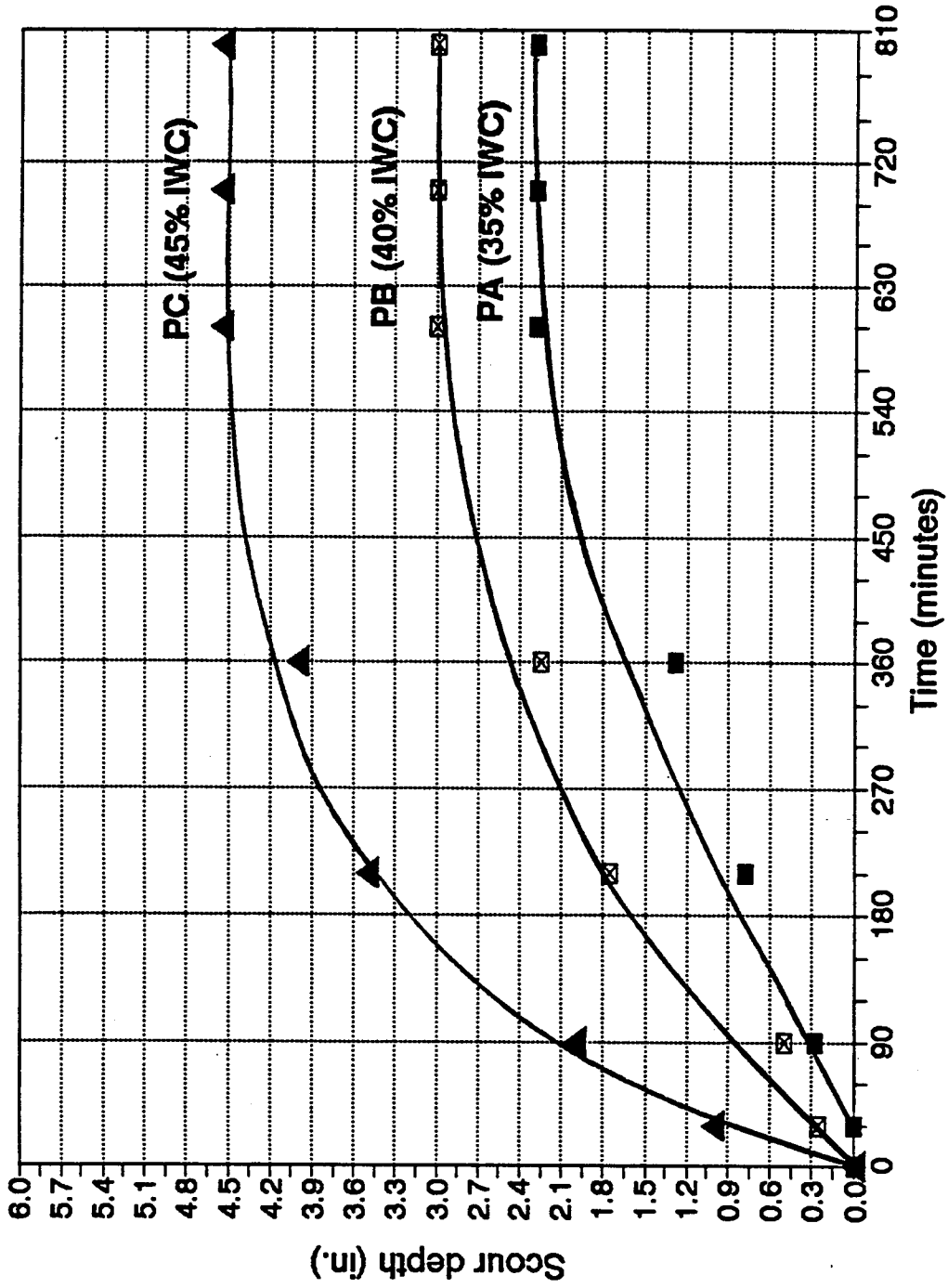


Figure 5-53. Effect of the IWC of Saturated Calyx on Scour Development for Run R34

5-5-4 Regression Analysis for Pier Scour in Saturated Cohesive Soils

As stated before, a multiple linear regression analysis was used utilizing SAS computer software in order to develop a general equation for estimating the scour depth in saturated cohesive soils.

Compared to unsaturated cohesive soil, the dimensionless parameter of soil shear strength, $(S/\rho V^2)$, is eliminated from equation 5-13 since this term has no physical meaning for saturated clays at high initial water contents. In several experiments with initial water content of 32% and above, different values of scour depth (starting from zero) were observed in spite of the torvane shear strength was measured to be close to zero. Therefore, this parameter could not be used as an indicator to explain the scour phenomena.

The compaction (Comp.) of saturated cohesive soil is mainly related to the water content, therefore this parameter is also removed. Furthermore, the critical Froude number, F_c , (criterion for the initiation of scour) was introduced to eliminate over prediction of scour ratio for experiments resulting in no scour. Thus, equation 5-13 after replacing F_r by $(F_r - F_c)$, reduces to:

$$\frac{d_s}{b} = f(IWC, F_r - F_c) \quad (5-17)$$

On the assumption that the critical Froude number is a function of initial water content of saturated cohesive soil, the scour ratios were plotted versus Froude numbers for each initial water content. The critical Froude number, F_c , which is defined as the value at which the scour ratio is zero, is determined by interpolation. A regression analysis using six data points was then carried out based on the assumption that the critical Froude number is a power function of the initial water content. This analysis with a correlation coefficient of 0.95, yielded:

$$F_c = \frac{0.035}{(IWC)^2} \quad (5-18)$$

The regression analysis of the data given in Table 5-6 based on equation 5-17, yielded:

$$\left(\frac{d_s}{b} \right)_p = 5.48 (IWC)^{1.14} (F_r - F_c)^{0.6} \quad (5-19)$$

where IWC is the initial water content ranging from 0.15 to 0.5. This equation was developed for Froude numbers varying between 0.18 and 0.506. The data for $(F_r - F_c) < 0$ and data of supercritical flow conditions were not included in the regression analysis in arriving at equation 5-19. The relatively high value of linear correlation coefficient, $R=0.89$, between the observed and predicted scour ratio indicates that the equation fits the data very well.

The best-fit regression equation output results from SAS computer software is presented in Table 5-7. Equation 5-19 was modified in order to form an envelope for all data points; it resulted in:

$$\left(\frac{d_s}{b}\right)_p = 5.5 (IWC) (F_r - F_c)^{0.6} \quad (5-20)$$

A comparison between the observed scour ratio given in Table 5-6 and predicted scour ratio by equations 5-19 and 5-20 is presented in Figure 5-54. The maximum scatter in the predicted scour ratio in Figure 5-54 for scour ratios greater than zero lies between ± 20 percent. This scatter was probably due to: 1) the duration of experiments were not sufficient to reach the final equilibrium scour depth; 2) the experimental inaccuracies in measuring the initial water content and Froude number (especially at high flows); 3) scale effects in conducting experiments in three different flumes; 4) most importantly, inaccuracy in defining the critical condition by equation 5-18.

An arbitrary criterion that a formula is satisfactory if the predicted scour ratio within 20% less-or over-prediction. This criterion is met by equation 5-20 and is represented by dashed lines in Figure 5-54.

The regression equation (5-20) was developed using data of subcritical flows up to Froude number of 0.5. Applying this equation for higher Froude numbers ($1 < F_r < 1.76$) results in

Table 5-7. Regression Output from SAS Program for Set 3

Dependent Variable: LOG(ds/b)
Analysis of Variance

Source	DF	Sum of Squares	Mean Square	F value	Prob>F
Model	2	0.47717	0.23858	53.087	0.0001
Error	13	0.05842	0.00449		
C total	15	0.53559			

Root MSE	Dep Mean	C.V.	R-Square	Adj-R-Sq
0.06704	-0.16295	-41.14152	0.8909	0.8741

Parameter Estimates

Variable	DF	Parameter Estimate	Standard Error	T for Ho: Parameter=0	Prob> [T]
INTERCEP	1	0.738837	0.19686108	3.753	0
IWC	1	1.139035	0.641456	1.776	0
Fr-Fc	1	0.606937	0.1189548	5.102	0

CORRELATION

CORR.	IWC	Fr-Fc	ds/b
IWC	1.0000	0.7705	0.8200
Fr-Fc	0.7705	1.0000	0.9298
ds/b	0.8200	0.9298	1.0000

Regression Models for Dependent Variable: LOG (ds/b)

Number in Model	R-Square	Adjusted R-Square	C(p)	MSE	Variables in Model
1	0.86445809	0.85477653	4.15312	0.00518539	Fr-Fc
1	0.67247191	0.64907705	27.03294	0.01253016	IWC
2	0.89091612	0.87413398	3.0000	0.00449421	IWC, Fr-Fc

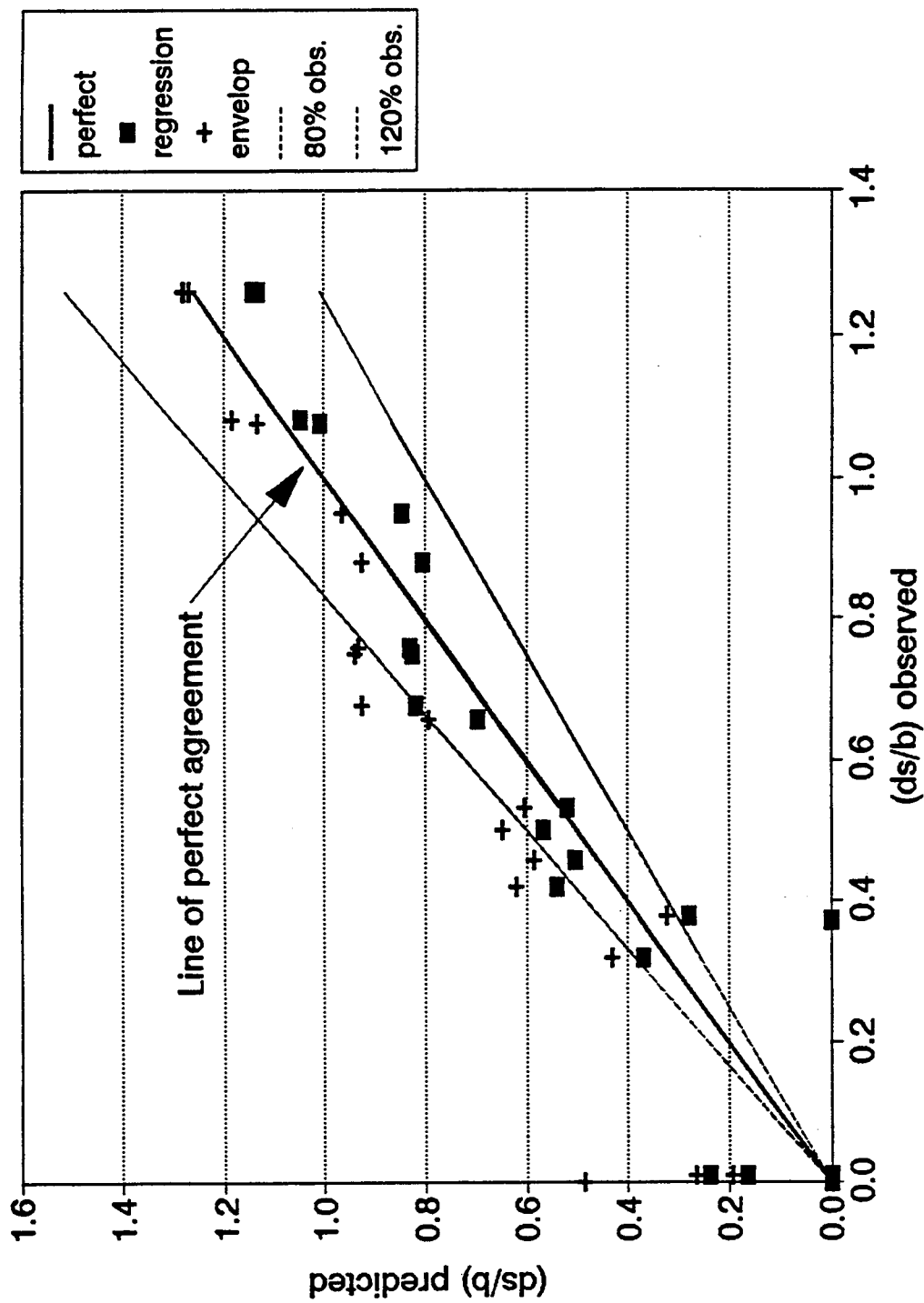


Figure 5-54. Comparison Between the Observed and Predicted Scour Ratios in Saturated Cohesive Soils

over-prediction by a factor up to 2 times. The best-fit regression equation for the data shown in Figure 5-51 (32% IWC of saturated clay, supercritical flow conditions) was developed. The regression analysis resulted in:

$$\left(\frac{d_s}{b}\right)_p = 2.5 (IWC) (F_r - F_c)^{0.6} \quad (5-21)$$

The comparison between equations 5-20 and 5-21 shows that the coefficient 5.5 in equation 5-20 is reduced by almost 50%.

5-5-5 Effect of Dry-Wet Cycle on Pier Scour in Saturated Cohesive Soils

In order to specify the effect of dry-wet cycle of saturated clay on pier scour, three test runs were conducted in the Four-foot wide flume. Each test run lasted for 16 hours with water depth of 2.28 inches and Froude number of 1.76.

The first run was performed for saturated clay at initial water content of 32% and compaction of 86%, and the maximum scour hole depth was recorded. The scour hole was let to dry for a period of 28 days resulting in reducing the initial water content to 25% and increasing the compaction to 91%.

Afterwards, the experiment was repeated using the bed configuration resulting from the first run with the same flow conditions. The second run lasted also for 16 hours without developing any additional scour.

The experiment was repeated for the third time at the

same flow conditions. Following the same procedures (120 days drying period), the initial water content was found to be reduced to 19% and the compaction was increased to 100% at the end of the drying period. No additional scour was reached beyond the scour that obtained in the first experiment.

The scope of these experiments, results, and the maximum cracks dimension at the end of each drying period are presented in Table 5-8.

Table 5-8. Effect of Dry-Wet Cycle on Saturated Clay

RUN No.	Dry period (days)	IWC %	Comp. %	ds/b	Cracks (in.)	
					width	height
1	0	32	86	0.9	0	0
2	28	25	91	0	0.433	2.52
3	120	19	100	0	0.875	5

Notes:

- All runs were performed at water depth= 0.19 ft and approach velocity= 4.4 ft/sec. ($F_r=1.76$).

The conclusion from these runs is that the dry-period reduces the initial water content which in turn results in an increase in the compaction of saturated clay. As a result, the resistance of saturated clay to scour is increased. Additional scour is not developed without changing the flow condition.

On the other hand, the dry period develops shrinking cracks on the soil surface. As the duration of the dry-period increases, the cracks become wider and deeper resulting in separating the soil surface around the pier into clusters, as shown in Figures 5-55 through 5-58.



Figure 5-55 Soil Surface Conditions after 6 Days of Dry Period.



Figure 5-56. Soil Surface Conditions after 22 Days of Dry Period.

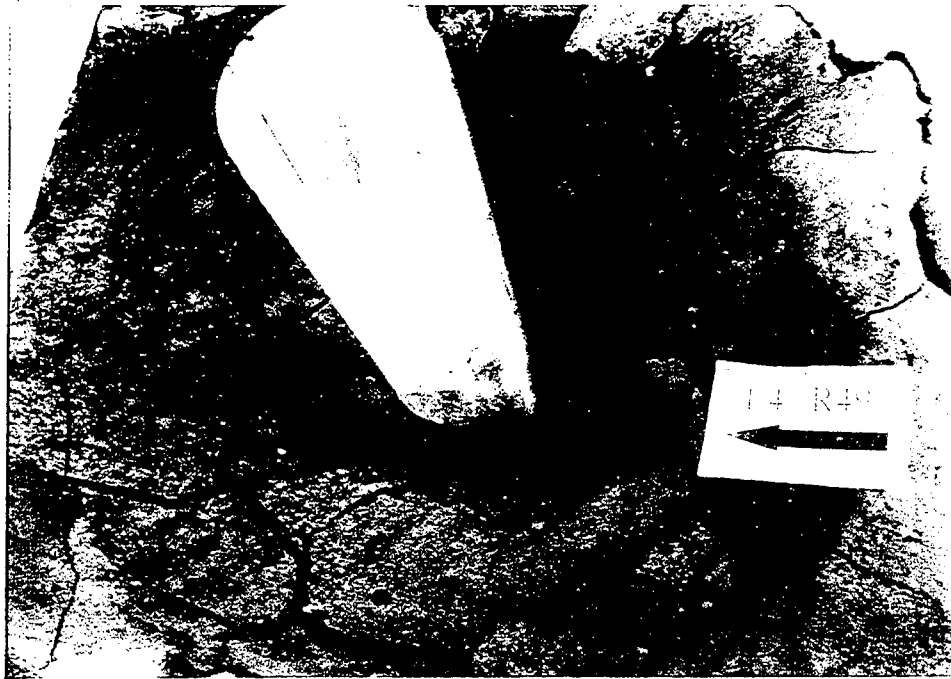


Figure 5-57. Soil Surface Conditions after 30 Days of Dry Period.



Figure 5-58. Soil Surface Conditions after 120 Days of Dry Period.

In prototype systems, the resulting blocks (much smaller crack size to pier diameter ratio) may become easily removed and carried away by the oncoming flow. However, the size of clusters in the model is exaggerated since the cluster size-to-pier diameter ratio is distorted, and no additional scour occurs. The effects of cracks size should be investigated further in future research to define the critical dry period that can lead to the removal of clay clusters.

5-5-6 General Equation for Pier Scour in Cohesive Soils

In this section, a generalized expression for predicting the maximum scour depth in both unsaturated and saturated cohesive soil was developed by combining the experimental data points of Sets 2 and 3. With the same procedure, the logarithmic values of (d_s/b) for all data points were regressed against the remaining dimensionless parameters in equation 5-13 after excluding the term $S/\rho V^2$ from the parameters list.

The best-fit regression equation which describes the data points is expressed as:

$$\left(\frac{d_s}{b} \right)_p = 0.85 (IWC)^{-0.72} F_r^{1.57} Comp.^{-1.92} \quad (5-22)$$

in which IWC is the initial water content varying between 0.15 and 0.5, and Comp. is the compaction of cohesive soil varying

between 0.58 and 1. This equation was developed for Froude numbers ranging from 0.18 to 0.506. The output results from SAS computer software is presented in Table 5-9. The value of correlation coefficient, $R=0.89$, indicates the strong correlation between the observed and predicted scour ratios.

For practical considerations, equation 5-22 was modified to be slightly more conservative; it resulted in:

$$\left(\frac{d_s}{b} \right)_p = 0.9 (IWC)^{-2/3} F_r^{3/2} Comp.^{-2} \quad (5-23)$$

The comparison between the observed and predicted scour ratio is presented in Figure 5-59. The dashed lines in this Figure illustrate the criterion of ± 20 percent less-or over-prediction. A comparison between the general equation (5-23) and other two equations for unsaturated (5-15) and saturated clay (5-20) is presented in Figure 5-60.

5-6 Sensitivity Analysis:

According to the International Standards Organization (ISO): "No measurement of a physical quantity can be free from uncertainties which may be associated with either systematic bias caused by errors in the standardizing equipment or a random scatter caused by a lack of sensitivity of the measuring equipment. The former is unaffected by repeated

Table 5-9. Regression Output from SAS Program for the General Equation

Dependent Variable: LOG(ds/b)
Analysis of Variance

Source	DF	Sum of Squares	Mean Square	F value	Prob>F
Model	3	1.67087	0.55696	87.658	0.0001
Error	48	0.30498	0.00635		
C total	51	1.97585			

Root MSE	Dep Mean	C.V.	R-Square	Adj-R-Sq
0.07971	-0.23433	-34.01583	0.8456	0.8360

Parameter Estimates

Variable	DF	Parameter Estimate	Standard Error	T for Ho: Parameter=0	Prob> [T]
INTERCEP	1	-0.0843	0.04900156	-1.721	0.2
IWC	1	-0.726934	0.10734223	-6.772	0
Fr	1	1.567336	0.11750503	13.338	0
Comp.	1	-1.917581	0.20956533	-9.15	0

CORRELATION

CORR.	IWC	Fr	Comp.	ds/b
IWC	1.0000	0.7986	0.2243	0.2471
Fr	0.7986	1.0000	0.2252	0.6294
Comp.	0.2243	0.2252	1.0000	-0.3938
ds/b	0.2471	0.6294	-0.3938	1.0000

Regression Models for Dependent Variable: LOG (ds/b)

Number in Model	R-Square	Adjusted R-Square	C(p)	MSE	Variables in Model
1	0.39610535	0.38402746	139.79465	0.0238641	Fr
1	0.15503952	0.13814031	214.75951	0.033144488	Comp.
1	0.06106346	0.04228473	243.98348	0.03667968	IWC
2	0.69816761	0.68584792	47.86158	0.01279312	Fr, Comp.
2	0.57640118	0.55911144	85.7276	0.01708097	IWC, Fr
2	0.2735229	0.24387078	179.91443	0.02870911	IWC, Comp.
3	0.84564553	0.83599838	4.00000	0.00635377	IWC, Fr, Comp.

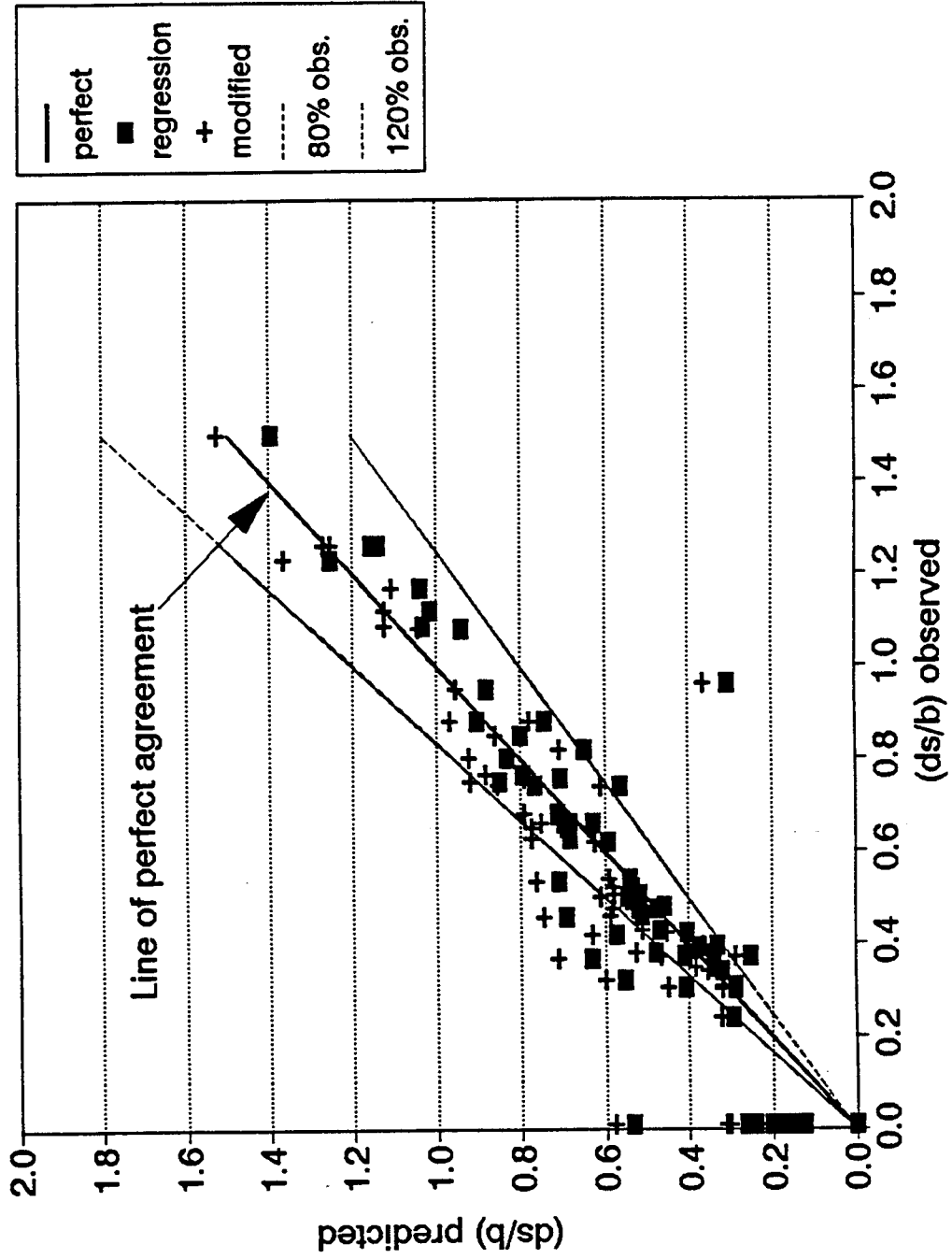


Figure 5-59. Comparison Between the Observed and Predicted Scour Ratios in Unsaturated and Saturated Cohesive Soil

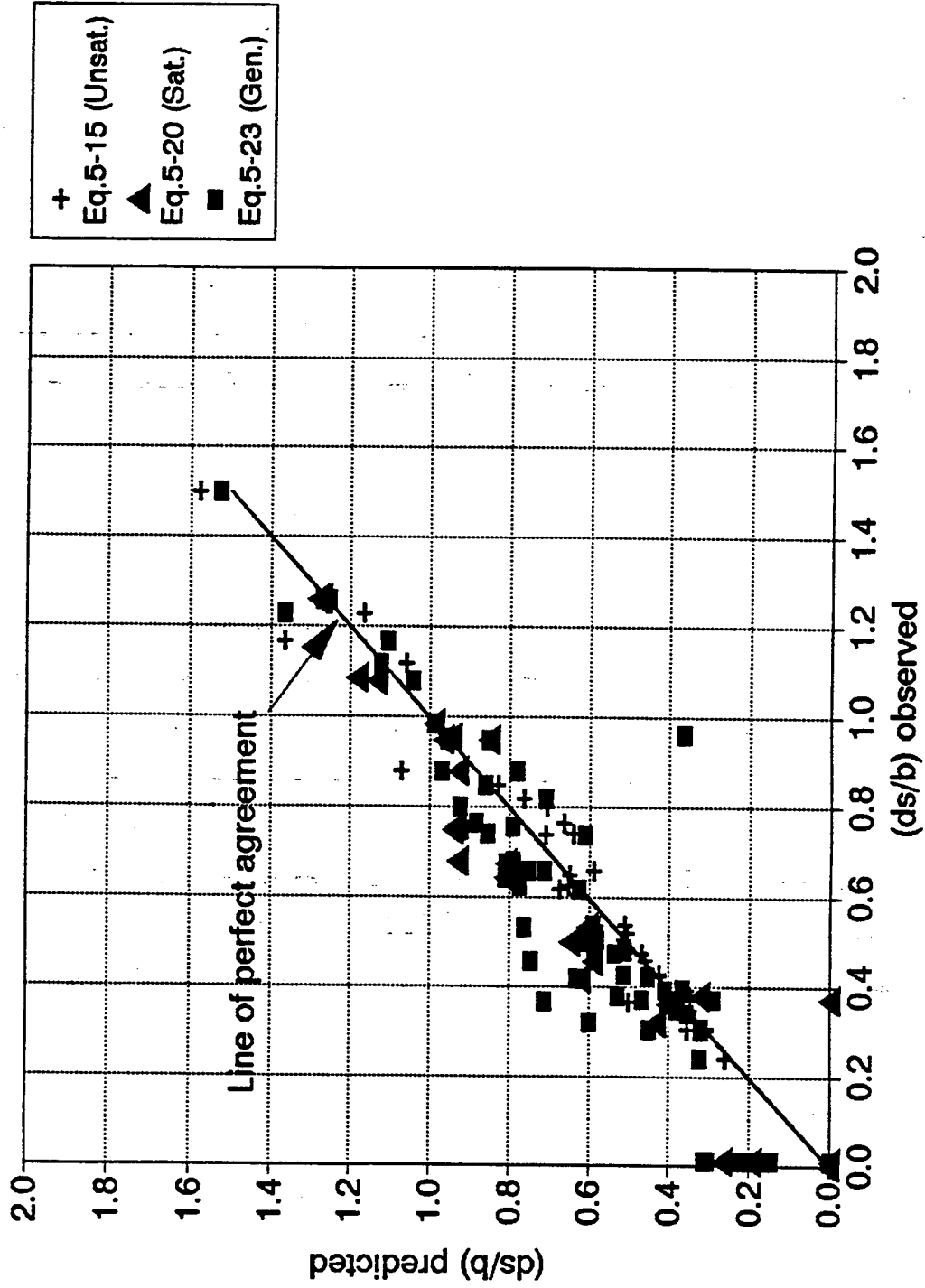


Figure 5-60. Comparison Between the Developed Equations

measurement and can only be reduced if more accurate equipment is used for the measurement. Repetition does, however, reduce the error caused by random scatter."

Another source of error is the sensitivity of derived quantities to discretization and computational procedures. Example of such estimates in alluvial channel measurements are: the estimation of area of cross section, discharge of water flowing through a section, average velocity of flow in a vertical, and bed material load.

In the present study, the uncertainties of different parameters measurement in the laboratory flumes are as follow:

a) Water depth measurements

Measurements of water depth were made by using a point gage with an accuracy of 0.005 ft. For the different sets of test runs, water depths varied between 1 ft and 0.3 ft which leads to have an estimated error of 0.5% to 2%.

b) Scour depth measurements

Scour holes were measured by means of the same point gauge. Since the scour depths for all test runs varied between 0.812 ft to 0.116 ft, the estimated error are in the range of 0.6% to 4.3%.

c) Velocity measurements

As mentioned before, the velocity measurements were carried out using a Marsh-Mc Birney 2-D magnetic velocity meter with an accuracy of $\pm 4\%$.

d) Soil preparation measurements

It can be reasonably assumed that the errors of measurement the clay content in sandy soil, initial water content, compaction, and soil shear strength are $\pm 1.5\%$, $\pm 1\%$, $\pm 1.5\%$, and $\pm 1\%$ respectively.

By using the Gaussian error propagation law, the absolute error in the predicted scour depth is:

$$(\sigma_{ds})^2 = \sum \left(\frac{\partial ds}{\partial i} \right)^2 \sigma_i^2 \quad (5-24)$$

where σ_i is the error in measuring the parameter i , $\partial ds / \partial i$ is the partial derivative of scour depth (ds) with respect to parameter i .

The sensitivity analysis had been done by applying the Gaussian propagation law on the developed equations.

Due to the error in measuring the water depth, approach velocity, clay content, soil shear strength, initial water content, and the degree of compaction, the absolute error in the predicted scour ratio for equations 5-11, 5-15, 5-20, and

5-23 can be determined respectively as:

$$(\sigma_{ds})^2 = \left(\frac{\partial ds}{\partial F_r} \right)^2 (\sigma_{F_r})^2 + \left(\frac{\partial ds}{\partial C} \right)^2 (\sigma_C)^2 \quad (5-25)$$

$$(\sigma_{ds})^2 = \left(\frac{\partial ds}{\partial IWC} \right)^2 (\sigma_{IWC})^2 + \left(\frac{\partial ds}{\partial F_r} \right)^2 (\sigma_{F_r})^2 + \left(\frac{\partial ds}{\partial S} \right)^2 (\sigma_S)^2 + \left(\frac{\partial ds}{\partial Comp.} \right)^2 (\sigma_{Comp.})^2 \quad (5-26)$$

$$(\sigma_{ds})^2 = \left(\frac{\partial ds}{\partial IWC} \right)^2 (\sigma_{IWC})^2 + \left(\frac{\partial ds}{\partial F_r} \right)^2 (\sigma_{F_r})^2 \quad (5-27)$$

$$(\sigma_{ds})^2 = \left(\frac{\partial ds}{\partial IWC} \right)^2 (\sigma_{IWC})^2 + \left(\frac{\partial ds}{\partial F_r} \right)^2 (\sigma_{F_r})^2 + \left(\frac{\partial ds}{\partial Comp.} \right)^2 (\sigma_{Comp.})^2 \quad (5-28)$$

where

$$(\sigma_{F_r})^2 = \left(\frac{\partial F_r}{\partial V} \right)^2 (\sigma_V)^2 + \left(\frac{\partial F_r}{\partial Y} \right)^2 (\sigma_Y)^2 \quad (5-29)$$

Utilizing the accuracy of the water depth measurement of 2%, scour depth measurements of 4.3%, velocity measurements of 4%, initial water content of 1%, and soil shear strength of 1%, the relative error of the predicted scour in the mixtures was found to be 9.7%, and it was found to be 9.2% for unsaturated and saturated cohesive soil.

For the general equation in cohesive soil, the relative error in the predicted scour depth was also calculated and found to be 11.6%. Tables 5-10 through 5-16 present an example of the sensitivity analysis determinations.

Table 5-10. Results of the Sensitivity Analysis for Set 1,
Run R15-PB

	Y	V	F _r	C
$\partial ds / \partial i$	-	-	3.551	- 0.7009
σ_i	0.0147	0.0403	0.008545	0.00075
$(\partial ds / \partial i) \sigma_i$	-	-	0.0303	- 0.00053
σ_i / i	0.02	0.04	0.04116	0.015
Absolute Error (σ_{ds}) = 0.0303 ft				
Relative Error (σ_{ds}/ds) = 8.77%				

Table 5-11. Results of the Sensitivity Analysis for Set 1,
Run R31-PC

	Y	V	F _r	C
$\partial ds / \partial i$	-	-	3.12214	- 0.7337
σ_i	0.019	0.0728	0.0135	0.006
$(\partial ds / \partial i) \sigma_i$	-	-	0.043	- 0.0044
σ_i / i	0.02	0.04	0.0414	0.015
Absolute Error (σ_{ds}) = 0.043 ft				
Relative Error (σ_{ds}/ds) = 9.7%				

Table 5-12. Results of the Sensitivity Analysis for
Set 2, Run R35-PA

	Y	V	F _r	IWC	S	Comp.
$\partial ds/\partial i$	-	-	4.66	-1.298	0	-2.03
σ_i	0.018	0.072	0.014	0.002	0.001	0.0087
$(\partial ds/\partial i) \sigma_i$	-	-	0.064	-0.002	0	-0.018
σ_i/i	0.02	0.04	0.021	0.01	0.01	0.015
Absolute Error (σ_{ds}) = 0.066 ft						
Relative Error (σ_{ds}/ds) = 8.8%						

Table 5-13. Results of the Sensitivity Analysis for
Set 2, Run R33-PC

	Y	V	F _r	IWC	S	Comp.
$\partial ds/\partial i$	-	-	2.398	-0.744	0	-0.578
σ_i	0.017	0.059	0.012	0.0015	0.002	0.013
$(\partial ds/\partial i) \sigma_i$	-	-	0.028	-0.001	0	-0.007
σ_i/i	0.02	0.04	0.041	0.01	0.01	0.015
Absolute Error (σ_{ds}) = 0.0285 ft						
Relative Error (σ_{ds}/ds) = 9.2%						

Table 5-14. Results of the Sensitivity Analysis for
Set 3, Run R23-PA

	Y	V	$F_r - F_c$	IWC
$\partial ds / \partial i$	-	-	5.103	0.5056
σ_i	0.0195	0.0428	0.0087	0.0048
$(\partial ds / \partial i) \sigma_i$	-	-	0.0444	0.00246
σ_i / i	0.02	0.04	0.1464	0.01
Absolute Error (σ_{ds}) = 0.0445 ft				
Relative Error (σ_{ds} / ds) = 9.2%				

Table 5-15. Results of the Sensitivity Analysis for
Set 3, Run R38-PC

	Y	V	$F_r - F_c$	IWC
$\partial ds / \partial i$	-	-	2.573	1.41
σ_i	0.025	0.126	0.02	0.0045
$(\partial ds / \partial i) \sigma_i$	-	-	0.0529	0.0064
σ_i / i	0.02	0.04	0.0607	0.01
Absolute Error (σ_{ds}) = 0.053 ft				
Relative Error (σ_{ds} / ds) = 8.5%				

Table 5-16. Results of the Sensitivity Analysis for
the General equation, Run R24-PA

	Y	V	F_r	IWC	Comp.
$\partial ds/\partial i$	-	-	2.183	-1.155	-0.822
σ_i	0.024	0.042	0.008	0.0045	0.0113
$(\partial ds/\partial i) \sigma_i$	-	-	0.019	-0.0046	-0.009
σ_i/i	0.02	0.04	0.0377	0.01	0.015
Absolute Error (σ_{ds}) = 0.0216 ft					
Relative Error (σ_{ds}/ds) = 11.6%					

An uncertainty of the predicted scour depth results from the uncertainty of the measured independent variables (F_r , C, IWC, S, Comp.) used in deriving the predicted equations. To study the sensitivity of the predicted equations to the variation in each of these parameters, each variable was increased by 2% and the predicted scour depth was determined. As shown in Tables 5-17 through 5-20, the maximum error in the predicted scour depth results mostly from the uncertainty in measuring the parameters V and Y, which are used in computing the Froude number. The magnitude of uncertainty in scour depth prediction due to a 2 percent uncertainty in measuring the Froude number is 4 percent.

Table 5-17. Error in the Predicted Scour Depth Due to 2% Error in the Measured Parameters for Set 1.

F_r	C	ds(ft)	Error %	Comments
0.204	0.1	0.325	0	Set 1, Run R13-PC (Base Condition)
0.208	0.1	0.3382	4	1.02 F_r
0.204	0.11	0.324	0.3	1.02 C
0.211	0.4	0.215	0	Set 1, Run R18-PC (Base Condition)
0.215	0.4	0.224	4	1.02 F_r
0.211	0.408	0.2120	1.4	1.02 C
0.227	0.2	0.337	0	Set 1, Run R32-PB (Base Condition)
0.231	0.2	0.351	4	1.02 F_r
0.227	0.204	0.335	0.6	1.02 C

Table 5-18. Error in the Predicted Scour Depth Due to 2% Error in the Measured Parameters for Set 2.

IWC	F_r	$S/\rho V^2$	Comp.	ds(ft)	Error%	Comments
0.2	0.336	33.17	0.58	0.787	0	Set 2, R35-PA (Base Condition)
0.204	0.336	33.17	0.58	0.7826	0.6	1.02 IWC
0.2	0.343	33.17	0.58	0.819	4	1.02 F_r
0.2	0.336	33.83	0.58	0.788	0.13	1.02 S
0.2	0.336	33.17	0.592	0.7646	2.8	1.02 Comp.
0.15	0.28	79.59	0.87	0.3359	0	Set 2, R33-PC (Base Condition)
0.153	0.28	79.59	0.87	0.333	0.9	1.02 IWC
0.15	0.285	79.59	0.87	0.349	3.8	1.02 F_r
0.15	0.28	81.18	0.87	0.336	0.03	1.02 S
0.15	0.28	79.59	0.887	0.326	2.9	1.02 Comp.

Table 5-19. Error in the Predicted Scour Depth Due to 2% Error
in the Measured Parameters for Set 3.

IWC	$F_r - F_c$	ds (ft)	Error %	Comment
0.4	0.349	0.324	0	Set 3, R34-PB (Base Condition)
0.408	0.349	0.330	1.8	1.02 IWC
0.4	0.355	0.327	0.9	1.02 ($F_r - F_c$)
0.35	0.424	0.293	0	Set 3, R38-PA (Base Condition)
0.357	0.424	0.2994	2	1.02 IWC
0.35	0.432	0.297	1.4	1.02 ($F_r - F_c$)

Table 5-20. Error in the Predicted Scour Depth Due to 2% Error
in the Measured Parameters for General Equation.

IWC	F_r	Comp.	ds (ft)	Error%	Comment
0.38	0.374	0.79	0.314	0	Gen. Eq., R28-PB (Base Condition)
0.388	0.374	0.79	0.309	1.6	1.02 IWC
0.38	0.381	0.79	0.324	3.18	1.02 F_r
0.38	0.374	0.806	0.302	3.8	1.02 Comp.

CHAPTER VI**SUMMARY, CONCLUSIONS, AND RECOMMENDATIONS****6-1 Summary**

Local scour around bridge piers and abutments has been recognized as a most serious and costly engineering problem for many decades. Severe scour in the vicinity of bridge piers often results in the instability and failure of the bridges.

In an attempt to understand, control and manage local scour, a series of studies was conducted earlier to observe and identify many of the basic principles governing the mechanics of local scour around bridge piers. Many investigators studied the behavior of local scour under variety of parameters such as flow conditions, mode of scour, Froude number, shape and dimension of piers, scour overlapping, contraction effect, flow depth, sediment size, angle of attack, and time.

It is important to recognize that all the previous scour studies were performed on sandy soils in spite of the fact that in a significant number of cases, the bed materials found at bridge sites are silty and clayey soils. The literature review revealed that the study of bridge pier scour in

sandy-clayey mixtures or in cohesive soils has not been previously investigated. Therefore, it is important to identify the basic soil characteristics and properties which influence soil erodability. As reported by Dunn (1950), Alizadeh (1974), Arulanandan (1975), Abt (1980), and Shaikh (1986), the parameters which were considered significant erosive indicator are the type and percentage of mineral clay, soil shear strength, cation exchange capacity, plasticity index, grain size distribution, pore fluid, moisture content, and sodium absorption ratio.

The main purpose of this study was to investigate bridge pier scour in a mixture of cohesive and non-cohesive soils and in unsaturated and saturated cohesive soils. These objectives were achieved by conducting three set of test runs for a total of one hundred and eleven experimental data points utilizing three different laboratory flumes located in the Engineering Research Center of Colorado State University.

For each test run, the flow condition was classified as steady gradually varied flow over the entire test flume length. The test runs were lasted until the near equilibrium scour depth was reached. The experimental program included subcritical as well as supercritical flow conditions (6 experiments).

The properties and characteristics of bed materials used in this study were presented in Section 4-3. In the first set (39 experiments), a Masonry sand of 0.55 mm mean grain size was mixed with 0, 5, 10, 20, 30, and 40 percent of cohesive soil mixture (containing 78% finer than sand sizes by weight). In the second set (39 experiments), the cohesive soil was first prepared at 20 and 15 percent of water content and then compacted at 58, 65, 73, 80, and 87 percent of degree of compaction. For the third set (33 experiments), the cohesive soil was saturated at initial water content of 32, 35, 40, and 45 percent.

The regression analysis of the experimental data resulted in equations 5-10, 5-14, and 5-19 for predicting the maximum scour ratio. These equations which were derived for 8-inch diameter pier size and 10-inch flow depth are given below. The expression for pier scour for clayey-sand mixtures (containing Montmorillinite clays) with up to 31 percent silt-clay content by dry weight from this study is given by:

$$\left(\frac{d_s}{b}\right)_p = 18.92 \left(\frac{F_r^{2.08}}{(1+C)^{1.88}} \right) \quad (5-10)$$

where C = fraction of cohesive soil finer than sand (up to 31 percent, or C < 0.31); b = pier diameter of 8". For flow and geometry conditions beyond the scope of the present experimental study, adjustments are needed based on previously established relationships. For example, in order to apply equation 5-10 to other circular pier sizes and flow depths, the right hand side of the equation must be multiplied by $(b_{desired}/b_{8''})^{0.6} (d_{desired}/d_{10''})^{0.167}$, where $b_{8''}$, $d_{10''}$ are pier diameter

of 8" and flow depth of 10" (in desired units), respectively; and b_{desired} , d_{desired} are desired pier diameter and flow depth, respectively. Similarly, other correction factors for flow angle of attack, pier shape, coarse size fraction, etc. must be applied using methodologies available in literature.

Selection of cohesive pier scour equation depends on the degree of soil saturation. Within the bounds of this study, Equations 5-14 and 5-19 can be used for this purpose.

For unsaturated cohesive soils:

$$\left(\frac{d_s}{b}\right)_p = 2.71 (IWC)^{-0.36} F_r^{1.92} \left(\frac{S}{\rho V^2}\right)^{0.023} (Comp.)^{-1.62} \quad (5-14)$$

where $d_s = 0$ for $F_r \leq 0.2$ and for Compaction ≥ 85 percent.

For saturated cohesive soils:

$$\left(\frac{d_s}{b}\right)_p = 5.48 (IWC)^{1.14} (F_r - F_c)^{0.6} \quad (5-19)$$

where $F_c = \frac{0.035}{IWC^2}$, and $d_s = 0$ for $F_r \leq F_c$.

Scour around circular piers is dominated by the intensity of flow in excess of critical values for various types of cohesive soils. The scouring action continues until the reduced shear intensity due to the development of a scour hole can no longer erode the material (critical shear conditions). As a result, the maximum pier scour relationships given by equations 5-14 and 5-19 do not express scour as a rate of erosion.

6-2 Conclusions

The conclusion from this experimental study can be listed as:

- 1) The presence of cohesive material in non-cohesive soils causes a reduction in the scour depth. The scour depth decreases as the clay content in sandy soil increases up to 40%. Beyond this clay content other parameters such as compaction, water content, etc become dominant.
- 2) In sandy soil, a new scour depth predictor is proposed in terms of Froude number and clay content. The scour depth is directly proportional to F_r^2 and inversely proportional to $(1+C)^2$, where C is clay content.
- 3) The side inclinations of the scour hole as a function of clay content is developed. As the clay content is increased, the angle of repose is decreased. This is due to the fact that the clay in sandy-clayey mixture, acts as a lubricant.
- 4) For unsaturated compacted cohesive soils, a new scour depth equation is proposed in terms of initial water content, Froude number, soil shear strength, and compaction. The scour depth is inversely proportional to the degree of compaction.
- 5) The slope of the scour hole in cohesive soils is may be much steeper than those in non-cohesive soils, and increases as the compaction of cohesive soil increases.

- 6) For saturated cohesive soils, a new scour depth predictor is developed as a function of initial water content, and Froude number. The scour depth decreases as the initial water content decreases.
- 7) The concept of critical Froude number (F_c) as a function of initial water content is used in defining the initiation of pier scour in saturated cohesive soil ($F_c=0.035/(IWC)^2$).
- 8) For saturated cohesive soils, it was observed that the time to reach the maximum scour depth (900 minutes) was much larger than those observed in sandy-clayey mixture (420 minutes).
- 9) For the time rate of scour, approximately 90 percent of maximum scour in sandy-clayey mixture occurred during the first 300 minutes, while the same percentage required the first 540 minutes in saturated cohesive soils.
- 10) For sandy-clayey mixture and unsaturated cohesive soil at low compactions, the scour holes were observed to be conical in shape and independent of bed material. However, for saturated cohesive soil at low water content and for unsaturated cohesive soil at high degree of compaction, the shape of the scour hole is more likely to be cylindrical with steeper side slopes.

6-3 Recommendations for Further Research

The findings of the present study should be applied to

the design of bridges in similar soils and channel characteristics. The empirical equations were developed and assumed generally representative of the scour depth in mixture of cohesive and noncohesive soils and in cohesive soils.

Due to wide variations in the properties of cohesive soils, the application of the developed equations in bed materials of different origin (such as Kaolinite) than those described in this study may be inadequate for scour depth estimation. There are many other factors that have not been covered in this study which may affect the shape and size of scour holes. Therefore, it is recommended that further studies should be pursued to extend the applicability of the developed equations. The following are suggested for further study:

- 1) In a manner similar to those procedures presented herein, tests should be conducted on other type of cohesive soils (for example soil with large amount of Kaolinite or Illite minerals clay have not been covered in this study).
- 2) All tests of this study were performed without changing the chemical properties of the cohesive soils and eroding fluid. Therefore it is recommended to investigate the effect of sodium adsorption ratio of clay soil and salt concentration of the eroding fluid on the scour depth.
- 3) In order to apply with confidence the proposed equations,

field measurements are needed to verify the conformity of model and prototype. Any discrepancies between the predicted scour and field measurements may indicate factors that should cover in further study.

- 4) Research on the effects of dry-wet cycle on pier scour in cohesive soils should be conducted in a larger scale.
- 5) The effect of sand content of the oncoming flow should be investigated to examine the abrasive effects of flows.
- 6) Defining the F_c for various types of cohesive soils at different initial water content should be studied.
- 7) It is recommended to check the influence of the shapes of flood hydrograph and sediment content of the flood flow on the behavior of pier scour in cohesive soils.
- 8) Throughout this study, the circular piers were aligned with the direction of the flow. It is suggested that tests be performed with different angles of attack and various pier shapes in order to investigate the effect of these parameters on the scour depth in cohesive soils.
- 9) It would be beneficial to test the development equations for very shallow flows ($Y/b < 0.2$) and for deep flows ($Y/b > 10.0$ to 20.0).

BIBLIOGRAPHY

- 1- Abdel-Rahmann, N.M., "The Effects of Flowing Water on Cohesive Beds". Thesis Presented to Laboratory for Hydraulic Research and Soil Mechanics, Swiss Federal Institute of Technology, Zurich, 1963.
- 2- Abdou, M.I., "Effect of Sediment Gradation and Coarse Material Fraction on Clear-Water Scour Around Bridge Piers", Ph.D. Dissertation, Colorado State University, September 1993.
- 3- American Society of Civil Engineers. "Sedimentation Engineering". Manual No.54.1975.
- 4- Ariathurai, R. and Arulanandan, K., "Erosion Rates of Cohesive Soils". Journal of Hydraulics Division, ASCE, Vol.104, No.HY2, February 1978.
- 5- Arulanandan, K., Loganathan, P. and Knone, R.B., "Pore and Eroding Fluid Influence on Surface Erosion of Soil". Journal of Geotechnical Division, American Society of Civil Engineers, Vol.101, No.GT1, January 1975.
- 6- Arulanandan, K., "Fundamental Aspects of Erosion of Cohesive Soils". Journal of the Hydraulics Division, ASCE, Vol. 101, No. HY5, May, 1975.
- 7- Anderson, H.W., "Physical Characteristics of Soil Related to Erosion". Journal of Soil and Water Conservation, July 1951.
- 8- Abt, S.R., "Scour at Culverts Outlets in Cohesive Bed Material". Ph.D. Dissertation, Colorado State University, Colorado, April 1980.
- 9- Alizadeh, A., "Amount and Type of Clay and Pore Fluid Influences on the Critical Shear Stress and Swelling of Cohesive Soils. Ph.D. Dissertation, University of California, 1974.
- 10- Bormann, N.E., "Equilibrium Local Scour Downstream of Grade-Control Structures". Ph.D. Dissertation, Colorado State University, September 1988.
- 11- Bohan, J.P., "Erosion and Riprap Requirements at Culvert and Storm-drain Outlets". U.S.Army Engineer Waterways Experiment Station, Vicksburg, Mississippi, 1970.

- 12- Bayazit, M., "Scour of Bed Materials in Very Rough Channels". Journal of Hydraulics Division, American Society of Civil Engineers, Vol. 104, No.HY9, Sep. 1978.
- 13- Carman, P.C."Permeability of Saturated Sands, Soil, and Clays. J. Agric. Sci. Vol.29, 1939, pp.262-273.
- 14- Carstens, M.R., "Similarity Laws for Localized Scour". Journal of the Hydraulics Division, American Society of Civil Engineering, May 1966.
- 15- Chen, Y.H., "Scour at Outlets of Box Culverts", Master's Thesis, Colorado State University, Fort Collins, Colorado, September, 1970.
- 16- Christensen, R.W. and Das, B.M., "Hydraulic Erosion of Remolded Cohesive Soils". Highway Research Board Special Report, No.135, 1973.
- 17- Collis-George, N., and Smiles, D.E., "An Examination of Cation Balance and Moisture Characteristic Methods of Determining the Stability of soil Aggregates, Journal of Soil Science, Vol.14, 1963, pp.21-32.
- 18- Daniel Hillel, "Soil and Water Physical Principles and Processes", 1971.
- 19- Dunn, I.S., "Tractive Resistance of Cohesive Channels". Journal of the Soil Mechanics and Foundations, Vol.85, No.SM5, June 1959.
- 20- Ettema, R., "Influence of Bed Material Gradation on Local Scour", University of Auckland, Report No.124, 1973.
- 21- Flaxman, E.M., "Channel Stability in Undisturbed Cohesive Soils." Journal of Hydraulics Division, American Society of Civil Engineers, Vol.89, No.HY6, PP.87-96, March 1963.
- 22- Fletcher, B.P. and Grace, J.L., "Practical Guidance for Estimating and Controlling Erosion at Culvert Outlets". U.S.Army Water-Ways Experiment Station, Vicksburg, Mississippi, 1972.
- 23- Grass, A.J., "Initial Instability of Fine Bed Sand". Journal of the Hydraulics Division, American Society of Civil Engineers, Vol.76, No.HY3, 1970.
- 24- Grissinger, E.H., Asmussen, L.E. and Espey, W.V. "Channel Stability in Undisturbed Cohesive Soils". Journal of Hydraulic Division, ASCE, Vol. 89, No HY6, November 1963.

- 25- Grissinger, E.H., "Resistance of Selected Clay Systems to Erosion by Water". Water Resources Research, Vol.2, No.1, 1966, pp.131-138.
- 26- Kamphuis, J.W., "Influence of Sand or Gravel on the Erosion of Cohesive Sediment". Journal of Hydraulic Research, Vol. 28, No. 1, Queen's University, Kingston, Ontario, Canada, 1990.
- 27- Kuti, E.G. and Yen, C., "Scouring of Cohesive Soils". Journal of the Hydraulics Research, Vol.14, No.3, 1976.
- 28- Laursen E.M., "Observations on the Nature of Scour". Proceedings of the Fifth Hydraulic Conference, June, 1952.
- 29- Lausley, L.M., Kappus, V., and Otwna, M.P., "Magnitude and Rate of Erosion at Culvert Outlets" Proceedings of the 12th Congress of the IAHR, Vol.3, Fort Collins, Colorado, 1967.
- 30 Lambe, T.W., "The Structure of Compacted Clay" Journal of the Soil Mechanics and Foundations Division, Proceedings of the ASCE, Vol. 84, No.SM 2, May, 1958.
- 31- Liou, Y., "Effects of Chemical Additives on Hydraulic Erodibility of Cohesive Soil". M.S. Thesis, Colorado State University, August 1967.
- 32- Liou, Y., "Hydraulic Erodibility of Two Pure Clay Systems", Ph.D. Dissertation, Colorado State University, August 1970.
- 33- Little, W.C. and Mayer, P.G., "Stability of Channel Beds by Armoring". Journal of Hydraulic Division, ASCE, Vol.102, No.HY11, November 1976.
- 34- Lyle, W. and Smerdon, E., "Relation of Compaction and other Soil Properties to Erosion Resistance of Soils". Transactions of the American Society of Agricultural Engineers, Vol.8, No.3, 1965, pp.419-422.
- 35- Mitchell J.K., "Fundamentals of Soil Behavior", Second edition, December 1992.
- 36- Martin, T.R., discussion of, "Experiments on the Scour Resistance of Cohesive Sediments". Journal of Geophysical Research, Vol.67 No.4, pp.1447-49, Washington, D.C. April 1962.

- 37- Masood, T., "Error Analysis in Measurements of Alluvial Channel". Thesis, Colorado State University, Fall, 1976.
- 38- Middleton, H.E., "Properties of Soils which Influence Soil Erosion". U.S. Department of Agriculture Technical Bulletin No.178, pp.16, 1930.
- 39- Moore, W.L. and Masch, F.D., "Experiments on the Scour of Cohesive Sediments". Journal of Geophysical Research, Vol.67, No.4, April, 1962.
- 40- Murray, W.A., "Erodibility of Coarse Sand-Clayey Silt Mixtures". Journal of the Hydraulics Division, ASCE, Vol.103, No.HY10, October 1977.
- 41- Masch, F.D., Espey, W.H., and Moore, W.L., "Measurements of the Shear Resistance of Cohesive Sediments." Proceedings of the Federal Inter-Agency Sedimentation Conference, Agricultural Research Service, Publication No.970, Washington, D.C, 1963, pp.151-155.
- 42- Noshi, H.M., "Experimental Study on the Effect of Sediment Gradation and Flow Hydrograph on Clear Water Local Scour Around Circular Bridge Piers". Master's Thesis, Colorado State University, December 1993.
- 43- Nickelson, J.R., "Experimental Study of Riprap Around Bridge Piers". Master's Thesis, Colorado State University, May 1992.
- 44- Paaswell, R.E., "Causes and Mechanisms of Cohesive Soil Erosion". Highway Research Board Special Report 135, pp. 52-74, 1973.
- 45- Partheniades, E., "Erosion and Deposition of Cohesive Soils". Journal of Hydraulics Division, ASCE, Vol.91, No.HY1, January, pp. 105-138, 1965.
- 46- Peele, T.C., "The Relation of Certain Physical Characteristics to the Erodibility of Soils". Soil Science Society of America, Vol.II, December, 1937.
- 47- Partheniades, E., and Paaswell, R.E., "Erodibility of Channels with Cohesive Boundary", Journal of the Hydraulics Division, ASCE, Vol.96, No.HY3, Proc. paper 7156, Mar., 1970, pp.755-771.
- 48- Quirk, J.P., and Schofield, R.K., "The Effect of Electrolyte Concentration on Soil Permeability", Journal of Soil Science, Vol.6, 1955, pp.163.

- 49- Robinson, A.R., "Model Study of Scour from Cantilevered Outlets". Transactions of the American Society of Agricultural Engineers, 1971.
- 50- Rouse, H., "Criteria for Similarity in the Transportation of Sediment", Proceedings of 1 st Hydraulic Conference, Bulletin 20, State University of Iowa, Iowa City, Iowa, March, 1940, PP.33-49.
- 51- Rectoric, R.J., "Critical Shear Stress in Cohesive Soils". Thesis presented to Texas A&M University at College Station, Tex., in 1964, in partial fulfillment of the requirements for the degree of Master of Science.
- 52- Rowell, D.I., "Effect of Electrolyte Concentration on the Swelling of Oriented Aggregates of Montmorillonites." Soil Science, Vol.96, 1963, pp.368.
- 53- Shaikh, A., "Surface Erosion of Compacted Clays." Ph.D. Dissertation, Colorado State University, 1986.
- 54- Shaikh, A., "Scour in Uniform and Graded Gravel at Culvert Outlets". Master's Thesis, Colorado State University, Fort Collins, Colorado, May, 1980.
- 55- Sargunam, A., Riley, P., and Arulanandan, F., "Physio-Chemical Factors in Erosion of Cohesive Soils". Journal of the Hydraulics Division, American Society of Civil Engineers, Vol.99, HY3, March 1973.
- 56- Schneider, V.R., "Mechanics of Local Scour". Ph.D. Dissertation, Colorado State University, Fort Collins, Colorado, December 1968.
- 57- Seed, H.B. and Chan, C.K., "Structure and Strength Characteristics of Compacted Clays". Journal of Soil and Mechanics and Foundation Division, American Society of Civil Engineers, Vol.85, No.SM5, October, 1959.
- 58- Simons, D.B. and Senturk, F., "Sediment Transport Technology" Water Resources Publications, Fort collins, Colorado, 1976.
- 59- Smerdon, E.T. and Beasley, R.P., "Critical Tractive Forces in Cohesive Soils". Agricultural Engineering, January 1961.
- 60- Sherard, J.L., Decker, R.S., and Ryka, N.L., "piping in Earth Dams of Dispersive Clay", presented at the june 12-14, 1972, ASCE Soil Mechanics and Foundation Conference hold at Purdue University, Lafayette, Ind.

- 61- Sargunam, A. "Influence of Minerology, Pore Fluid Composition and Structure Of the Erosion of Cohesive Soils. Ph.D. Dissertation Univ. of Calif. , Davis, 1973.
- 62- Verwey, E.J.W., and Overbeek, J.T., G., "Theory of the Lyophobic Colloids, Elsevier Publishing Co., New York, N.Y., 1948.
- 63- Walter Hans Graf" Hydraulics of Sediment Transport", Mc Graw-Hill Co., New York, 1971.
- 64- White, C.M., "The Equilibrium of Grains on the Bed of a Stream" Royal Society, Proceedings A174, 1940.

